Functional characterisation of ANKRD1 and its regulation by RASSF1A and YAP1 signalling

DISSERTATION

Zur Erlangung des Doktorgrades der Naturwissenschaften

(Doctor rerum naturalium Dr. rer. nat.)

Angefertigt am Institut für Genetik

Fachbereich Biologie und Chemie

der Justus-Liebig-Universität Giessen

Vorgelegt von

Adriana Patricia Jiménez Carrera

Giessen, Januar 2017

1. Gutachter: Prof. Dr. Reinhard Dammann
Institut für Genetik
Fachbereich Biologie und Chemie
der Justus-Liebig-Universität Giessen

2. Gutachter: Prof. Dr. M. Lienhard Schmitz
Institut für Biochemie
Fachbereich Medizin
der Justus-Liebig-Universität Giessen

ERKLÄRUNG

Hiermit erkläre ich, dass ich die vorliegende Doktorarbeit selbständig und ohne unzulässige fremde Hilfe oder Benutzung anderer als der angegebenen Hilfsmittel angefertigt habe. Alle Textstellen, die wörtlich oder sinngemäß aus veröffentlichten Schriften entnommen sind, und alle Angaben, die auf mündlichen Auskünfte beruhen, sind als solche kenntlich gemacht. Bei den von mir durchgeführten und in der Dissertation erwähnten Untersuchungen habe ich die Grundsätze guter wissenschaftlicher Praxis, wie sie in der "Satzung der Justus-Liebig-Universität Gießen zur Sicherung guter wissenschaftlicher Praxis" niedergelegt sind, eingehalten.

Giessen, den 31.01.2017 …….

Adriana Patricia Jiménez Carrera

Während dieser Arbeit ist eine Publikation mit dem Titel "*The tumor suppressor RASSF1A induces the YAP1 target gene ANKRD1 that is epigenetically inactivated in human cancers and inhibits tumor growth*" entstanden. Die Publikation ist in der Revisionsphase bei der Zeitschrift "Oncotarget".

Eine weitere Publikation als Ko-Autorin wurde 2016 veröffentlicht mit dem Titel "*The dual specificity phosphatase 2 gene is hypermethylated in human cancer and regulated by epigenetic mechanisms*". T. Haag, A.M. Richter, M.B. Schneider, A.P. Jiménez, and R.H. Dammann. BMC Cancer 2016. Die Ergebnisse dieser Publikation wurden bei dieser Arbeit nicht mit einbezogen.

For Claude

Index

ABBREVIATIONS

β	Beta
Δ	Delta
ΔNp63	N-terminus truncated p63 isoform
ΔNp73	N-terminus truncated p73 isoform
µ	Micro
AJUBA	LIM protein AJUBA
AMOT	Angiomotin
ANKRD1	Ankyrin Repeat Domain 1/CARP
APS	Ammonium persulfate
ATM	Ataxia telangiectasia mutated
Aza	5'-Aza-2'-desoxycytidine
BAX	BCL2-associated X protein
BBC3	BCL2 binding component 3/PUMA
bp	Base pair
CDKN1A	Cyclin-dependent Kinase Inhibitor 1A/p21
cDNA	Complementary DNA
CoBRA	Combined bisulfite restriction analysis
Co-IP	Co-immunoprecipitation
CpG	Cytosine and guanine dinucleotides
CDK6	Cyclin dependent kinase 6
CYR61	Cysteine-rich angiogenic inducer 61
CTGF	Connective tissue growth factor
C-terminal	Carboxyl-terminal
Ctrl	Control
d	Day
D. melanogaster	*Drosophila melanogaster*
ddH_2O	Water
DMEM	Dulbecco's modified Eagle Medium
DNA	Deoxyribonucleic acid
DNAse	Deoxyribonuclease
dNTP	Nucleoside triphosphate
Dox	Doxycycline

ECL	Enhanced chemiluminescence
E. coli	*Escherichia coli*
EDTA	Ethylenediaminetetraacetic acid
e.g.	Example given
et al.	and others
EtOH	Ethanol
FACS	Fluorescence-activated cell sorting
FCS	Fetal calf serum
Fig.	Figure
FSC	Forward light scatter
g	Acceleration of gravity
g	Gram
G418	Geneticin
GAPDH	Glyceraldehyde-3-phosphate dehydrogenase
GFP	Green fluorescent protein
h	Hour(s)
HCC	Hepatocellular carcinoma
HRP	Horsera dish peroxidase
ind.	Induction
Ivm	*In vitro* methylated
JNK	c-Jun N-terminal kinase
kDa	kilo Dalton
l	Liter
LATS	Large Tumor Suppressor
M	Molar
m	Milli
MAPK	Mitogen-activated protein kinase
MDM2	Human homologue of mouse double minute 2
$MgCl_2$	Magnesium chloride
min	Minutes
MST	Mammalian STE20 like Kinase
NF2	Neurofibromatosis type II
ON	Over night
p16	Tumor suppressor protein p16, CDKN2A
PBS	Phosphate buffered saline

PCR	Polymerase chain reaction
PEI	Polyethylenimine
pH	Negative of the logarithm to base 10 of the activity of hydrogen
PS	Penicillin and streptomycin
PVDF	Polyvinylidene difluoride
RA	Ras-association domain
RASSF	Ras Association Domain Family
RNA	Ribonucleic acid
RNAse	Ribonuclease
rpm	Revolutions per minute
RT	Room temperature
RT-PCR	Reverse transcriptase PCR
qRT-PCR	Quantitative real time PCR
s	Seconds
SAM	S-adenosylmethionine
SARAH	Sav/Rassf/Hpo domain
SDS	Sodium dodecyl sulphate
S	Serine
siRNA	Small interfering RNA
T	Threonine
TBE	Tris borate EDTA buffer
TBS	Tris buffered saline
TE	Tris EDTA buffer
TEAD	TEA domain family
TEMED	N,N,N′,N′-Tetramethylethane
TET ON	Tetracycline-controlled gene expression
TGF- β	Transforming growth factor beta
TP53	Tumor suppressor protein p53
TP73	Tumor suppressor protein p73
U	Enzyme unit
WNT	Wnt signaling
Y	Tyrosine
YAP1	Yes-Associated Protein 1
YFP	Yellow fluorescent protein

SUMMARY

The Hippo pathway controls organ size and is involved in both cell proliferation as well as in apoptosis. In cancer, the signalling via Hippo is deregulated and promotes tumor growth. The proto-oncogene YAP1 is the downstream transcriptional co-activator of this pathway with its function depending on the binding to several transcription factors such as TEAD, SMAD and TP73. The tumor suppressor gene RASSF1A is one of the main regulators of the Hippo signalling; however, *RASSF1A* is epigenetically silenced in cancer. In the literature, there are indications for the role of RASSF1A in the regulation of the pro-apoptotic function of the Hippo pathway. The aim of this study was to analyse the regulatory role of RASSF1A on YAP1 target genes. Therefore, a YAP1-inducible cell line was generated and further characterised after induction of YAP1 and co-expression with RASSF1A.

An important observation in this study was the oncogenic potential of YAP1. The induction of YAP1 promotes cell proliferation by activation of pro-proliferative genes and by the transcriptional repression of tumor suppressor genes such as *TP53, RASSF1A, BAX, CDKN1A* and *BBC3*. Expression screenings by microarray revealed novel potential YAP1 target genes that are regulated by RASSF1A. In addition, microscopy and flow cytometry data showed that the expression of RASSF1A triggers the nuclear translocation of YAP1 inducing nuclear deformation, cell cycle arrest and apoptosis. In addition, it was observed that RASSF1A and YAP1 repress the expression of growth-associated genes and growth factors such as MDM2. Further analysis indicated that RASSF1A neutralizes the oncogenic function of YAP1 by activation of the YAP1 target genes *ANKRD1, AJUBA, BAX* and *CDKN1A*. RASSF1A activates Hippo signalling via the SARAH (Sav/Rassf/Hpo) domain and, together with YAP1, regulates the expression of the target gene *ANKRD1*. The further characterisation of ANKRD1 indicated its potential function as tumor suppressor gene. ANKRD1 inhibits cell growth and is silenced by promoter methylation in lung and in prostate cancer cell lines. At the protein level, ANKRD1 stabilises TP53 via reduction of the level of MDM2, which results in the transcriptional activation of *CDKN1A* and *BAX*. Previous reports suggested ANKRD1 as co-activator of TP53. In this study, the knockdown of ANKRD1 by siRNA and promoter assays corroborated the obtained findings and the data from the literature. The data from this work suggest a novel mechanism of RASSF1A and YAP1 interaction, namely to regulate TP53 and the G1/S cell cycle transition via the Hippo pathway and ANKRD1. The inactivation of *RASSF1A* by aberrant promoter methylation results in the deregulation of the signalling, which promotes cell proliferation by the action of the oncogene YAP1.

ZUSAMMENFASSUNG

Der Hippo Signalweg kontrolliert die Organgröße bei der Regulation der Zellproliferation und Apoptose. Bei Krebs ist der Hippo Signalweg dereguliert und fördert das Tumorwachstum. Das Proto-Onkogen YAP1 ist der transkriptionale Co-Aktivator dieses Signalwegs, und seine Funktion hängt von der Bindung an unterschiedliche Transkriptionsfaktoren wie TEAD, SMAD und TP73 ab. Das Tumorsuppressor-Gen *RASSF1A* ist einer der Hauptregulatoren des Hippo Signalwegs, jedoch ist *RASSF1A* in Krebszellen epigenetisch inaktiviert. In der Literatur gibt es Hinweise auf die Rolle von RASSF1A bei der Regulation der pro-apoptotischen Funktion des Hippo Signalwegs. Das Ziel dieser Arbeit war die Analyse der regulatorischen Rolle von RASSF1A auf die YAP1-Zielgene. Daher wurde eine YAP1-induzierbare Zelllinie generiert und charakterisiert sowohl nach der Induktion von YAP1 als auch nach Expression von RASSF1A.

Eine wichtige Beobachtung dieser Studie war die potentielle onkogene Funktion von YAP1. Die Induktion von YAP1 fördert die Zellproliferation durch Aktivierung von pro-proliferativen Genen sowie durch die Transkriptionsrepression von Tumorsuppressor-Genen wie *TP53, RASSF1A, BAX, CDKN1A* und *BBC3*. Transkriptom-Analysen mittels Microarrays zeigten neue potentielle YAP1-Zielgene, die durch RASSF1A reguliert werden. Darüber hinaus zeigten Mikroskopie- und Durchflusszytometrie- Daten, dass die Expression von RASSF1A die nukleare Translokation von YAP1, Zellkernveränderung, Zellzyklus-Arrest und Apoptose induziert. Zusätzlich wurde beobachtet, dass RASSF1A und YAP1 die Expression von Wachstums-assoziierten Genen und Wachstumsfaktoren wie MDM2 unterdrücken. Weitere Analysen zeigten, dass RASSF1A die pro-proliferative Funktion von YAP1 durch Aktivierung der YAP1-Zielgene *ANKRD1, AJUBA, BAX* und *CDKN1A* neutralisiert. RASSF1A aktiviert den Hippo Signalweg über die SARAH-Domäne (Sav/Rassf/Hpo) und reguliert zusammen mit YAP1 die Expression des Zielgens *ANKRD1*. Die weitere Charakterisierung von ANKRD1 zeigte seine potentielle Funktion als Tumorsuppressor-Gen. ANKRD1 hemmt das Zellwachstum und ist durch Promoter-Methylierung in Lunge und in Prostatakrebs-Zelllinien inaktiviert. Auf Proteinebene stabilisiert ANKRD1 die Expression von TP53 durch Verringerung von MDM2, was zu einer transkriptionellen Aktivierung von *CDKN1A* und *BAX* führt. Die Literatur berichtet, dass ANKRD1 ein möglicher Co-Aktivator von TP53 sei. Die Ergebnisse dieser Studie bestätigten die erhaltenen Befunde und die Angaben aus der Literatur.

Diese Ergebnisse deuten auf einen neuen Mechanismus von RASSF1A und YAP1 hin, um TP53 und den G1/S Zellzyklus-Übergang über den Hippo Signalweg und ANKRD1 zu regulieren. Die epigenetische Inaktivierung von *RASSF1A* führt zu der Deregulierung des Signalwegs, was widerum die Zellproliferation durch die Wirkung des Onkogens YAP1 fördert.

1. INTRODUCTION

1.1 Cancer

Cancer is a result from the progressive acquisition and accumulation of genetic and epigenetic alterations in cells and tissues (Hanahan and Weinberg, 2011). In normal cells or quiescent cells, the balance of growth-suppressing tumor suppressor genes and growth-promoting oncogenes is essential for maintaining the genomic integrity. During cancer initiation genomic and epigenetic aberrations ocurr, which cause genomic instability (Risch and Plass, 2008). These alterations include the amplification of proto-oncogenes, deletions or translocation of genomic loci, changes in the epigenetic methylation pattern and loss of heterozygosity of tumor suppressor genes (Hanahan and Weinberg, 2011; Risch and Plass, 2008).

Genomic amplification and hypomethylation of promoter regions is associated with the activation of proto-oncogenes, which contributes to carcinogenesis (Feinberg *et al*., 2016). The depletion of genomic loci and the hypermethylation of CpG islands in the promoter region or at the first exon of tumor suppressor genes can lead to transcriptional gene silencing and the subsequent loss of gene expression (Feinberg *et al*., 2016; Risch and Plass, 2008). Alterations in DNA methylation affect genes that encode e.g. for DNA repair proteins, non-coding RNAs or for proteins involved in cell adhesion. The expression of these methylated genes changes and therefore, diverse cellular signalling pathways and the cell cycle are altered (Feinberg *et al*., 2016; Risch and Plass, 2008). The cell cycle is a critical process, which is strictly regulated to avoid hyperproliferation and genetic instability. In cancer cells, the cell cycle progression is deregulated. The silencing or inactivation of the principal regulators of the cell cycle checkpoints and apoptosis plays an essential role in promoting tumor progression (Hanahan and Weinberg, 2011).

The imbalance in the expression between tumor suppressor genes and oncogenes disturbs the genomic integrity of the cells, which results in uncontrolled cell growth and the resistance to cell death.

1.2 The Hippo pathway

The Hippo pathway is a kinase cascade that regulates organ size and plays an important role in cell differentiation, proliferation and apoptosis (Saucedo and Edgar, 2007); thus its deregulation is a key factor for tumorigenesis, tumor growth and metastasis (Saucedo and Edgar, 2007). According to recent reports, there is a crosstalk between the Hippo signalling and other cellular pathways such as MAPK, TGF-β and WNT signalling (Reddy and Irvine, 2013; Sun and Irvine, 2013; Varelas *et al*., 2010; Varelas *et al*., 2008).

The components of the Hippo pathway were first discovered in *Drosophila melanogaster* by genetic mosaic screens for mutated genes that produce cellular proliferation (Xu and Rubin, 1993). Among the discovered genes, novel tumor suppressor genes were found with homologues in humans such as *PTEN*, *Salvador (Sav)*, large tumor suppressor gene *Warts/LATS* and Hippo (*hpo/MST)* (Justice *et al*., 1995; Tapon *et al*., 2002; Xu and Rubin, 1993). Years later, the components of the signalling were further described to promote apoptosis and to control cell proliferation in *D. melanogaster* (Justice *et al*., 1995; Tapon *et al*., 2002; Xu and Rubin, 1993). This signalling pathway received the name from the Hippo (*hpo)* Ste-20 family protein kinase (Tapon *et al*., 2002). In *D. melanogaster*, loss-of-function mutants of *Hpo* promoted tissue overgrowth in eyes and wings (Wu *et al*., 2003). The Hpo kinase was also described to phosphorylate Salvador and to interact with the tumor suppressor Warts (Wu *et al*., 2003).

To date, the components of the Hippo pathway are described in three categories: the upstream regulatory elements, the core components and the downstream transcriptional effectors (Fig. 1). The principal components of the Hippo pathway in *D. melanogaster* are: Fat, Merlin/NF2 (Mer/NF2), Expanded (Ex), Kibra, Mats, Warts (Wts), Salvador (Sav), Hippo (Hpo) and the transcriptional regulator Yorki (Yki) (Fig. 1). Both in *D. melanogaster* and in mammals, the upstream regulatory components are a transmembrane protein (e.g. Fat) and the membrane-associated cytoplasmic tumor suppressor protein Merlin/NF2 (Lallemand *et al*., 2003; Zhang *et al*., 2010). The activation of the pathway is still under investigation. Some reports suggest the activation of the Hippo pathway by high cell density, since the upstream component Merlin/NF2 regulates the function of Yki/YAP1 in association with cell-cell adhesion, cell polarity, cell junctions and mechanotransduction (Elbediwy *et al*., 2016; Kim *et al*., 2011; Lallemand *et al*., 2003; Zhao *et al*., 2007). As

indicated in figure 1, the pathway is initiated by the transmembrane protein Fat, by regulation of the membrane-associated proteins Mer, Ex and the scaffold protein Kibra that activate the phosphorylation of Hpo, Sav and Wts. Wts in turn regulates the transcriptional function of Yki (Fig.1). In *D. melanogaster*, the transcriptional activator Yki interacts with the transcription factors Scalloped (Sc) and Homothorax (Hth) to promote cell survival and cell proliferation e.g. in eye development (Peng *et al*., 2009; Wu *et al*., 2008; Zhang *et al*., 2008). Some of the target genes of Yki in *D. melanogaster* are *bantam, e2f1* and *Drosophila Myc* (*dMyc*) (Fausti *et al*., 2012; Neto-Silva *et al*., 2010; Peng *et al*., 2009).

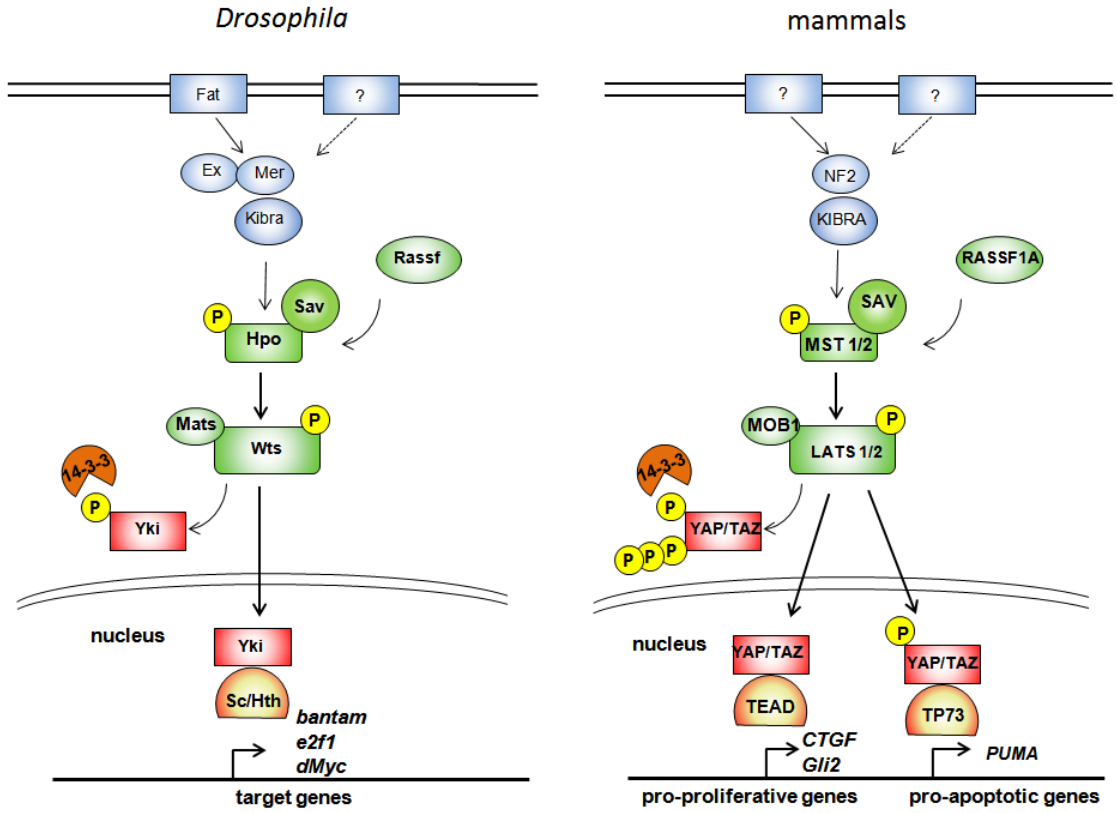

Figure 1: Components of the Hippo pathway in *D. melanogaster* and mammals. An extracellular stimulus activates a transmembrane protein (Fat in *D. Melanogaster*. G-protein coupled receptor and E-cadherin in mammals), which regulates the membrane-associated proteins Mer/NF2, Expanded (Ex) and Kibra/KIBRA that in turn activate the Hippo kinase cascade (Hpo/MSTs; Wts/LATSs). The kinase cascade is also activated by the members of the RAS association domain family (Rassf/RASSF1A) via the SARAH (Sav/Rassf/Hpo) domain. The active Hpo/MSTs kinases together with the scaffold protein Sav/SAV phosphorylate the Wts/LATSs kinases. Subsequently, the Wts/LATSs kinases together with the scaffold protein Mats/MOB1 phosphorylate Yki/YAP1. The phosphorylation of the transcriptional activator Yki/YAP1 plays different roles such as cytoplasmic retention and degradation (via 14-3-3) or nuclear translocation. To regulate the expression of the specific target genes, Yki/YAP1 binds to several transcription factors, such as Scalloped (Sc) and Homothorax (Hth) in *D. melanogaster* and TEAD or TP73 in mammals. In blue: the upstream components. In green: the core proteins. In red: the transcriptional activator Yki/YAP1, which binds to the transcription factors (in orange).

The homologue Hippo components in mammals are very conserved (Saucedo and Edgar, 2007). The large tumor suppressor proteins 1 and 2 (LATS1 and LATS2) are the homologues of Wts; the STE20-like kinases (MST1 and MST2) are the homologues of Hpo; SALVADOR (WW45 or SAV) is the homologue of Sav and MOBKL1A and MOBKL1B (MOB1) are the homologues of Mats. The transcription effectors in mammals are the Yes-associated protein 1 (YAP1) and its paralogue TAZ (Yki homologue) (Lei *et al*., 2008) (Fig. 1). The induction or activation of this pathway in mammals are still not clear, but recent reports suggest the upstream activation by G-protein coupled receptor signalling, which depending of the extracellular stimuli, represses or activates the Hippo pathway (Yu *et al*., 2012). For example, serum-borne lysophosphatidic acid and sphingosine 1-phosphophate inhibit LATSs (LATS1/2) phosphorylation by binding the G12/13-coupled receptors, while glucagon or epinephrine activate the LATS1/2 kinases (Yu *et al*., 2012). Another mechanism of regulation of the Hippo kinase cascade in mammals is via Angiomotin (AMOT), which is an upstream component of the Hippo pathway that binds to Mer/NF2 activating the kinase cascade (Li *et al*., 2015b). Also, E-cadherin and β-catenin regulate the Hippo pathway by activation of Mer/NF2 (Kim *et al*., 2011).

The members of the RAS association domain family (RASSFs) represent further important regulatory proteins of the Hippo kinases (Schagdarsurengin *et al*., 2010). The RASSF members that contain a SARAH (Sav/Rassf/Hpo) interaction domain at the C-terminus, such as RASSF1A, activate the autophosphorylation of the MSTs kinases (MST1/2) (Dittfeld *et al*., 2012; Hwang *et al*., 2007). MSTs and SAV also present a SARAH interaction domain, which is essential for the interaction with regulatory factors such as RASSF1A and Raf1 (O'Neill *et al*., 2004; Schagdarsurengin *et al*., 2010). As indicated in figure 1, the activated MSTs/SAV complex phosphorylates the LATSs kinases (Chan *et al*., 2005). LATSs activate the scaffold protein MOB1 and both together, phosphorylate YAP1 that is a transcriptional regulator (Fig. 1). Active YAP1 translocates into the nucleus (Matallanas *et al*., 2007; Wang *et al*., 2016) and acts as co-activator with several transcription factors, such as TEAD (Zhao *et al*., 2008), SMAD (Grannas *et al*., 2015) or TP73 (Fig. 1) (Matallanas *et al*., 2007; Strano *et al*., 2001). Depending on the cellular context, YAP1 regulates the expression of target genes involved either in cell proliferation or apoptosis by binding to the corresponding transcription factors (Matallanas *et al*., 2007; Zhao *et al*., 2008). The pro-apoptotic function of the Hippo pathway is described in

association with RASSF1A and with the interaction of YAP1 with TP73 by regulating the expression of *BAX* and *BBC3*, also known as *PUMA* (see Fig. 1) (Basu *et al*., 2003; Matallanas *et al*., 2007).

The roles of the phosphorylation and the nuclear translocation of YAP1 are still controversial in the literature. LATSs phosphorylate YAP1 at five serine sites within a HXRXXS consensus motif (Zhao *et al*., 2010a; Zhao *et al*., 2007). Several reports suggest that the phosphorylation in $YAP1^{S127}$ is responsible for the nuclear translocation of YAP1(Matallanas *et al*., 2007; Zhao *et al*., 2007). In contrast, other reports have demonstrated that this phosphorylation site of YAP1 by LATSs is essential for the cytoplasmic retention of YAP1 for further cleavage by 14-3-3 and proteosomal degradation (see Fig. 1) (Basu *et al*., 2003).

1.3 Deregulation of the Hippo pathway in cancer

The Hippo signalling was first described as a tumor suppressor pathway in *D. melanogaster* (Justice *et al*., 1995; Tapon *et al*., 2002; Wu *et al*., 2003). In mammals, some of the components of the Hippo signalling (e.g. NF2, MSTs, LATSs and RASSF1A) are described as tumor suppressor genes, which are deregulated in cancer. For example, the inherited heterozygous mutation of the *NF2* tumor suppressor gene is a risk factor for familial Neurofibromatosis type 2 (Gutmann, 1997; Lallemand *et al*., 2003). The loss of the wild-type allele of *NF2* promotes tumor development in the nervous system and metastasis (Gutmann, 1997; Lallemand *et al*., 2003). In addition, the loss of *NF2* is associated with the destabilisation of adherens junctions, hyperplasia of hepatocytes and the formation of hepatocellular carcinoma (HCC) (Lallemand *et al*., 2003; Zhang *et al*., 2010). The human Hippo kinases MST1/2 are hypermethylated in soft tissue sarcoma (Seidel *et al*., 2007). LATS1/2 are associated with MDM2 and the phosphorylation of $TP53^{S15}$ (Aylon *et al*., 2006; Furth *et al*., 2015). However, LATS1/2 are downregulated by hypermethylation in lung cancer (Sasaki *et al*., 2010). LATS1/2 are also silenced by tumor-specific mutations in non-small cell lung cancer and in esophageal squamous cell carcinoma (Ishizaki *et al*., 2002; Strazisar *et al*., 2009).

The deregulation of the tumor suppressor gene *RASSF1A* and of the proto-oncogene *YAP1* in cancer is well characterised in the literature. RASSF1A regulates the cell cycle progression and induces apoptosis by several mechanisms. For example, RASSF1A regulates the cell cycle by stabilisation of the microtubule network (Dallol *et al*., 2004; Dallol *et al*., 2009; Rong *et al*., 2004) and by inhibiting Cyclin D1 (Agathanggelou *et al*., 2003). RASSF1A regulates cell death by destabilising MDM2 via the interaction with the death-domain-associated protein (Song *et al*., 2008) and by stimulation of modulator of apoptosis (MOAP-1) in response to the presence of active KRAS (Foley *et al*., 2008). Moreover, RASSF1A activates the Hippo signalling by promoting the gene expression of pro-apoptotic genes (Dittfeld *et al*., 2012; Matallanas *et al*., 2007). Thereby the silencing of *RASSF1A* affects cellular stability and diverse pathways. Extensive studies have demonstrated that *RASSF1A* is epigenetically inactivated in several types of cancer including lung (Dammann *et al*., 2000), in pancreatic carcinoma (Dammann *et al*., 2003), prostate (Liu *et al*., 2002), HCC (Schagdarsurengin *et al*., 2003) and Merkel cell carcinoma (Dammann *et al*., 2001; Helmbold *et al*., 2009). *RASSF1A* methylation was suggested as a potential epigenetic biomarker for breast cancer (Shukla *et al*., 2006). In addition, the hypermethylation of *RASSF1A* is associated with poor prognosis in hepatoblastoma and neuroblastoma (Sugawara *et al*., 2007; Yang *et al*., 2004) as well as in metastasis (Liu *et al*., 2005). In contrast to the tumor suppressor RASSF1A, *YAP1* is described as a proto-oncogene in HCC and in gastric cancer (Kang *et al*., 2011; Xu *et al*., 2013). Furthermore, tumor tissues have shown an elevated YAP1 expression compared to normal tissue due to amplification of the *YAP* gene locus (Chr. 11q22) in oral squamous cell carcinoma, primary intracranial ependymomas and glioblastoma (Modena *et al*., 2006; Orr *et al*., 2011; Snijders *et al*., 2005). In lung and in gastric cancer, the amplification of *YAP1* correlates with poor prognosis (Kang *et al*., 2011; Wang *et al*., 2010). The overexpression of *YAP1* is associated with chemoresistance in HCC (Huo *et al*., 2013), in ovarian cancer (Xia *et al*., 2014) and in pancreatic cancer cells (Yuan *et al*., 2016). In addition, YAP1 is involved in tumorigenesis, proliferation and metastasis by interacting as co-factor with TEADs, SMADs and ß-catenin (Grannas *et al*., 2015; Rosenbluh *et al*., 2012; Varelas *et al*., 2010; Zhao *et al*., 2008), inducing among others the expression of pro-proliferative genes such as the *connective tissue growth factor (CTGF)*, *cyclin dependent kinase 6 (CDK6)*, *cysteine-rich angiogenic inducer 61 (CYR61)*, and *c-Myc* (Schutte *et al*., 2014; Xie *et al*., 2013; Zhao *et al*., 2008).

These data suggest that the oncogenic function of YAP1 and the silencing of *RASSF1A* by promoter hypermethylation contribute to the deregulation of the Hippo signalling and hereby promoting cellular instability and tumorigenesis.

1.4 Yes-associated protein 1 (YAP1)

The *Yes-associated protein* (*YAP*) gene is located at the chromosome 11q22. This gene encodes for nine YAP isoforms by differential splicing (Gaffney *et al*., 2012). The major and best-characterised isoform is YAP1, which is the transcriptional activator of the Hippo pathway (Sudol *et al*., 2012). As mentioned before, the function of YAP1 differs depending of the binding to the transcription factors, which either promote or restrict proliferation. YAP1 interacts and binds to several factors such as TEAD (Sudol *et al*., 1995), SMADs (Grannas *et al*., 2015), different isoforms of TP63 and TP73 (Levy *et al*., 2008a; Matallanas *et al*., 2007; Tomlinson *et al*., 2010), ErbB4 (Komuro *et al*., 2003), RUNX (Basu *et al*., 2003) and β-catenin (Rosenbluh *et al*., 2012).

Figure 2: Protein structure of YAP1 with corresponding binding motifs. YAP1 has a length of 504 aminoacids (aa) and a molecular weight of 65 kDa. YAP1 contains a TEAD binding domain (TEAD), a WW motif (WW), a SH3 binding motif (SH3), a transactivation domain (TAD) and PDZ motif (PDZ) with the FLTWL consensus sequence, which is essential for the nuclear translocation of YAP1.

As indicated in figure 2, YAP1 contains a TEAD binding domain between amino acids 47 and 154 at the N-terminus. Between amino acid 74 and 204, YAP1 contains a WW domain to bind PPxY consensus sequences (Sudol *et al*., 1995; Sudol *et al*., 2012). At the carboxyl terminus, YAP1 contains a SH3-binding motif, a transcriptional activation domain (TAD) and a PDZ binding motif (Fig. 2) (Oka *et al*., 2010; Sudol *et al*., 1995; Sudol *et al*., 2012). The PDZ domain contains a FLTWL motif that is essential for the nuclear translocation of YAP1 (Oka *et al*., 2010). The binding of YAP1 to the different transcription factors is essential for the expression of pro-proliferative or of pro-apoptotic genes. Both the TEAD binding domains and the PDZ binding motif are necessary for the interaction between YAP1 and TEAD (Li *et al*., 2010; Sudol *et al*., 2012). The YAP1/TEAD complex regulates

the expression of *CTGF, AJUBA* and *ankyrin repeat domain protein 1* (*ANKRD1*) (Zanconato *et al*., 2015). YAP1 is also involved in the regulation of the target genes of the ErbB4 tyrosin kinase (Komuro *et al*., 2003). The ErbB4 receptor is a membrane associated tyrosine kinase. After activation of the tyrosine kinase, the C-terminus of ErbB4 is cleavaged and interacts with the WW domain of YAP1 (Komuro *et al*., 2003). The complex consisting of YAP1 and the fragment of ErbB4 translocate into the nucleus to regulate the gene expression of the target genes (Komuro *et al*., 2003). The WW domain is also important for the interaction of YAP1 with TP73 and with RUNX (Basu *et al*., 2003; Strano *et al*., 2001).

The stability, cellular localization and function of YAP1 are modulated by phosphorylation. LATS1/2 are the main regulators of YAP1. LATS1/2 interact with YAP1 through PPxY consensus sequence in the WW domain (Hao *et al*., 2008; Macias *et al*., 2002). LATS1/2 phosphorylate YAP1 in a HXRXXS context in S61, S109, S127, S164 and S381 (Zhao *et al*., 2010a; Zhao *et al*., 2007). Three of the LATSs phosphorylation sites are located in the TEAD domain of YAP1. In addition, other components of the Hippo pathway such as AMOT and the LIM protein AJUBA also indirectly regulate YAP1 by regulation of LATS1/2 (Das Thakur *et al*., 2010; Paramasivam *et al*., 2011; Zhao *et al*., 2011). In addition, YAP1 is phosphorylated by c-Abl on Y357 in response to DNA damage, thereby increasing the affinity of YAP1 to TP73 (Keshet *et al*., 2015; Levy *et al*., 2008a). In contrast, the protein kinase B (Akt) phosphorylates YAP^{S127} to induce the interaction with 14-3-3 and the further degradation of YAP1 (Basu *et al*., 2003). In recent years, a crosstalk between YAP1 and the MAPK signalling has been described. For example, MAPK8 (JNK1) and MAPK9 (JNK2) phosphorylate YAP1 at T119, S138, T154, S317 and T362 (Tomlinson *et al*., 2010). The phosphorylation of YAP1 by the MAPKs stabilises the interaction of YAP1 to ΔNp63, regulating the UV-induced apoptosis (Tomlinson *et al*., 2010). The regulation of YAP1 by MAPKs has also been associated with the oncogenic function of YAP1 in gastric cancer, in cholangiocellular tumors, gallbladder tumors (Kang *et al*., 2011; Li *et al*., 2014; Li *et al*., 2015a), and in association with the oncogenic KRAS in pancreatic ductal adenocarcinoma (Kapoor *et al*., 2014; Zhang *et al*., 2014). Other kinases that phosphorylate YAP1 are ERK2, PKCα, MAPK (p38) and CK1 (Muranen *et al*., 2016; Tomlinson *et al*., 2010; Zhao *et al*., 2010b).

1.5 RAS association domain family (RASSF)

The RAS association domain family is composed of ten members, also known as RASSF1 to RASSF10. The RASSFs are described as a family of tumor suppressor genes, which are frequently silenced in cancer (Richter *et al*., 2009). The RASSFs are involved in microtubule stabilisation, apoptosis and in the regulation of the cell cycle (Richter *et al*., 2009; Rong *et al*., 2004; Song *et al*., 2009b). This gene family is distributed in two subgroups, according to the localization of the Ras-association domain (RA). RASSF1, RASSF2, RASSF3, RASSF4, RASSF5 and RASSF6 contain the RA domain at the carboxyl terminus (C-terminal RASSFs), wheras RASSF7, RASSF8, RASSF9 and RASSF10 present the RA domain at the amino terminus (N-terminal RASSFs). The RA, or *RalGDS/AF-6,* domain is characteristic for the Ras effectors and Ras-related GTPases (Dammann *et al*., 2000). Another feature that differs between the subgroups is the presence of the SARAH domain, which is only found in the C-terminal RASSFs (Schagdarsurengin *et al*., 2010). The SARAH domain is a protein-protein interaction domain, which allows e.g. the interaction between the members of the C-terminal RASSFs and the SARAH domain of MSTs and SALVADOR (Dittfeld *et al*., 2012; Schagdarsurengin *et al*., 2010). The RASSF members also contain a protein kinase C conserved region, or C1 domain, and the ATM domain with putative phosphorylation sites for ATM kinase (ataxia telangiectasia mutated) (Richter *et al*., 2009). As example, the protein structure of RAS association domain family 1 (RASSF1A) is indicated in figure 3.

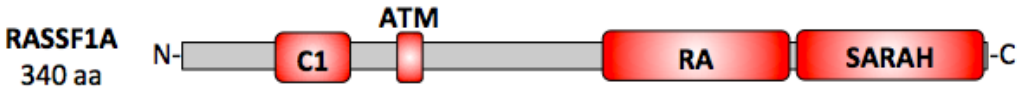

Figure 3: Protein structure of RASSF1A with corresponding binding motifs. RASSF1A has a length of 340 amino acids (aa) and a molecular weight of 40 kDa. RASSF1A contains a protein kinase C motif (C1), an ATM domain (ATM) with putative phosphorylation sites for ATM kinase, a RA domain (RA) and the SARAH (Sav/Rassf/Hpo) domain at the carboxyl terminus, which mediates the interaction between RASSF1A and the MSTs.

In the year 2000, Dammann *et al.* identified RASSF1 by yeast-two-hybrid screens through its interaction with XPA, a DNA excision repair protein (Dammann *et al*., 2000). The *RASSF1* gene is located on chromosome 3p21.3 and contains eight exons. The *RASSF1* gene encodes for seven isoforms, which are transcribed by splicing using two alternative

promoters (1α and 2γ) (Dammann *et al*., 2000; Richter *et al*., 2009). The main isoforms with a biological relevance are RASSF1A and RASSF1C. Both isoforms have opposing functions in cancer. The isoform RASSF1A is the best-investigated RASSF member and, as previously described, it is frequently inactivated in cancer cells by promoter hypermethylation (CpG island of promoter 1α). In contrast, in the literature the RASSF1C isoform has been described to promote proliferation and metastasis in cancer (Amaar *et al*., 2006; Reeves *et al*., 2013).

RASSF1A co-localizes with tubulin and among its principal functions are microtubule stabilisation (Dallol *et al*., 2004; Rong *et al*., 2004), inhibition of cell cycle progression (Rong *et al*., 2007) and activation of the Hippo pathway (Dittfeld *et al*., 2012). RASSF1A regulates the cell cycle by several mechanisms, for example by repression of Cyclin A2 and Cyclin D1 (Ahmed-Choudhury *et al*., 2005; Shivakumar *et al*., 2002). RASSF1A, together with Aurora A, modulates the CDC20/anaphase-promoting complex (Liu *et al*., 2008; Song *et al*., 2009b). In this study, the function of the RASSF1A isoform in the regulation of the Hippo signalling was analysed. RASSF1A activates the Hippo signalling through the SARAH domain (Dittfeld *et al*., 2012). The proto-oncogene Raf1 inhibits the activation of MST2 by sequestering and binding to the SARAH domain of MST2 (O'Neill *et al*., 2004). The Raf1-MST2 complex is dissociated by RASSF1A, which allows the binding of RASSF1A to MST2 and the activation of the Hippo kinase cascade (Matallanas *et al*., 2007). Moreover, other reports have suggested that RASSF1A triggers the translocation of YAP1 into the nucleus, stabilises the interaction of YAP1 with TP73 and regulates the expression of the pro-apoptotic genes *BBC3* and *BAX* (Levy *et al*., 2008a; Matallanas *et al*., 2007; Strano *et al*., 2001).

In contrast to RASSF1A, the other C-terminal RASSFs are poorly investigated. To date RASSF1A, RASSF2 and RASSF5 are directly associated with the activation of both MSTs (Cooper *et al*., 2009; Ni *et al*., 2013; Praskova *et al*., 2004; Schagdarsurengin *et al*., 2010; Song *et al*., 2010). RASSF2 is silenced for example in thyroid cancer (Schagdarsurengin *et al*., 2010), in gastric cancer (Maruyama *et al*., 2008) and in pheochromocytoma (Richter *et al*., 2015). RASSF5 has been identified as a tumor suppressor e.g. in osteosarcoma cells in association with the Hippo pathway (Zhou *et al*., 2014) and in association with TP53 (Calvisi *et al*., 2009; Donninger *et al*., 2015).

1.6 Ankyrin repeat domain protein 1 (ANKRD1)

The ankyrin repeat domain protein 1 (ANKRD1) was first described as a nuclear protein in cardiomyocytes and to be important for heart development, transcriptional regulation and stretch sensing (Cinquetti *et al*., 2008; Ishiguro *et al*., 2002; Jeyaseelan *et al*., 1997; Mikhailov and Torrado, 2008). The *ANKRD1* gene, also known as *CARP (cardiac ankyrin repeat protein),* is a target gene of YAP1 (Li *et al*., 2013; Zanconato *et al*., 2015). Other factors that regulated the gene expression of *ankrd1* in mice are Nkx2, Gata-4 and Sp3 (Chen *et al*., 2012; van Loo *et al*., 2007; Zou *et al*., 1997).

Figure 4: Protein structure of ANKRD1 with corresponding binding motifs. ANKRD1 has a length of 319 amino acids (aa) and a molecular weight of 40 kDa. ANKRD1 contains a coil-coil domain (CC), a PEST domain for the proteasomal degradation and four ankyrin interaction motifs (ANK).

ANKRD1 is located both in the nucleus as well as at the Z-disc complexes in skeletal and heart muscle cells (Ishiguro *et al*., 2002). As indicated in figure 4, ANKRD1 contains a coil-coil domain and a PEST motif, which is important for the proteasomal degradation and four ankyrin motifs of 33 amino acids each (Fig. 4) (Badi *et al*., 2009; Mikhailov and Torrado, 2008; Mosavi *et al*., 2004). *In silico* prediction analyses suggest that ANKRD1 also contains a caspase-3 cleavage site, a nuclear localization signal, a nuclear export signal and several putative phosphorylation and glycosylation sites (Mikhailov and Torrado, 2008). The ankyrin motifs are protein-protein interaction domains, which are observed in several proteins such as in the members of the INK4 family of tumor suppressor genes and in the tumor suppressor 53 binding protein 2 (Mosavi *et al*., 2004). ANKRD1 is a key player for the stress response in cardiomyocytes by interaction with TITIN, DESMIN, YB1, MYPN and CASQ2 (Mikhailov and Torrado, 2008; Miller *et al*., 2003; Torrado *et al*., 2005). Other interaction partners of ANKRD1 are p50 (subunit of NF-kappa β) (Liu *et al*., 2015; Mohamed and Boriek, 2012), nucleolin (Almodovar-Garcia *et al*., 2014), myopalladin (Ishiguro *et al*., 2002) and TP53 (Kojic *et al*., 2010).

The function of ANKRD1 is still under investigation and there are few reports in the literature about its role in cancer. In mice, *ankrd1* knockout resulted in a complete lack of phenotype (Barash *et al*., 2007). ANKRD1 is a transcriptional co-factor that negatively regulates the expression of cardiac genes (Jeyaseelan *et al*., 1997). Mutations and the deregulation in the expression of *ANKRD1* are associated with cardiomyopathies and heart anomalies (Arimura *et al*., 2009; Bogomolovas *et al*., 2015; Crocini *et al*., 2013; Duboscq-Bidot *et al*., 2009; Torrado *et al*., 2006). ANKRD1 is the transcriptional regulator of *MMP13* and *MMP10* (Almodovar-Garcia *et al*., 2014). In cancer, *ANKRD1* has been described as possible proto-oncogene in intestinal tumorigenesis in association with the WNT pathway and with TGF-β signalling (Labbe *et al*., 2007). In ovarian cancer, ANKRD1 negatively regulates the cellular response to cisplatin and chemotherapy (Lei *et al*., 2015; Scurr *et al*., 2008). In contrast, ANKRD1 acts a potential tumor suppressor gene in HCC by fenretinide-induced apoptosis (Park *et al*., 2005) and in rhabdomyosarcomas (Ishiguro *et al*., 2002). In 2005, Han *et al.* observed that ANKRD1 together with GADD153, is involved in hypoxia-induced apoptosis (Han *et al*., 2005). Recently ANKRD1 is related with the TP53 and with the JNK-mediated apoptosis in mice cardiomyocytes (Mazelin *et al*., 2016; Shen *et al*., 2015). Other reports suggest ANKRD1 to be a co-activator of TP53 and thereby induce the expression of *CDKN1A* and *BAX* (Kojic *et al*., 2010; Shen *et al*., 2015).

Aims of this study

The Hippo pathway has been described as a pro-apoptotic kinase cascade that is activated by the tumor suppressor gene RASSF1A for regulation the transcriptional function of YAP1. The function of the transcriptional regulator YAP1 depends on the binding to specific transcription factors. There is evidence suggesting that RASSF1A regulates the apoptotic function of the Hippo pathway by promoting and stabilising the binding of YAP1 to the tumor suppressor gene TP73 and the subsequent transcriptional regulation of the pro-apoptotic genes. However, the mechanism behind the apoptotic function of the Hippo pathway needs to be elucidated in more detail. Therefore, the main purpose of this study was the identification and the functional characterisation of YAP1 target genes that are co-regulated by the tumor suppressor gene RASSF1A.

In order to analyse the regulatory function of RASSF1A on the YAP1 target genes, the following secondary aims were proposed for this study:

- Create and characterise a YAP1-inducible cell system.
- Conduct a comparative whole transcriptome study using the YAP1-inducible system after expression of RASSF1A.
- Identify novel candidate target genes for validation, which are regulated by RASSF1A and YAP1, taking into account the fold expression change and the biological function.
- Validate the expression level of the principal candidate genes by qRT-PCR.
- Confirm these results with another method such as promoter assays and western blotting.
- Perform functional analyses of the best candidate gene such as colony formation assays, overexpression and promoter assays.
- Clarify the transcriptional function of the other C-terminal RASSFs in the regulation of the novel target genes compared to the RASSF1A mediated regulation.

2. MATERIALS AND METHODS

2.1 MATERIALS

2.1.1 List of Materials

2.1.1.1 Chemicals

5'-Aza-2'-desoxycytidine	Sigma-Aldrich Chemie GmbH, Steinheim, Germany
Acrylamide	Merck KGaA. Darmstadt, Germany
Agar agar	Merck KGaA. Darmstadt, Germany
Agarose beads with FLAG	Sigma-Aldrich Chemie GmbH, Steinheim, Germany
Ammonium persulfate (APS)	Serva electrophoresis GmbH, Heidelberg, Germany
Agarose	Biozym Scientific GmbH, Oldendorf, Germany
Bacto trypton	Becton Dickinson and company, France
Boric acid	Sigma-Aldrich Chemie GmbH, Steinheim, Germany
Bovine serum albumin (BSA)	Thermo Scientific, Schwerte, Germany
Bromphenol blue	Carl Roth GmbH, Karlsruhe, Germany
β-Mercaptoethanol	Sigma-Aldrich Chemie GmbH, Steinheim, Germany
Chloroform	Carl Roth GmbH, Karlsruhe, Germany
Complete protease inhibitor mix	Roche GmbH, Mannheim, Germany
DAPI	Serva electrophoresis GmbH, Heidelberg, Germany
DEPC water	Carl Roth GmbH, Karlsruhe, Germany
Dulbecco's modified Eagle Medium (DMEM)	GIBCO®, Life Technologies GmbH, Darmstadt, Germany
Dimethylsulfoxide (DMSO)	Sigma-Aldrich Chemie GmbH, Steinheim, Germany
Disodium hydrogen phosphate	Carl Roth GmbH, Karlsruhe, Germany
dNTPs	Thermo Scientific, Schwerte. Germany
EDTA	Carl Roth GmbH, Karlsruhe, Germany
Ethanol	Merck KGaA. Darmstadt, Germany
Ethidium bromide	Carl Roth GmbH, Karlsruhe, Germany
Fetal calf serum (FCS)	PAA Laboratories GmbH, Cölbe, Germany
Fetal calf serum tetracycline free (FCS for Tet-On cells)	Biochrom GmbH, Merck KGaA. Darmstadt, Germany
Formaldehyde	Carl Roth GmbH, Karlsruhe, Germany
Formamide	Carl Roth GmbH, Karlsruhe, Germany
Giemsa	Sigma-Aldrich Chemie GmbH, Steinheim, Germany
Glucose	Carl Roth GmbH, Karlsruhe, Germany

Glycerol	Carl Roth GmbH, Karlsruhe, Germany
Glycine	Carl Roth GmbH, Karlsruhe, Germany
Glycogen	Sigma-Aldrich Chemie GmbH, Steinheim, Germany
HEPES	Carl Roth GmbH, Karlsruhe, Germany
Immobilon Western Chemiluminescent HRP substrate	Millipore GmbH, Schwalheim, Germany
Hydrochloric acid	Carl Roth GmbH, Karlsruhe, Germany
Hydroquinone	Merck KGaA. Darmstadt, Germany
Isopropyl alcohol	Merck KGaA. Darmstadt, Germany
Magnesium chloride	Merck KGaA. Darmstadt, Germany
Methanol	Merck KGaA. Darmstadt, Germany
Milk powder	Carl Roth GmbH, Karlsruhe, Germany
NP40	AppliChem GmbH, Darmstadt, Germany
Opti-MEM®	GIBCO®, Invitrogen GmbH, Karlsruhe, Germany
OrangeG	Carl Roth GmbH, Karlsruhe, Germany
Phosphate buffered saline (PBS)	GIBCO®, Invitrogen GmbH, Karlsruhe, Germany
Phenol	Carl Roth GmbH, Karlsruhe, Germany
Phenol/Chloroform/Isoamyl alcohol	Carl Roth GmbH, Karlsruhe, Germany
Propidium iodide	Sigma-Aldrich Chemie GmbH, Steinheim, Germany
Protein A agarose beads	Calbiochem, Merck, Darmstadt, Germany
RPMI	GIBCO®, Life Technologies GmbH, Darmstadt
Sodium acetate	Merck KGaA. Darmstadt, Germany
Sodium chloride	Carl Roth GmbH, Karlsruhe, Germany
Sodium dodecylsulfate (SDS)	Carl Roth GmbH, Karlsruhe, Germany
Sodium deoxycholate	Sigma-Aldrich Chemie GmbH, Steinheim, Germany
Sodium dihydrogen phosphate	Carl Roth GmbH, Karlsruhe, Germany
Sodium metabisulfite	Sigma-Aldrich Chemie GmbH, Steinheim, Germany
SYBR® Select Master Mix	Life Technologies GmbH, Darmstadt, Germany
TEMED	Carl Roth GmbH, Karlsruhe, Germany
Tris base	Carl Roth GmbH, Karlsruhe, Germany
Triton X100	Carl Roth GmbH, Karlsruhe, Germany
TRIzol®	GIBCO®, Invitrogen GmbH, Karlsruhe, Germany
Tween20	Sigma-Aldrich Chemie GmbH, Steinheim, Germany
Yeast extract	Carl Roth GmbH, Karlsruhe, Germany

2.1.1.2 Size and molecular weight standards

100 bp DNA ladder	Thermo Scientific, Schwerte, Germany
1 kb DNA ladder	Thermo Scientific, Schwerte, Germany
PageRuler Prestained protein ladder	Thermo Scientific, Schwerte, Germany

2.1.1.3 Antibiotics

Ampicillin	Sigma-Aldrich Chemie GmbH, Steinheim
Blasticidin	Invitrogen Life technologies GmbH, Darmstadt
Chloramphenicol	Sigma-Aldrich Chemie GmbH, Steinheim
Doxycycline	Invitrogen Life technologies GmbH, Darmstadt
Kanamycin	Applichem GmbH, Darmstadt
Geneticin (G418)	Biochrom, Berlin
Penicillin (10 U/µl)/ Streptomycin (10 µg/µl) solution	GIBCO®, Invitrogen GmbH, Karlsruhe
Zeocin	Invitrogen Life technologies GmbH, Darmstadt

2.1.1.4 Transfection reagents

JetPei	Polyplus-Transfection SA, Illkrich, France
Lipofectamine™	Invitrogen Life technologies GmbH, Darmstadt, Germany
Lipofectamine® RNAiMAX	Invitrogen Life technologies GmbH, Darmstadt, Germany
Polyethylenimine (PEI)	Polyplus-Transfection SA, Illkrich, France
Turbofect	Thermo Scientific, Schwerte, Germany
X-tremeGENE HP	Roche Applied Science, Mannheim, Germany
X-tremeGENE 9	Roche Applied Science, Mannheim, Germany

2.1.1.5 Enzymes

DNaseI (1U/µl)	Thermo Scientific, Schwerte, Germany
FastAP, thermosensitive (1 U/µl)	Thermo Scientific, Schwerte, Germany
Methyltransferase *SssI* (20 U/µl)	New England BioLabs, Schwalbach
MMLV Reverse Transcriptase (200 U/µl)	Promega GmbH, Mannheim, Germany
Proteinase *K* (20 µg/µl)	Thermo Scientific, Schwerte, Germany
Ribolock (40U/µl)	Thermo Scientific, Schwerte, Germany

RNaseA (10 µg/µl)	Thermo Scientific, Schwerte, Germany
SAM	New England BioLabs, Schwalbach, Germany
T4 DNA Ligase (3 U/µl)	Thermo Scientific, Schwerte, Germany
Taq-DNA-Polymerase	AG Dammann. Isolated from an *E. coli* strain expressing Taq- polymerase
TrypLE ^{TM} Express (Trypsin)	GIBCO®, Invitrogen GmbH, Karlsruhe, Germany

Restriction endonucleases

BglII	Thermo Scientific, Schwerte, Germany
BamHI	Thermo Scientific, Schwerte, Germany
HindIII	Thermo Scientific, Schwerte, Germany
SalI	Thermo Scientific, Schwerte, Germany
TaqI	Thermo Scientific, Schwerte, Germany
XhoI	Thermo Scientific, Schwerte, Germany
XmaI	Thermo Scientific, Schwerte, Germany

2.1.1.6 Kits and microarrays

CloneJET PCR cloning kit	Thermo Scientific, Schwerte, Germany
Dual Luciferase® Reporter Assay System	Promega, Heidelberg, Germany
EZ DNA Methylation kit	Zymo Research, USA
GFP-Trap®	ChromoTek GmbH, Planegg-Martinsried, Germany
MSB®Spin PCRapace	Invitek GmbH, Berlin, Germany
NucleoSpin® Extract II	Macherey-Nagel GmbH, Düren, Germany
NucleoSpin® Plasmid QuickPure	Macherey-Nagel GmbH, Düren, Germany
NucleoBond® Xtra Midi	Macherey-Nagel GmbH, Düren, Germany
QIAquickChange Lightning	Agilent, USA
Gene Chip® human gene 2.0 ST arrays	Affymetrix, UK
GeneChip WT terminal labeling and controls reagent kit	Affymetrix, UK

2.1.1.7 Antibodies for western blots

Table 1. List of antibodies and the corresponding dilution.

Name	Dilution	Company
ANKRD1 (H-120) rabbit polyclonal IgG	1:500	Santa Cruz Biotechnology, Santa Cruz, Inc., CA, USA
BAX (06-499) rabbit polyclonal IgG	1:1000	EMD Millipore, Massachusetts, USA
GAPDH (FL-335) rabbit polyclonal IgG	1:2000	Santa Cruz Biotechnology, Santa Cruz, Inc., CA, USA
GFP rabbit polyclonal IgG	1:2000	AG Renkawitz (University of Giessen, Institute for Genetic)
Flag (M2) mouse monoclonal IgG	1:1000	Santa Cruz Biotechnology, Santa Cruz, Inc., CA, USA
MDM2 (Ab-2) mouse monoclonal IgG	1:1000	Calbiochem® Merck KGaA. Darmstadt, Germany
mp53 (1C12) mouse polyclonal IgG	1:1000	New England BioLabs, Schwalbach, Germany
HRP (goat anti-rabbit/ mouse, IgG HRP-conjugated)	1:2000	Santa Cruz Biotechnology, Santa Cruz, Inc., CA, USA
YAP1 (H-125) rabbit polyclonal IgG	1:200	Santa Cruz Biotechnology, Santa Cruz, Inc., CA, USA

2.1.1.8 Vectors

The expression and luciferase reporter vectors used in this project were verified by restriction digestion and sequencing.

Table 2. List of vectors used in this study.

Vector name	Resistance	Manufacturer	Remark
pCMV-Flag-Tag1	Kanamycin	Addgene, England	empty vector
pCMV-Flag-RASSF1A	Kanamycin	AG Dammann (University of Giessen. Institute for Genetic)	
pCMV-RASSF1A-ΔSARAH	Kanamycin	AG Dammann	depletion of SARAH domain
pCMV-Flag-RASSF2A	Kanamycin	AG Dammann	
pCMV-Flag-RASSF3	Kanamycin	AG Dammann	
pCMV-Flag-RASSF4A	Kanamycin	AG Dammann	
pCMV-Flag-RASSF5A	Kanamycin	AG Dammann	
pCMV-Flag-RASSF6A	Kanamycin	AG Dammann	
pCMV-Flag-YAP1	Kanamycin	AG Dammann	

pCMV-YAP1-T119A	Kanamycin	Jiménez. AG Dammann	Pointmutation
pCMV-YAP1-S127A	Kanamycin	Jiménez. AG Dammann	Pointmutation
pCMV-YAP1-S138A	Kanamycin	Jiménez. AG Dammann	Pointmutation
pCMV-YAP1-S127E	Kanamycin	Goetze. AG Dammann	Pointmutation
pDNR-LIB-ANKRD1	Chloramphenicol	Biocat BC018667	cloning vector *ANKRD1* cloned via SfiI (introduction of *BglII* site 9 bp before the TSS)
pCMV-Flag-ANKRD1	Kanamycin	Jiménez. AG Dammann	Cloned from pDNR-LIB-ANKRD1 via *BglII/XhoI*
pcDNA3	Ampicillin	AG Dammann	empty vector
pcDNA3-p73	Ampicillin	AG Stiewe (University of Marburg. IMT)	
pcDNA3-deltap73	Ampicillin	AG Stiewe	
pcDNA3.1-mCherry	Ampicillin	AG Dammann	empty vector
mCherry-YAP1	Ampicillin	Jiménez. AG Dammann	cloned from pCMV-Flag-YAP1 via *BglII/BamHI*
mCherry-YAP1-T119A	Ampicillin	Jiménez. AG Dammann	pointmutation
mCherry-YAP1-S127A	Ampicillin	Jiménez. AG Dammann	pointmutation
mCherry-YAP1-S138A	Ampicillin	Jiménez. AG Dammann	pointmutation
mCherry-YAP1-S127E	Ampicillin	Goetze. AG Dammann	pointmutation
pcDNA-Myc	Ampicillin	AG Dammann	
pcDNA-Max	Ampicillin	AG Dammann	
pcDNA4TO-Myc	Zeocin	Thermo Fisher Scientific, Germany	empty vector
pcDNA4TO-Flag-ANKRD1	Zeocin	Jiménez. AG Dammann	Cloned from pCMV-Flag-ANKRD1 via *BamHI/XhoI* and *BglII/XhoI*
pcDNA4TO-YAP1	Zeocin	Jiménez. AG Dammann	cloned via *BglII*
pEGFP-C2	Kanamycin	Clontech Inc., France	empty vector
pEYFP-C2	Kanamycin	Clontech Inc., France	empty vector
pEGFP-RASSF1A	Kanamycin	AG Dammann	
pEYFP-RASSF1A	Kanamycin	AG Dammann	
pEYFP-RASSF2A	Kanamycin	AG Dammann	
pEYFP-RASSF3	Kanamycin	AG Dammann	
pEYFP-RASSF4A	Kanamycin	AG Dammann	
pEYFP-RASSF5A	Kanamycin	AG Dammann	
pEYFP-RASSF6A	Kanamycin	AG Dammann	
pEYFP-MST1	Kanamycin	AG Dammann	

pEYFP-MST2	Kanamycin	AG Dammann	
pEGFP-ANKRD1	Kanamycin	Traum. AG Dammann	cloned from pCMV-Flag-ANKRD1 via *BglII/XhoI* *BglII/SalI*
pEYFP-ANKRD1	Kanamycin	Traum. AG Dammann	cloned pCMV-Flag-ANKRD1 via *BglII/XhoI* *BglII/SalI*
pEGFP-p53	Kanamycin	AG Schmitz (University of Giessen. Department of Biochemistry)	
pEGFP-lamin B1	Kanamycin	AG Dobreva (MPI Bad Nauheim)	
pEYFP-YAP1	Kanamycin	Jiménez. AG Dammann	cloned from pCMV-Flag-YAP1 via *BglII/BamHI*
pEYFP-YAP1-T119A	Kanamycin	Jiménez. AG Dammann	pointmutation
pEYFP-YAP1-S127A	Kanamycin	Jiménez. AG Dammann	pointmutation
pEYFP-YAP1-S138A	Kanamycin	Jiménez. AG Dammann	pointmutation
pEYFP-YAP1-S127E	Kanamycin	Goetze. AG Dammann	pointmutation
pJET1.2/blunt	Ampicillin	Thermo Scientific, Germany	cloning vector
pJet-ANKRD1promoter	Ampicillin	Jiménez. AG Dammann	cloning vector
pRL-null (renilla luciferase)	Ampicillin	Promega, Germany	luciferase vector
pRL-ANKRD1 (renilla luciferase)	Ampicillin	Traum. AG Dammann	luciferase vector cloned from pJet-ANKRD1promoter via *HindIII/XmaI*
pRL-RASSF1A 0.5 kb (renilla luciferase)	Ampicillin	AG Dammann	luciferase reporter vector
pRL-RASSF1A 2.3 kb (renilla luciferase)	Ampicillin	AG Dammann	luciferase vector
pGL2-basic (firefly luciferase)	Ampicillin	AG Schmitz	luciferase vector
pGL3 (firefly luciferase)	Ampicillin	AG Dammann	luciferase vector
pGL-BAX (firefly luciferase)	Ampicillin	AG Schmitz	luciferase vector
pGL-MDM2 (firefly luciferase)	Ampicillin	AG Schmitz	luciferase vector
pGL-p21 (firefly luciferase)	Ampicillin	AG Schmitz	luciferase vector
pGL-p53 synthetic TP53 target sites (13x) (firefly luciferase)	Ampicillin	AG Schmitz	luciferase vector

2.1.1.9 Chemically- competent *E. coli* strains

The following *E. coli* strains were used for plasmid amplification.

Table 3. List of *E. coli* strains.

Strain	Genotype	Company
DH5α	supE44 lacU (80lacZM15) hsdR17 recA endA1 gyrA96 thi-1 relA1	ATCC53868
TAM I	mcrA D(mrr-hsdRMS-mcrBC) F80lacZDM15 DlacX74 recA1 araD139 (ara-leu)7697 galU galK rpsL endA1 nupG	Active Motif, Rixensart, Belgien
XL10-Gold	TetrD(*mcrA*)*183* D (*mcrCB-hsdSMR-mrr*)*173 endA1 supE44 thi-1 recA1 gyrA96 relA1 lac* Hte, F´ *proAB lacI*qZD*M15* Tn*10* (Tetr) Amy Camr	Stratagene**,** Agilent Technologies, Germany

2.1.1.10 Human cell lines

During this study, the following cell lines were used for transfections, colony formation, DNA and RNA isolation (see Table 4). The cells were cultivated at 37°C under 5% CO_2 concentration with the appropriate media containing 10% FCS and 1% penicillin and streptomycin (PS). The TREx293 cells were cultivated in DMEM with 1% PS and 10% FCS tetracycline free serum. The cells were stored in DMEM or RPMI media with 10% DMSO in liquid nitrogen.

Table 4. Human cell lines.

Cell line	Origin	Medium
A427	non-small cell lung cancer	RPMI
A549	lung adenomacarcinoma	DMEM
Buf1280	Melanoma	DMEM
C8161	malignant melanoma	DMEM
H322	bronchioalveolar carcinoma	RPMI
H358	bronchioalveolar carcinoma	RPMI
HEK293T	human embryonic kidney cells	DMEM
HeLa	cervical carcinoma	DMEM
IGR-1	metastasis from malignant melanoma	DMEM
LNCaP	prostate carcinoma	RPMI
MCF-7	breast adenocarcinoma	RPMI
MeWo	Melanoma	DMEM
Sk-Mel13	Melanoma	DMEM
Sk-Mel28	Melanoma	DMEM
T47D	breast cancer	DMEM
TREx293	embryonic kidney cells expressing Tet repressor, *YAP1* or *ANKRD1* in tetracycline dependent manner	DMEM

2.1.1.11 Hepatic primary tumors and normal liver tissues

Primary human liver cancer and matching normal tissue samples used for methylation analysis were obtained from patients of the City of Hope Medical Center (Duarte, CA, USA.) or from the University of Halle-Wittenberg (Steinmann *et al*., 2011). The local committee of medical ethics and the patients approved the use. Samples names: 2800 (T/N), 2844 (T/N), 974 (T/N), 1117 (T/N), 3084 (T/N). T=Tumor. N=Normal liver tissue.

2.1.2 Primers

During this study, the following primers were used (Table 5 - Table 9). All primers were provided desalted by Life Technologies GmbH. They were dissolved in DEPC water to a stock concentration of 100 µM, after that they were diluted and mixed to primer mix solutions with the forward and reverse primers each at 10 µM concentration for CoBRA and semiquantitative PCRs and at 2 µM concentration for quantitative real time PCR. The primer pairs for CoBRA and semiquantitative PCRs were optimized with respect to the annealing temperature during PCR (55°C to 62°C).

Table 5. Sequencing primers.

Primer name	Sequence (5´-3´)
EGFPSeqU	*GCCGCCGGGATCACTCTCG*
PCMV	*GCGGTAGGCGTGTACGG*
T7	*TAATACGACTCACTATAGGG*
Mcherryseq1	*GAACGCGCCGAGGGCCG*

Table 6. Primers for *ANKRD1* promoter region.

Primer name	Sequence (5´-3´)	Product size
ANKRD1UHD3	*AAGCTTCATGTCATGTGCTAATTATGGCCAG*	606 bp
ANKRD1LXma	*TCCAACCCGGGAACCGAAGTAACACTCC*	

Table 7. Primers for CoBRA.

Primer name	**Sequence (5´-3´)**	**Product size** (annealing temperature)
ANKRD1BSU1	*AAGGAATTTTTGGAGTTGGTTTTGT*	139 bp (56°C)
ANKRD1BSL1	*CACCTACCTCTAAATTAACTCCTAATAAAAA*	
MU379 (for *RASSF1A*)	*GTTTTGGTAGTTTAATGAGTTTAGGTTTTTT*	
ML730 (for *RASSF1A. 1st PCR*)	*ACCCTCTTCCTCTAACACAATAAAACTAACC*	(55 °C)
ML561 (for *RASSF1A 2nd PCR*)	*CCCCACAATCCCTACACCCAAAT*	205 bp (54 °C)

Table 8. Primers for semi- and quantitative real-time PCR.

Primer name	**Sequence (5´-3´)**	**Product size** (annealing temperature)
ANKRD1RTF1	*AGCGCCCGAGATAAGTTGCT*	240 bp (60°C)
ANKRD1RTR1	*CACCAGATCCATCGGCGTCT*	
BaxRTF	*AACTGGGGCCGGGTTGTCGC*	196 bp (62°C)
BaxRTRew	*CGCGGTGGTGGGGGTGAGG*	
CTGFRTF1	*CATCTTCGGTGGTACGGTGT*	295 bp (62°C)
CTGFRTR1	*GACCAGGCAGTTGGCTCTAA*	
UGAP389	*TGGAGAAGGCTGGGGCTCAT*	176 bp (60°C)
LGAP545	*GACCTTGGCCAGGGGTGCTA*	
PUMARTFW	*GCGGCGGATGGCGGACGA*	188 bp (60°C)
PUMARTRW	*CTGACGTCCACCGGGCGGGT*	
p21RTF	*CCTTGTGCCTCGGTCAGGGGAG*	183 bp (62°C)
p21RTR	*GGCCCTCGCGCTTCCAGGAC*	
P53RTU1	*TCAGATCCGTGGGCGTGAGCG*	235 bp (62°C)
P53RTL1	*GGGGGTGGGAGGCTGTCAGTGG*	
UHE2ab	*GGCTGGGAACCCGCGGTG*	239 bp (60°C)
L27111	*TCCTGCAAGGAGGGTGGCTTCT*	
YAP1RTFW1	*TGTCTTCTCCCGGGATGTCTCAGG*	215 bp (62°C)
YAP1RTRW1	*TGAGGGCAGGGTGCTTTGGTTG*	
MDM2RTF1	*ATCAGGCAGGGGAGAGTGAT*	288 bp (62°C)
MDM2RTR1	*CCTCAACACATGACTCTCTGGA*	
AJUBARTF1	*GGATGGCATCCCCTTCACAGTGG*	196 bp (60°C)
AJUBARTR1	*CATCCGGCAGTCCTCACAGTGGT*	
U148P16	*GCTGCCCAACGCACCGAATAGT*	157 bp (60°C)
L287P16	*CTCCCGGGCAGCGTCGTG*	
P73RTFW	*CAGCAGCCACAGCGCCCAGTC*	191 bp (60°C)
P73RTRW	*GGGCCCCCAGGTCCTCAATGG*	
RSF2ARTF	*TCCTCCAGGGCCCATGTGAGC*	237 bp

RSF2RTR	*TTGCTGGGGTCTCGGCTATCTCC*	(60°C)
RSF3RTF	*AGCAGGGCCCAGAACAGACACAC*	215 bp
RSF3RTR	*CCCCGCTTTAATCAGGCTTCCAC*	(60°C)
RSF4ARTF	*CCAGAATCCTGCATGGGCCATG*	203 bp
RSF4ARTR	*CGTCAGACGCAGGGCTTGGAA*	(60°C)
RASF5CRTF	*TGCAGCCTGGACGAGGAACTGG*	252 bp
RASF5ACRTR	*CCGCCGGAGTTTCAGATGCACTT*	191 bp
RSF5ARTF	*GCACCCTCACCGTGACCTTCAGC*	(60°C)
RSF6ARTR	*GCCACATCACTGCTAATTTCTTCTGCA*	166 bp
RSF6ARTF	*GTCCCCAGGATTTTGCTCTTCACATT*	(60°C)

Table 9. Mutagenesis primers.

Primer name	**Sequence (5´-3´)**
ANKRD1_BglIIF1	*CAGTACCATCATGTTGGCTGAAGAGATCTTGTATGTTTTTCTGTCGTG*
ANKRD1_BglIIR1	*CCACGACAGAAAAACATACAAGATCTCTTCAGCCAACATGATGGTACTG*
YapT119AU1	*GAACATGCTGTGGAGCCAGGGCTCCTGCAG*
YapT119AL1	*CTGCAGGAGCCCTGGCTCCACAGCATGTTC*
YapS127AU1	*GAGAAGCTGGAGAGGCATGAGCTCGAACATGCT*
YapS127AL1	*AGCATGTTCGAGCTCATGCCTCTCCAGCTTCTC*
YapS138AU1	*GTCCCAGGAGCAACAGCTCCCAACTGCAG*
YapS138AL1	*CTGCAGTTGGGAGCTGTTGCTCCTGGGAC*
YapS127EU1	*ACTGCAGAGAAGCTGGAGATTCATGAGCTCGAACATGCTGTGG*
YapS127EL1	*CCACAGCATGTTCGAGCTCATGAATCTCCAGCTTCTCTGCAGT*
YapS138EU1	*GGGTCAGTGTCCCAGGTTCAACAGCTCCCAACTGCAG*
YapS138EL1	*CTGCAGTTGGGAGCTGTTGAACCTGGGACACTGACCC*
mCherrydelgF	*GGGTAAGCCATAGAGATCTTGTACAGCTCGTCCA*
mCherrydelgR	*TGGACGAGCTGTACAAGATCTCTATGGCTTACCC*

2.1.3 Media

All media were prepared in the Institute for Genetic from the University of Giessen and autoclaved before use.

DMEM for 10 l

pH 7.25 adjusted with HCl	DMEM	133 g
	$NaHCO_3$	3.7 g
	HEPES	59.6 g

RPMI for 10 l		
pH 7.25 adjusted with HCl	RPMI	133 g
	$NaHCO_3$	2 g
	HEPES	50 mM
LB medium for 1 l		
pH 7.5 adjusted with HCl	Bacto trypton	10 g
	Yeast extract	5 g
	NaCl	10 g
Sorting medium for FACS	PBS (1X)	
	HEPES	25 mM

2.1.4 General buffers and solutions

Loading Dye (6X) for 50 ml	Saccharose	22.5 g
	TBE buffer (10X)	6 ml
	OrangeG	0.5 g
Mowiol for slides	Glycerol	6 g
	MOWIOL	2.4 g
	Tris (pH 8.5)	0.2 M
	DABCO	0.1%
Proteinase *K* buffer		
Adjusted pH to 7.6	Tris	50 mM
	EDTA	25 mM
	NP40	0.5%
	SDS	0.5%
TBE buffer (10X)	Tris	1 M
	EDTA	10 mM
	Boric acid	0.8 M
TE buffer (1X)		
pH adjusted to 7.6 with HCl	Tris	10 mM
	EDTA	1 mM

2.1.5 Buffers for SDS-PAGE and western blot

Separation gel buffer	Tris/HCl pH 8.8	1.5 M
Stacking gel buffer	Tris-HCl pH 6.8	0.5 M

Blotting buffer

For 1 l	NaH_2PO_4	1 M (20 ml)
	Na_2HPO_4	0.5 M (14 ml)

Flag lysis buffer

pH adjusted to 7.4 with HCl	Tris	50 mM
	NaCl	150 mM
	EDTA	1 mM
	Triton X100	0.5%
	1x Complete proteinase inhibitor/ 50 ml buffer	

Laemmli buffer

pH adjusted to 6.8 with HCl	Tris	140 mM
	Glycerol	20 %
	SDS	4 %
	β-Mercaptoethanol	1 M
	Bromphenol blue	0.01 %

SDS-PAGE running buffer (10X)	Tris	250 mM
	Glycine	1.92 M
	SDS	0.1 %

TBS buffer (10X)

pH adjusted to 7.6 with HCl	Tris	200 mM
	NaCl	1.4 M
	0.02 % Tween20 for TBS-T	

FACS sorting media	PBS	1x
	EDTA	1 mM
	HEPES	25 mM

2.1.6 Basic commodities

2.1.6.1 Consumables

Amersham Hybond-P PVDF membrane	GE Healthcare, Munich, Germany
Cryotubes (2 ml)	Sarstedt AG & Co., Nümbrecht, Germany
Cell culture dishes	Sarstedt AG & Co., Nümbrecht, Germany
Cell scraper	Sarstedt AG & Co., Nümbrecht, Germany
Reaction tubes (1.5 ml, 2 ml)	Sarstedt AG & Co., Nümbrecht, Germany
Falcon tubes (50 and 15 ml)	Sarstedt AG & Co., Nümbrecht, Germany
FACS tubes	
Gloves (rotiprotect nitril)	Carl Roth GmbH & Co. KG, Karlsruhe, Germany
PCR tubes and 8-well strip	TechnoPlastic Products AG, Trasadingen, Switzerland
Plates 96 well plates for luminometer	Greiner bio-one GmbH, Hampshire, UK
Petri dishes	Sarstedt AG & Co., Nümbrecht, Germany Techno Plastic Products AG, Trasadingen, Schweiz
Pipet tips (10, 20, 100, 200, 1000 µl)	Greiner bio-one GmbH, Hampshire, UK
Scalpel	B. Braun Melsungen AG, Melsungen, Germany
Sterile filters	Sartorius AG, Göttingen, Germany
Tubes for qRT-PCR	Biozym Scientific GmbH, Hessisch Oldendorf, Germany
Whatman paper	Carl Roth GmbH & Co., Karlsruhe, Germany

2.1.6.2 Equipment

Autoclav Technoclav	Technomara AG, Wallisellen, Switzerland
Acculab precision scale VIC-123	Sartorius AG, Göttingen, Germany
Acculab precision scale VIC-5101	Sartorius AG, Göttingen, Germany
Blotting chambers	BioRad, Munich, Germany
Block heater QBD2	Grant Instruments Ltd. Cambridge, UK
Electrophoresis chambers	PEQlab Biotechnologie GmbH, Erlangen, Germany
FACS CANTO II	BD Biosciences, Heidelberg, Germany
FACS Aria III	BD Biosciences, Heidelberg, Germany
Freezer -80°C DF8517	Labotec GmbH, Göttingen, Germany
Gel documentation transilluminator	Decon Science Tec GmbH, Hohengandern, Germany
Microplate luminometer	ORION L, Berthold Detection Systems, Pforzheim, Germany
Magnetic mixer (VMS-C7)	VWR International GmbH, Darmstadt, Germany
MALDI-TOF-MS	AG Lochnit. Amersham Bioscience Group

Microwave	Cinex Electronic GmbH, Aschenberg
Molecular Imager VersaDoc	Bio-Rad, Hercules, CA, USA
Neubauer chamber	LO - Laboroptik Ltd, Lancing, UK
pH meter, pH 211	Microprocessor Hanna Instruments, Kiel, Germany
Pipetting aid	PZ HTL S.A.,Warszawa, Poland
Power supply	Bio-Rad Laboratories Inc., Hercules, CA, USA
Rotor-Gene3000	Corbett Research, Germany
Tecan Infinite M200 PRO	Tecan GmbH, Grödig, Austria
Versadoc	BioRad, Munich, Germany
Vortexer	VWR International GmbH, Darmstadt, Germany

2.1.6.3 Centrifuges

Centrifuge 5418	Eppendorf GmbH, Hamburg, Germany
Fresco 17 Centrifuge	Heraeus, Hanau, Germany
Multifuge 1S/1S-R	Heraeus, Hanau, Germany
Pico 17 Centrifuge	Heraeus, Hanau, Germany

2.1.6.4 Incubators

HERAcell 150	Thermo Electron LED GmbH, Langenselbold, Germany
Incubator shaker TH30	Edmund Bühler GmbH, Hechingen
Laboratory incubator Type B6	Thermo Electron LED GmbH, Langenselbold, Germany

2.1.6.5 Microscopes and camera

Axio Observer.Z1 (inverse microscope)	Zeiss, Wetzlar, Germany
Camara Orca-ER, HAMAMATSU	Zeiss, Wetzlar, Germany
Fluorescence microscope	Zeiss, Wetzlar, Germany

2.1.6.6 Shakers

Shaker Rotamax 120	Heidolph Instruments GmbH & Co. KG, Schwabach, Germany
Shaker Roto-Shake Genie	Scientific Industries Inc., Bohemia, N.Y., USA
Thermomixer compact	Eppendorf-Netheler-Hinz GmbH, Germany

2.1.6.7 PCR Thermocyclers

Mastercycler	Eppendorf-Netheler-Hinz GmbH, Hamburg, Germany
Mastercycler Gradient	Eppendorf-Netheler-Hinz GmbH, Hamburg, Germany

2.1.6.8 Water baths

WB10 P-D	Industriegesellschaft GmbH, Dresden Germany
AL-5 Lauda	Dr. R. Wobser GmbH &Co. KG, Lauda-Königshofen, Germany

2.1.7 Software

BioEdit Sequence Alignment Editor Version 7.1.3.0	Ibis biosciences, Carlsbad, USA
Image J	National Institutes of Health, Bethesda, USA
Mascot Server	Matrix science
Python vs. CoBRA	https://launchpad.net/python.vs.cobra, Frederick Turczek
R project version 3.1.3	R Foundation
Rotor-Gene6	Corbett Research, Qiagen, Hilden, Germany
UCSC Genome Browser	University of California, Santa Cruz, USA
Motic Images Plus 2.0	Motic Deutschland GmbH, Wetzlar, Germany
Simplicity software	ORION L, Berthold Detection Systems, Pforzheim, Germany
BDFacsDivaTM Version 6.1.3.	BD Biosciences
Volocity version 6.3	PerkinElmer

2.2. METHODS

2.2.1 Molecular cloning

2.2.1.1 Restriction digestion

Molecular cloning describes the insertion of a DNA fragment into a specific expression vector. In this work, the cDNA of *ANKRD1* and *YAP1* were cloned into different expression vectors. Furthermore, the promoter region of *ANKRD1* was cloned into a luciferase reporter vector. To avoid a religation of the target vector, most of the cloning vectors were treated by double digestion as indicated in Table 2. By the digestion with one enzyme, an extra dephosphorylation step was performed using 5 units of FastAP, 1x of the corresponding buffer, ddH_2O, and an incubation at 37°C for 30 min. To obtain the inserts from the original vectors, 15 µg of the original vector with insert (pDNR-LIB-ANKRD1 and CMV-YAP1) were digested overnight (ON), and separately also the target vectors (10 µg plasmid), with the restriction enzymes at the corresponding temperature. Afterwards, the fragments were purified by preparative gel electrophoresis (1% gel) using the gel extraction kit from Macherey- Nagel.

To clone the promoter of *ANKRD1*, a 606 bp region before the transcription start site was amplified by PCR (see appendix 1). The primers used for this propose are listed in Table 6. The primers created *HindIII* and *XmaI* restriction sites in the amplified fragment, which were used for the cloning into the cloning vector (pJet) and later in the renilla luciferase vector (pRL-null). The amplified fragment and digested pRL vector were purified with preparative gel electrophoresis and gel extraction kit from Macherey- Nagel.

2.2.1.2 Ligation and transformation

Following restriction digestion and purification, the purified fragments were ligated. For that, the vector background and the isolated insert at a ratio of 1:5 were ligated ON at room temperature (RT) using the T4 ligase and the corresponding buffer from Fermentas.

The amplification of the constructs was performed by transformation of competent *Escherichia coli* (*E. coli*) strains (*DH5α*, *TAM I* or *XL10-Gold*) (Table 3). 30 µl of competent cells on ice were mixed with 1 µl of plasmid. The mixture was incubated for 30

min on ice, before the heat shock at 42°C for 45 s. The transformed cells were incubated for 2 min on ice and mixed with 250 µl SOC medium. After 1 h incubation at 37°C, 100 µl of this aliquot was plated on LB-plates with the necessary antibiotics (ampicillin: 60 µg/ml; kanamycin: 50 µg/ml; chloramphenicol: 30 µg/ml final concentration) and incubated ON at 37°C.

2.2.1.3 Plasmid preparation and glycerol stock cultures

To gain large amounts of the plasmids, midi and mini preparations had to be performed. The transformed *E. coli* cells were grown in LB liquid medium with the specific antibiotic at 37°C ON. Next day, the plasmids were purified according to the kits from Macherey-Nagel GmbH & Co. KG. For the glycerol stocks, 750 µl of the *E. coli* suspension were supplemented with 250 µl sterile 80% glycerol, mixed thoroughly and stored at -80°C. The correctness of the plasmid sequences and orientation were verified by restriction digestion and by conventional sequencing. The sequences were further analysed using the BioEdit software. The functionality of the generated plasmid was controlled by fluorescent microscopy, qRT-PCR and at the protein level by western blotting.

2.2.2 Mutagenesis

During this work, mutagenesis steps were performed for various reasons e.g. to create specific restriction sites (*BglII* sites) in pDNR-LIB-ANKRD1, to create the YAP1 point mutants (YAP1-S127A, YAP1-S127E, YAP1-T119A, YAP1-S138A, YAP1-S127E), or to delete a nucleotide to bring the insert in frame, since the reading frame is essential for the correct expression of the fusion protein (mCherry-YAP1). The mutagenesis primers were created using the *in silico* tool of Stratagene and are listed Table 9. The mutagenesis PCR was performed with the Quick Change Lightning Site-Directed Mutagenesis Kit from Agilent Technologies with the settings indicated in Table 16.

2.2.3 Cell culture

2.2.3.1 Cell lines and transfections

This work is a cell culture based study. The cell lines used, their origin and respective growth medium are listed in Table 4. The cell lines were cultivated in DMEM or RPMI containing 10% FCS and PS at 37°C under 5% CO_2 concentration. The cells were transfected at a confluence of 60-80% in serum free media (Opti-MEM from Gibco) with 4 or 10 µg plasmid DNA in 6-well or 10 ml plates respectively. HEK293T and TREx293 cells were transfected using PEI. LNCaP cells were transfected with Lipofectamine from Invitrogen. A549 and T47D were transfected using Turbofect from Fermentas. A427 cells were transfected using X-tremGENE HP from Roche according with the instructions of the manufacturers. The transfected cells were further used for expression analyses, promoter assays, colony formation, growth curves, as well as for protein, RNA and DNA isolation.

2.2.3.2 Promoter assays

The promoter assays performed in this study were used to corroborate the effect of the putative transcription factor or activators on the promoters of target genes. The activation of the cloned promoter is linked experimentally to the luciferase activity. The measurements of reporter activity were performed using the Dual-Luciferase Reporter Assay System, which also contains the catalytic enzyme to oxidate luciferin. The generated light intensity was measured by the microplate illuminometer ORION L. The obtained data were normalized to the corresponding control vectors.

The promoters of *p53, p21, MDM2* and *BAX* were cloned into pGL-vectors (firefly luciferase) and were obtained from the AG Schmitz (Department of Biochemistry, University of Giessen). The p53 vector is an artificial construct with 13 binding sites of TP53 in a pGl luciferase vector. A fragment of 606 bp of the ANKRD1 promoter was cloned into pRL-null vector as previously indicated in 2.2.1.1. The luciferase vector pRL-RASSF1A (length promoter: 0.5 kb) was created by Dr. Kiehl in the AG Dammann.

For the promoter assays, HEK293T or the YAP1-inducible TREx293 cells were co-transfected with 2 µg of the luciferase vector (*RASSF1A*, *ANKRD1*, *TP53, p21, MDM2* or *BAX*) together with 1.7 µg of the transcription factor or activator. The transfection

efficiency was controlled using 0.3 µg of the corresponding control empty vector (pGL2 or pGL3 for the renilla luciferase vectors or pRL-null for the firefly luciferase vectors). For the respective normalization, mock transfections were performed by co-transfection of the respective empty vector together with the transcription factors or activator. 24 h post transfection, the cells were lysed with 200 µl of the 1x passive lysis buffer from the Dual-Luciferase Reporter Assay kit. The cell lysate was spun down for 1 min at 10000 rpm. 20 µl of the lysate were analysed in the illuminometer ORION L.

The firefly luciferase activity was measured by adding 33 µl Lar II buffer (provided in the Dual-Luciferase Reporter Assay kit). To stop the firefly luciferase activity and to measure the renilla luciferase activity, 33 µl of Stop&Glo buffer with the diluted substrate Stop&Glo 50X (1:50) was added (provided in the Dual-Luciferase Reporter Assay kit). The obtained measurements were normalized in three steps: first to the corresponding vector for the transfection efficiency, secondly, the values were normalized to the sample transfected with the luciferase reporter vectors and overexpression empty vectors; finally, each sample was normalized to the corresponding sample co-transfected with the luciferase empty vector and with the overexpression vector of the transcription factor.

2.2.3.3 Colony formation and growth curves

In order to investigate the effect of ANKRD1 on cell growth, colony formation assays and growth curves were performed. For the colony formation assay HEK293T, A427, LNCaP and T47D cells were seeded in 6-well plates. The following day, the cells were transfected in triplicates with 4 µg plasmid. A427, LNCaP and T47D cells were transfected with pCMV-ANKRD1 or with the pCMV-empty vector as control. The H293T cells were transfected as previously described either with pcDNA4TO-ANKRD1 or with pcDNA4TO-empty vector. The overexpression of ANKRD1 was proved by semiquantitative PCR as indicated in figure 17. 24h after transfection, the culture medium was supplemented with geneticin (G418) or zeocin for the selection as indicated in Table 10. After approximately three weeks, the colonies were stained with GIEMSA in a dilution of 1:10 with water.

For the statistical analysis, the number of the colonies in the technical triplicates was counted, the mean value was determinated and normalized relative to the cells transfected

with the empty control vector. For the standard deviation, the mean values of the biological triplicates were used and plotted in figure 17.

Table 10. Antibiotic concentration for colony formation.

Cell line	Antibiotic	Concentration
A427	G418 (30.000 U/ml)	5 µl/ml
A549	G418	50 µl/ml
HEK293T	Zeocin (100 mg/ml)	7 µl/ml
LNCaP	G418	33.34 µl/ml
T47D	G418	100 µl/ml

The growth curves of LNCaP and A549 cells were generated after ectopic expression of ANKRD1. For this proposes, the cells were transfected either with 4 µg pCMV empty vector or with 4 µg pCMV-ANKRD1 vector. After 48 h selection with G418, 2 x 10^5 cells were plated under antibiotic selection pressure in duplicates. Every 24 h the cell number of the duplicates was counted using the Neubauer chamber. The cell number of day one was used as start point to quantify the fold change of the cell number over the experimental time period.

2.2.3.4 Generation of stable cell line

The stable cell lines were generated using the Tet-On inducible system from Invitrogen, which allows a site directed regulation or activacion of a specific gene. The TREx293 cells are stably transfected with a *tetracycline response element* (TRE) repressor and with a plasmid containing a TRE promoter and the gene of interest. The adding of tetracycline or its derivate doxycycline (Dox) produces the release of the repressor from TRE leading to the free promoter, which then allows the high transcription of the downstream gene of interest.

For the generation of the ANKRD1 and YAP1 stable cell lines, cDNAs of *YAP1* or *ANKRD1* were cloned into pcDNA4TO Myc vector as indicated in Table 2. 10 µg of the vectors were transfected in the TREx293 cells in 10 cm plates. The cells were cultivated in DMEM with 10% tetracycline free serum and PS under the same conditions described above. The vector containing the Tet repressor is blasticidin resistant and the pcDNA4TO Myc vector is zeocin resistant. After three weeks of selection by blasticidin (5 µg/ml) and

zeocin (500 µg/ml), the individual clones were isolated and extended. The induction of *YAP1* or *ANKRD1* was performed using Dox in a final concentration of 2µg/ml. The individual clones and the pool of clones were further used for transfection, expression and protein analysis.

2.2.3.5 Knockdown assays by small interfering RNA

Small interfering RNA (siRNA) is a double stranded small non-coding RNA, which binds complementary to the mRNA sequence of its target genes to enhance its degradation (Fire *et al*., 1998). During the natural gene regulation by siRNA in cells, the precursor siRNA is cleaved into small 20-25 bp length RNA in the DICER protein complex. The siRNA duplex loads one strand on the RNA-induced silencing complex (RISC), in which the target mRNA is scanned and cleaved (Esteller, 2011). In this study, the ANKRD1 knockdown was performed with the commercial siRNA from Dharmacon.

	5'- 3' sequences
Non-targeting pool (5 nmol)	*UGGUUUACAUGUCGACUAA* *UGGUUUACAUGUUGUGUGA* *UGGUUUACAUGUUUUCUGA* *UGGUUUACAUGUUUUCCUA*
Human ANKRD1 siRNA SMARTpool (5 nmol)	*CUACAAGACCUCUCGCAUA* *GAACCAAAGCAAUAUUCGA* *CGAAUUCCGUGAUAUGCUU* *GCUAUAAGAUGAUCCGACU*

HEK293T cells were transfected at a confluence of 80% either with 50 pmol of a non-targeting siRNA control pool or with 50 pmol of the siRNA for ANKRD1 using the Lipofectamine® RNAiMAX from Invitrogen. For the transfection, 50 pmol siRNA were diluted in 100 µl Opti-MEM; 10 µl Lipofectamine were prepared also in 100 µl Opti-MEM and mixed with the corresponding siRNA dilution. Before the transfection, 800 µl of Opti-MEM was added to the cells. Both siRNA/Lipofectamine mixes were incubated for 20 min at room temperature (RT) and added to the cells with Opti-MEM. After 6 h, the medium was changed to DMEM and the transfected cells were incubated for 4 days under the same conditions described in 2.2.3.1. The cells were then harvested for RNA isolation and expression analysis.

2.2.4 DNA isolation

The isolation of DNA was perfomed at RT. Before DNA isolation, the cells were washed twice with 1x PBS and harvested by scraping. The cells were centrifuged at 13000 rpm for 30 s. The cell pellet was resuspended in 400 µl Proteinase *K* buffer. 15 µl of Proteinase *K* (20 mg/ml) was added to the cells and incubated ON at 55°C. The following day, DNA was isolated by phenol/chloroform extraction. To this effect, 500 µl of phenol were added to the cell lysate and mixed vigorously. The phase separation was performed by centrifugation at 13000 rpm for 3 min. The upper aqueous layer containing the nucleic acids was transferred into a new tube. 500 µl phenol/chloroform/isoamyl alcohol mix were added to the sample and mixed for 1 min. After a centrifugation step of 13000 rpm for 3 min, the upper aqueous layer was isolated and mixed with 500 µl chloroform. The DNA/chloroform mix was centrifuged for 3 min at 13000 rpm. The supernatant was transferred into a new reaction tube. The DNA was precipitated by adding 1/10 volume of 3 M NaAc and 1 volume of isopropyl alcohol. The sample was centrifuged for 3 min at 13000 rpm. The DNA pellet was washed in 150 µl 70% ethanol (EtOH) and after a further centrifugation step for 5 min at 13000 rpm, the pellet was dried for 10 min at RT. The DNA was resuspended in TE-buffer. Subsequently, a RNaseA digestion was performed by adding 2 µl RNaseA and an incubation step at 37°C for 10 min. The DNA concentration was determinated using the TECAN apparatus.

2.2.5 RNA isolation

The cells used for RNA isolation were washed once with 1x PBS and lysed with 1 ml TRIzol. To the lysates 200 µl chloroform were added and mixed thoroughly. After an incubation for 3 min at RT, the samples were centrifuged at 12000 rpm for 10 min at 4°C. The upper aqueous layer was transferred into a new reaction tube and mixed with 500 µl isopropyl alcohol. After thoroughly mixing the sample, another centrifugation step at 12000 rpm for 10 min at 4°C was performed. The RNA pellet was washed with 150 µl of 70% EtOH diluted in DEPC water and centrifugated for 5 min. The supernatant was discarded and the pellet was dried at RT for maximal 3 min. Depending on the size of the pellet 20 – 50 µl DEPC water were added. Before the measurement of the concentration, the RNA samples were incubated for 10 min at 65°C and subsequently for 30 min at 37°C. The integrity of the isolated RNA was verified by agarose gel electrophoseresis in a 1% agarose

gel. The isolated RNAs were subsequently used for the reverse transcriptase PCR and for the expression analyses by quantitative real time PCR.

2.2.6 Methylation analysis

The methylation of the *ANKRD1* and *RASSF1A* promoter was analysed using bisulfite PCR followed by restriction analysis.

2.2.6.1 *In vitro* methylation (*ivm*)

In vitro methylated DNA (*ivm* DNA) was used as positive control for the methylation analyses. 2 µg genomic DNA in 164 µl ddH_2O were supplemented with 20 µl Buffer 2, 1 µl SAM (200x), 15 µl *SssI* (4 U/µl) and incubated ON at 37°C. After the first 2-3 h of incubation, another 1 µl SAM was added. Following the incubation the sample was diluted with 100 µl TE-buffer. Subsequently, the *ivm* DNA was purified with phenol/chloroform extraction as indicated in 2.2.4.

2.2.6.2 DNA bisulfite conversion

During the DNA bisulfite conversion all unmethylated cytosines (Cs) are converted into uracil by desulphonation, while all methylated Cs are maintained as Cs, since the methyl group protects the cytosine from the hydrolytic deamination thus avoiding its conversion to uracil. For this purpose, 2 µg of genomic DNA (cell line DNA, tumor and matched normal tissue DNA) were diluted in 18 µl of ddH_2O and supplemented with 2 µl of 3 M NaOH. The samples were incubated for 15 min at 37°C. Thereafter, 12 µl of 0.1 M hydroquinone and 208 µl of 1.9 M sodium metabisulfite were added. The sample mix was incubated at 50°C ON. The following day, the DNAs were purified using the MSB®Spin PCRapace kit. The purified bisufite DNA was supplemented with 5 µl 3M NaOH to remove the sulfur group. Afterwards, the DNA was precipitated by EtOH and the DNA pellet was resuspended in 30 µl TE buffer. Thereafter, a PCR with the bisulfite treated DNA was performed. The region of interest from each cell line or tissue was amplified by PCR using the specific primers for bisulfite DNA indicated in Table 7. The *ivm* DNA was also bisulfite treated and further used for the PCR.

2.2.6.3 Combined bisulfite restriction analysis (CoBRA)

The CoBRA method allows the qualitative determination of the methylation status of the promoter region of a gene. The generated PCR product was subsequently digested with a restriction enzyme, which recognizes a palindromic sequence within a CG context. In this work, the restriction enzyme *TaqI* was used for the digestion both for *ANKRD1* as well as for *RASSF1A*. The restriction site of this enzyme is TCGA. Thus the digestion can only take place if the CG of interest was methylated before the bisulfite treatment.

For the CoBRA analysis, the PCR from the *ivm* DNA was used as positive control and as negative control, a mock digestion without enzyme was performed. In this study, 8.5 µl of the PCR product were used for the restriction digestion with *TaqI* and 8.5 µl of the PCR product was used for the mock digestion. The samples were digested at 65°C for 60 min. Thereafter, the CoBRA digest was analysed by gel electrophoresis on a 2% agarose gel.

2.2.7 Agarose gel electrophoresis (AGE)

Agarose gel electrophoresis is a molecular method for separating DNA fragments according to their molecular size. For the study, 1% and 2% agarose gels in Tris-Borate-EDTA (TBE) buffer containing ethidium bromide for were used for the visualization of DNA and RNA fragments. Ethidium bromide intercalates with the nucleic acids and fluoresces under UV-light.

1% gels were employed for RNA, genomic DNA, vector digests and preparative digests. 2% gels served to analyse PCR products and the CoBRA fragments. The gels were run at 200 volts for approx. 12-20 min. As molecular size standards, DNA ladders of 1 kb or 100 bp ladder from Fermentas were used.

2.2.8 Polymerase chain reaction (PCR)

The polymerase chain reaction is a biochemical method to amplify a particular DNA sequence using specific primers, which are short DNA fragments complementary to the target region. PCR consists of three steps: denaturation, annealing and extension. During the denaturation, the double DNA strand melts open at 94°C to single stranded DNA to

initiate a new PCR cycle and to stop all enzymatic reactions from the previous cycle. In the second (annealing) step, the primers bind to the single stranded DNA template at the target region, thus the polymerase can attach to the template. The temperature of annealing is variable (50 to 62°C) and depends on the melting temperature of the primer set. The last step (extension) occurs at 72°C; this is the ideal working temperature for the polymerase at which it copies that part of the DNA template defined by the position of the forward and reverse primer.

2.2.8.1 Reverse transcriptase PCR (RT-PCR)

To analyse the expression of genes at the transcriptional level, the RNA isolated from the cells (as described in 2.2.5), was reverse transcribed into cDNA. For this purpose, 2 µg of RNA was digested with DNAse I to remove the remaining DNA and plasmid from a sample. For the digestion, the RNA samples were supplied with 1 µl DNaseI, 2 µl DNaseI buffer and 0.5 µl Ribolock and filled to a final volume of 20 µl with DEPC water. The digestion was performed at 37°C for 30 min, afterwards, the enzyme was inactivated at 65°C for 10 min.

For the subsequent RT-PCR, 1 µg of RNA was mixed with 5 µl MMLV buffer (5x), 8 µl dNTPs (2.5 mM), 1 µl oligodT (10 pmol/µl) and 1 µl hexamers (10 ng/µl). The conditions for the RT-PCR are described in Table 11. After 10 min incubation at 62°C, 0.5 µl MMLV reverse transcriptase was added to the samples, and further incubated at 42°C as indicated in Table 11.

Table 11. Settings for RT-PCR.

Temperature	Time	
62°C	10 min	
Cool samples on ice		Adding of 0.5 µl MMLV Reverse transcriptase and 0.5 µl Ribolock
42°C	60 min	
90°C	5 min	
4°C	Pause	

Following the reverse transcription the cDNA was diluted 1:5. The generated cDNA was used as template for the semi- and quantitative real time PCR.

2.2.8.2 Semiquantitative PCR

The semiquantitative PCR serves to determinate the expression of a gene in a qualitative form. In this study, the semiquatitative PCR was used to control the reverse transcription of RNA into cDNA, overexpressions and gene inductions. Furthermore, it was used to visualize the endogenous level of target genes and *GAPDH*. The expression level of the housekeeping gene *GADPH* was used as control and for the normalization of the gene expression of the target genes. The semiquantitative PCR products were analysed by agarose gel electrophoresis in a 2% TBE gel using a DNA ladder marker of 100 bp as size marker.

The primers used here are the same as for the quantitative real time PCR. The annealing temperatures, the concentration of $MgCl_2$, the number of cycles for the optimal visualization as well as the addition of formamide were determined and displayed in Table 8 and in Table 12. The cycler conditions are annotated in Table 13.

Table 12. Parameters for semiquantitative PCR (fill up with ddH_2O for a final reaction volume of 25 µl).

Gene	Cycles	10x NH_4 buffer in µl	$MgCl_2$ (50mM) in µl	Primer (10nM) mix in µl	dNTPs (2.5mM) in µl	*Taq* in µl	Formamide in µl
ANKRD1	34	2.5	1	2	2	0.5	0
BAX	32	2.5	1.25	2	2	0.5	0
CDKN1A	32	2.5	1.25	2	2	0.5	0
CTGF	36	2.5	1	2	2	0.5	1
GAPDH	23	2.5	0.75	2	2	0.5	0
MDM2	30	2.5	1	2	2	0.5	0
PUMA	29	2.5	1.5	2	2	0.5	1
TP53	36	2.5	1.5	2	2	0.5	0
TP73	39	2.5	1.5	2	2	0.5	1
RASSF1A	34	2.5	0.75	2	2	0.5	1
RASSF2	35	2.5	0.75	2	2	0.5	0
RASSF3	30	2.5	0.75	2	2	0.5	0
RASSF4	34	2.5	0.75	2	2	0.5	0
RASSF5	33	2.5	0.75	2	2	0.5	0
RASSF6	33	2.5	0.75	2	2	0.5	0
YAP1	35	2.5	0.75	2	2	0.5	1

Table 13. Settings for semiquantitative PCR.

Step	Time	Temperature	
Initial denaturation	5 min	95°C	
Denaturation	30 s	94°C	**Cycles:** variable
Annealing	30 s	60°C / 62°C	
Extension	30 s	72°C	
	4 min	72°C	

2.2.8.3 Quantitative real time PCR (qRT-PCR)

Quantitative real time PCR (qRT-PCR) is a technique that is used to amplify and simultaneously quantify a target DNA molecule. The quantity can be either an absolute number of copies or a relative amount when normalized to DNA input or additional normalizing genes. For this study, the SYBR green from Life Technologies was used. The SYBR green intercalates with the DNA. After each cycle, the light emission of the SYBR green is measured, detected and obtained in the raw data.

One qRT-PCR reaction sample consists of 5 µl SYBR, 2 µl ddH_2O, 1 µl of 4 nM primer mix and 2 µl cDNA. The primers used and the respective optimal temperatures are listed in Table 8. The qRT-PCR data were measured in triplicates in Rotor Gene 3000 from Corbett Research. The raw data were processed with the corresponding program using the comparative quantification between the samples. The calibrator for this quantification was the control sample transfected with empty vector. The raw data were normalized to the respective *GAPDH* expression and relative to the respective control sample (set to 1). The settings used for the qRT-PCR are described in Table 14.

Table 14. Settings for qRT-PCR.

Step	Time	Temperature	
Initial denaturation	5 min	95°C	
Denaturation	20 s	94°C	**Cycles:** 40 X
Annealing	20 s	60°C / 62°C	
Extension	30 s	72°C	
	4 min	72°C	

2.2.8.4 PCR for CoBRA

For the methylation analysis by CoBRA, the promoter region of *ANKRD1* and *RASSF1A* were amplified by PCR using the specific primers indicated in Table 7 and bisulfite converted DNA. The selectivity of PCR relies on the specificity of the primers. The primer-design technique is important for improving the PCR product yield and for avoiding the formation of unspecific products. The primers used for CoBRA PCR were tested at different temperatures to define the optimal annealing conditions (Table 7). Their specificity for bisulfite DNA and not for genomic DNA was also verified.

The CoBRA PCR reaction for *ANKRD1* consist of 2.5 µl 10X NH_4 buffer, 2 µl dNTPs (2.5 mM), 1.75 µl of 50 mM $MgCl_2$, 0.5 µl Taq DNA-Polymerase, 5 µl bisulfite DNA (300 ng), 2 µl of 10 nM primer mix and 11.25 µl ddH_2O. For *RASSF1A*, a seminested PCR was perfomed adding formamide to the reaction samples. The settings used for the thermocycler are described in Table 15. The amplifications were checked by agarose gel electrophoresis loading 5 µl of the PCR products onto a 2% TBE gel. Subsequently, the PCR products can be digested enzymatically as described in 2.2.6.3. After the *TaqI* digestion, the PCR fragments were analysed by agarose gel electrophoresis in a 2% TBE gel using a 100 bp DNA ladder as size marker.

Table 15. Settings for CoBRA PCR.

Step	Time	Temperature	
Initial denaturation	2 min	95°C	
Denaturation	20 s	95°C	**Cycles:** 45 X
Annealing	20 s	variable	
Extension	30 s	72°C	
Final extension	4 min	72°C	
	∞	4°C	

2.2.8.5 Mutagenesis PCR

As previously described in 2.2.2, the vector mutagenesis was performed using the Quick Change Lightning Site-Directed Mutagenesis Kit and the mutagenesis PCR. Here the whole vector is amplified using the complementary mutagenic primers listed in Table 9 and the thermocycler settings from Table 16.

Table 16. Settings for mutagenesis PCR.

Step	Time	Temperature	
Initial denaturation	2 min	95°C	
Denaturation	20 s	95°C	**Cycles:** 17 X
Annealing	10 s	60°C	
Extension	variable	68°C	
Final extension	5 min	68°C	
	∞	4°C	

2.2.9 Protein extraction

For protein preparation, the cell lines were transfected beforehand in 10 cm plates at a confluence of 60-80% and incubated in as described in 2.2.3.1. Prior to the isolation, the cells were washed once with 1x PBS. For the whole cell lysis 0.5 - 1 ml (depending on the finally density and further uses) of cold lysis buffer with protease inhibitor mix was added to the cells. The cells were scraped off and transferred to a pre-cooled reaction tube. The cell lysates were incubated at 4°C in a rotation device for 30 min. To remove the cell debris, the lysates were centrifuged at 10000 rpm for 10 min at 4°C. Afterwards, the cleared cell lysates were used for the co-immunoprecipitation assays or denatured by adding of 2x Laemmli buffer and boiling at 95°C for 5 min. The rest of the lysate was stored at -80°C.

Before freezing, the protein concentration was determined by Bradford assay using a standard curve with different dilutions of bovine serum albumin. 10 µg of denatured protein lysate was loaded per lane in a 10% SDS gel and further analysed by gel electrophoresis and western blotting. By protein denaturation, the SDS in the Laemmli buffer provides the samples with a negative charge and the β-mercaptoethanol disturbs the hydrogen bonds and disulphide bridges.

2.2.10 Co-Immunoprecipitation (Co-IP)

The Co-Immunoprecipitation assays (Co-IPs) performed during this study were used to determine the protein-protein interaction between ANKRD1 and TP53 and MDM2. This method is based on immunoprecipitation to capture and purify a primary target (or antigen) as well as other secondary targets, which are bound to the primary target by native interactions.

For this purpose, HEK293T cells were transiently transfected either with Flag-/GFP-empty vector or with Flag-/GFP-ANKRD1 (primary target). 72 h after transfection, the cells were lysed with 1 ml Flag lysis buffer for the Flag Co-IPs or with 200 µl RIPA lysis buffer (included in the GFP-Trap® kit) for the GFP Co-IPs. The lysate preparation was performed as previously mentioned by 30 min rotation at 4°C and a centrifugation step of 10 min at 4°C. An aliquot of the cell lysate taken before the Co-IP was used as input to control the overexpression and the protein level of GAPDH, TP53 and MDM2. The enrichment of ANKRD1 with a Flag tag and the Co-IP of the interacting proteins were performed using agarose beads coupled with an anti-FLAG antibody. The immunoprecipitated GFP-ANKRD1 and its interacting proteins were enriched using the GFP-Trap® system from ChromoTek.

The anti-Flag and anti-GFP beads were equilibrated before adding to the protein lysates. 50 µl of anti-Flag beads were washed twice with 1 ml cold 1x TBS and spun down at 4°C for 5 s. The suspension with anti-GFP beads (25 µl) was equilibrated by washing three times in 500 µl dilution buffer (included in the GFP-Trap® kit) and spun down at 2500 x *g* for 2 min at 4°C as indicated in the manufacturer's instructions. After equilibration, the beads were added to the pre-cleared cell lysates and incubated ON under constant rotation at 4°C. The following day, the anti-Flag beads were centrifuged and washed twice with cold 1x TBS as previously described. The anti-GFP beads were washed twice with 500 µl wash buffer (included in the GFP-Trap® kit) and centrifuged at 2500 x *g* for 2 min at 4°C. After the final wash step, the supernatant was completely removed and 30 µl Laemmli buffer were added to the beads. The input samples and the Co-IPs samples were denatured at 95°C for 5 min and further analysed by SDS-polyacrylamide-gel-electrophoresis and western blotting.

2.2.11 SDS-Polyacrylamide-Gel-Electrophoresis (SDS-PAGE)

The SDS-Polyacrylamide-gel-electrophoresis (SDS-PAGE) technique serves to separate proteins according to their molecular weight. In this work, the SDS-PAGE together with western blotting were widely used, for example to determinate protein overexpression, endogenous protein levels, fusion proteins and to analyse the Co-IPs.

The used SDS-Polyacrylamide gels consisted of a 4% stacking gel and of a 10% separation gel. The exact composition of the gels is indicated in Table 17. N, N, N', N'-tetramethylethylenediamine (TEMED) and 10% ammonium persulfate (APS) were used for the polymerisation. For the electrophoresis, the chamber containing the gels was filled with 1x SDS running buffer. Pre lane, 10 µg of denatured protein lysates were loaded in three technical triplicates. The electrophoresis was performed at a constant voltage of 120 V for 80 min. Afterwards, the SDS gels containing the proteins were used for the western blot.

Table 17. SDS-Polyacrylamide gel composition (for 2 gels).

Components	Stacking gel (4%)	Separating gel (10%)
ddH_2O	6.1 ml	4.1 ml
Acrylamide	1.3 ml	3.3 ml
Stacking gel buffer 0.5M Tris HCl pH 6.8	2.5 ml	-
Separating gel buffer 1.5M Tris HCl pH 8.8	-	2.5 ml
10% SDS	100 µl	100 µl
10% APS	50 µl	50 µl
TEMED	5 µl	10 µl

2.2.12 Western blot

The separated proteins were transferred by wet blotting onto a PVDF membrane from Amersham for the subsequent immunodetection with antibodies. Before the transfer, the membrane was activated with methanol for 10 s and equilibrated in transfer buffer (1x) for 20 min. The western blot chambers were filled with transfer buffer (1x). The transfer was performed by 350 mA for 2 h at 4°C.

The proteins on the PDVF membrane were detected with specific antibodies (see Table 1). The non-specific binding of antibodies was avoided by prior blocking with 3% skimmed

milk powder in 1x TBS-T for 1 h. The blocked membrane was cut according to the molecular weight of the proteins to be investigated using the prestained page rule size markers of Fermentas as reference. The membrane fragments were incubated ON with the respective antibody dilution (in 3% skimmed milk powder in 1x TBS-T, see Table 1) at 4°C under constant rotation.

Next day, the membranes were washed three times with 1x TBS-T for 5 min at 4°C. Thereafter, the membranes were incubated for 1 h at 4°C with the corresponding HRP-labeled secondary antibody. The membranes were then washed three times for 5 min with 1x TBS-T. The individual membrane fragments were scanned in the Versadoc scan system of BioRad using the ECL kit from Immobilon Western for the detection of HRP activity from the secondary antibody. The imaging data of the three technical samples were further analysed for the statistical analysis. The protein amount detected on the membranes was quantified using the ImageJ software. For this propose, the intensity of each individual protein band was measured taking into account areas of identical size and the light intensity. The background of the membrane fragment was also determined and subtracted from the total measured protein intensity. Thus, the values (after background substraction) were normalized to the respective GAPDH level and protein level on the control sample. The mean and standard deviation were obtained from the biological replicates as indicated in figure 19 and figure 26.

2.2.13 Fluorescence-activated cell sorting (FACS)

In this study, cell cycle analysis and the cell sorting by FACS was performed in cooperation with the FACS core facility of the Institute of Clinical Immunology of the University of Giessen.

The flow cytometry technique allows the fluorescence measurement of individual cells. In this method, a beam of monochromatic light is directed onto a hydrodynamically focused stream of fluid. Each suspended particle or cell passing through the beam scatters the ray and produces a fluorescent mark (in this case GFP). The emitted light has a longer wavelength than the light source. The detectors use the combination of scattered and fluorescent light for the analysis of fluctuations in brightness, which deliver information about the physical and chemical structure of each individual particle. The fluorescence-

activated cell sorting or FACS is an advanced technique that combines the flow cytometry analysis and cell sorting, in which the single cells are detected and separated according to their specific fluorescence signal.

2.2.13.1 Flow cytometry

To analyse the cell cycle distribution, the YAP1-inducible TREx293 cells were transfected in 10 cm plates (density of 70-80%) as described in 2.2.3.1 with one of the following vectors: GFP-empty vector, YFP-empty vector, YFP-RASSF1A, GFP-RASSF1A, YFP-RASSF2, YFP-RASSF3, YFP-RASSF4, YFP-RASSF5, YFP-RASSF6, or with YFP-MST1 and YFP-MST2 (2 x 10 cm plates for each transfection). Eight hours post transfection, the cell medium was changed to DMEM. The following day, the YAP1 induction with Dox (2µg/ml) was started in one set of the samples and after 72 h induction, the cells were fixed and prepared for flow cytometry.

To avoid the loss of dead cells, the detached dead cells and the living cells from the plate were transferred to a 15 ml tube and pelleted at 1500 rpm for 3 min. Thereafter, the cells were washed twice in 5 ml 1x PBS. The cells were resuspended in 1.5 ml 1x PBS to obtain single cells. Using a vortexer (lowest level), 3.5 ml ice-cold 100% EtOH were added dropwise. The cell fixation with EtOH was performed with an ON incubation at -20°C.

The following day, the fixed cells were pelleted at 1500 rpm for 3 min and washed twice in 1x PBS. To avoid the intercalation of propidium iodide with the dsRNA, RNaseA (5 µg/ml) was added to the samples and incubated at 37°C for 30 min. After the RNAseA digestion, the cells were analysed. For this purpose, 100 µl cells were transferred to a FACS tube and supplemented with 5 µl propidium iodide. Depending on the amount of cells, this mix was diluted with 1x PBS; the volume of propidium iodide was also adjusted accordingly. The red fluorescence emitted by propidium iodide possesses a different wavelength than YFP, therefore allowing the differentiation of both. The transfected cells are gated according to their DNA content (sub G1, G0/G1, S, M phase). The measurements were performed using the BD FACSCanto with the following settings: to measure the diffraction at a flat angle, forward scatter was adjusted at FCS = 220 mV. To determine the granularity of the cells, the size and structure of the nucleus, the side scatter was adjusted at SSC = 319 mV. The detection of the transfected cells occurred via the FITC channel (= 280 mV). For the

measurement of the DNA content the PE channel was set at 330 mV. The gates were selected to enclose the transfected cells. Afterwards the data were processed using the software: BDFacsDivaTM Version 6.1.3.

2.2.13.2 Fluorescence-activated cell sorting

The RNA used for the microarrays was isolated from the YAP1-inducible TREx293 cells, which were sorted beforehand for GFP transfected cells. For this purpose, the YAP1-inducible TREx293 cells were seeded in 10 cm plates. Next day, the cells were transfected at a density of 70% either with 10 µg GFP-empty vector or GFP-RASSF1A (2 x 10 cm plates for each transfection). Six hours after transfection, the cell medium was changed to DMEM. The following day (24h after transfection), the YAP1 induction with Dox (2µg/ml) was started in one plate transfected with GFP-empty and in one plate transfected with GFP-RASSF1A. The other two plates were treated with water as mock induction. After 72 h induction of YAP1, the four transfected cell plates were prepared for sorting. For that, the cells were washed twice with 1x PBS and trypsinized. Afterwards, the cells were resuspended in DMEM medium to inactivate the trypsin and were transferred to a 15 ml dark tube. The cells are pelleted at 1500 rpm for 3 min and washed twice in 10 ml 1x PBS, since the phenol red color of the DMEM media can disturb the sorting. Thereafter, the cells were resuspended in 10 ml sorting medium, which contains cold 1x PBS with 1mM EDTA and 25mM HEPES. In this condition, the dark tubes with the samples were transported on ice to the FACS core facility. Before sorting, the cells were sterile filtered in the sorting medium using cell filters with pores of 40 µm.

The living cells were sorted at 4°C in the BD Biosciences FACS Aria III flow cytometer. The optimization of the experiment was performed together with the personal of the core facility. The settings used for the sorting are listed in Table 18.

One million living cells with a positive GFP signal were sorted and collected in a new 15 ml tube containing DMEM media. The purity of the GFP signal from the sorted cells was analysed after sorting as shown in appendix 2. Immediately after the verification of the GFP purity, the cells were pelleted at 1500 rpm for 3 min at 4°C. The supernatant medium was discarded and the cells were lysed with 1 ml TRIzol and stored at -20°C for the further RNA isolation next day.

Table 18. Settings for cell sorting.

Parameter	Setting	Parameter	Setting
Frequency	47.1	Phase mask	0
Amplitude	24.8	Single cell	Off
Phase	0	Sweet spot	On
Drop delay	27.65	Frist drop	207
Attenuation	off	Plates voltage	5,000
Precision	0-16-0	Voltage centering	85
Yield mask	0	Sheath pressure	45.00
Purity mask	16		

2.2.14 Microarrays

The microarray analyses were performed in collaboration with the AG Boettger of the Max Planck Institute in Bad Nauheim.

The microarrays were used to find those genes with differential expression after YAP1 induction and RASSF1A overexpression compared to corresponding control and uninduced cells. The microarrays used for this propose were the HuGene version 2.0 ST arrays from Affymetrix, which cover the whole transcriptome and include probes to measure both messenger RNAs and long intergenic non-coding RNA transcripts.

For the microarrays, 250 ng of RNA from the sorted cells with a GFP signal (described in 2.2.13.2) was isolated as described in 2.2.5. The sample labelling and hybridisation were performed by the AG Boettger using the Affymetrix® GeneChip WT terminal labeling and controls reagent kit according to the manufacturer's instructions. Colleagues of AG Boettger also performed the data extraxtion and normalization using the software and the probes library from Affymetrix.

To find the potential target genes, which are differently expressed after YAP1 induction and RASSF1A expression, the obtained relative gene expression levels were normalized to the expression of microarray internal controls. The differentially expressed up- and downregulated genes were found by normalization of the samples with YAP1 induction and RASSF1A expression in relationship to the control cells. Thus, the relative gene

expression from the samples: GFP/YAP1 ind.; RASSF1A/unind. and RASSF1A/YAP1 ind., were normalized relative to the control sample, which are the cells transfected with GFP empty and without induction of YAP1 (GFP/ unind. cells). After the normalization, the samples were sorted by descending differential expression of the cells with a YAP1 induction and RASSF1A expression relative to the control cells without YAP1 induction and without RASSF1A (GFP/ unind. cells). The top 10 differential up- and downregulated genes (without miRNAs and pseudogenes) are listed in Table 19. The unbiased analysis of the top differential up- and down-regulated genes is listed in Table 21 and Table 22 (appendix 5 and 6).

2.2.15 Fluorescence microscopy

In this study, the localization of YAP1 in the presence of RASSF1A was analysed by fluorescence microscopy using overexpression constructs both for GFP-RASSF1A and mCherry-YAP1 or mCherry-YAP1 point mutations. HEK293T cells were seeded on sterile coverslips on 6-well plates. The following day, the cells were co-transfected at a density of 20% with the corresponding mCherry and GFP constructs. Six hours after transfection, the media were changed to DMEM and the cells were incubated for another 2 days. The third day, the cells were washed twice with 1x PBS and fixed for 15 min by cold 3.7 % formaldehyde. The cells were washed three times with 1x PBS and subsequently permeabilized with cold 0.2% Triton X followed by three wash steps with 1x PBS. Afterwards, the nuclear staining was performed with freshly prepared DAPI (1 mg/ml) by an incubation for 5 min. The cells were briefly washed three times with 1x PBS. For the mounting, the coverslips are flipped onto a slide with a drop of Mowiol. The images were captured using the 63X zoom lens of Axio Observer.Z1 microscope from ZEISS with a camera Orca-ER HAMAMATSU and Volocity software. In addition, n =100 co-transfected cells were analysed in more detail and counted for the corresponding statistical analysis.

From each co-transfection, the nuclear morphology of 100 cells was analysed using the DAPI staining and sorted in these three categories: entire nucleus, deformed or apoptotic. The localization of the mCherry signal was also analysed using the function "*navigation"* from the Volocity software, in which the individual channels can be set on or off and the light intensity can be changed, without affecting the original picture. The localization of the

mCherry signal was determinated in the same 100 cells as for the nuclear morphology and it was sorted in the following two categories: “mCherry signal in the cytosol and nucleus”, and “mCherry signal in nucleus”. The GFP signal was characterised by the localization either in the whole cell or at the microtubules as fusion protein with RASSF1A.

2.2.16 Statistical analysis

The statistical and correlation analyses were performed using R (version 6.3), a programming language for creating graphics including linear and nonlinear modeling, classic statistical tests, time-series analysis, classification and clustering.

The bar graphs showed in this work were produced in Excel. Unless otherwise indicated, the graphs present the means of biological triplicates ± standard deviation. The p-values were quantified using R by Student’s unpaired t-test, with the assumption that the data are distributed normal and the zero hypothesis is true. The differences were considered significant if $p < 0.05$. The correlation data were performed by simple linear regression analysis in R. The p-values were calculated with the corresponding t-test for the regression coefficients and were considered as significant if $p < 0.05$. The *Chi* square test was used to analyse the significance of the observed differences from the flow cytometry data. The statistical test was performed assuming that the data are *chi*-squared distributed and the zero hypothesis is true.

3. RESULTS

The Hippo pathway regulates the organ size and plays an important role in both proliferation and apoptosis (Edgar, 2006; Harvey *et al*., 2013). The function of the Hippo signalling in cancer is still controversial, since it is regulated by the tumor suppressor RASSF1A but the main downstream co-activator is YAP1, which is an oncogenic protein (Kang *et al*., 2011). In addition, YAP1 regulates the expression of both pro-proliferative genes as well as of tumor suppressor genes by binding e.g. to the TEADs or TP73 transcription factors (Basu *et al*., 2003; Wang *et al*., 2016; Wang *et al*., 2010).

According to various studies, *RASSF1A* is known to be epigenetically inactivated in several types of cancers (Dammann *et al*., 2000; Richter *et al*., 2009; Schagdarsurengin *et al*., 2003). The genomic amplification of *YAP1* in cancer cells and the further silencing of *RASSF1A* by promoter hypermethylation might contribute to cellular instability and tumorigenesis. The main focus of this study was to dissect the role of RASSF1A in the cellular function of the YAP1 signalling and its deregulation in cancer.

3.1 Role of RASSF1A in the Hippo pathway

3.1.1 RASSF1A regulates the expression of YAP1 target genes

In order to investigate the effect of RASSF1A on the regulation of the Hippo pathway, the expression of the potential YAP1 target genes, namely *ANKRD1, CTGF, BBC3, CDKN1A* and *BAX* (Fig. 5) were analysed by qRT-PCR 72h after transfection of YAP1 and RASSF1A in HEK293T cells. YAP1 is well known to induce the expression of *CTGF* (Zhao *et al*., 2008); for this reason, the upregulation of *CTGF* was used as control for the functional activity of YAP1.

The potential target genes such as *BAX, CDKN1A*, and *BBC3*, which were previously reported to be involved in the pro-apoptotic signalling of the Hippo Pathway, did not exhibit an obvious deregulation after the co-transfection of RASSF1A and YAP1 as checked by semiquantitative PCR (Fig. 5A). YAP1 significantly increased the expression of *CTGF* and *ANKRD1* (Fig. 5B-5C). However, compared to YAP1 overexpression, the

expression of *ANKRD1* increased further after the co-transfection of RASSF1A and YAP1 (Fig. 5A-5C). *ANKRD1* is known to be a target gene of YAP1 (Li *et al*., 2013). The increase in *ANKRD1* expression after co-transfection of both RASSF1A and YAP1 was up to 4-fold compared to the control (p-value 0.007) and up to 2-fold more than the upregulation with YAP1 alone (p-value 0.04) (Fig. 5C).

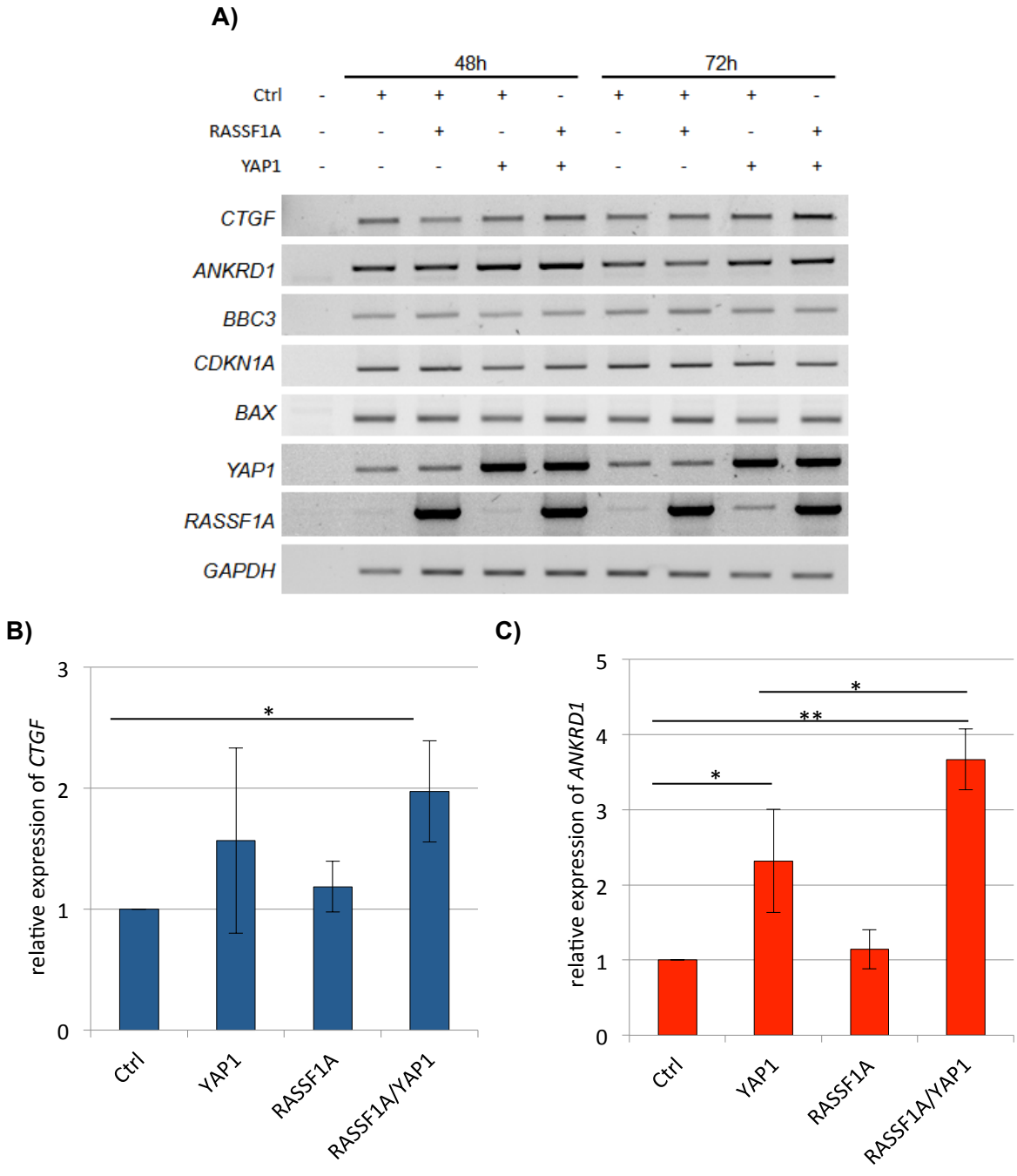

Figure 5: Induction of *ANKRD1* and *CTGF* in HEK293T cells. A) Semi-quantitative PCR of YAP1 target genes (*CTGF, ANKRD1, BAX, CDKN1A, BBC3)* and controls (*RASSF1A, YAP1* and *GAPDH)* 48h and 72h after transfection in HEK293T cells. Ctrl: *Flag-empty* vector; RASSF1A: *Flag-RASSF1A*; YAP1: *Flag-YAP1* **B)** Quantitative analysis of *CTGF* expression level in HEK293T cells transfected with Ctrl empty plasmid, YAP1 and/or RASSF1A plasmid. Expression was analysed by qRT-PCR, normalized to *GAPDH* and control transfection was set to 1. **C)** Quantitative analysis of *ANKRD1* level by qRT-PCR. p-values: * $p<0.05$, ** and $p<0.01$ (t-test).

3.1.2 Characterisation of the YAP1-inducible cell line

The transient transfection of YAP1 and the co-transfection with RASSF1A resulted in a significant induction of *ANKRD1* expression. In order to validate the previous findings and to obtain a more precise idea on the regulation events, YAP1 was stably transfected into a tetracycline inducible TREx293 cell line, also known as Tet-On inducible system. The TREx293 cells were cultivated in DMEM medium containg 10% tetracycline-free serum. The expression of YAP1 was activated by adding doxycycline (Dox). Control cells were also created, in which the empty vector was stably transfected and used to analyse the expression of the YAP1 target genes in a system with endogenous *YAP1* expression (Fig. 6A). Here, the expression of *YAP1*, *ANKRD1, BAX, CDKN1A* and *BBC3* was unaffected in the Dox-treated TREx293 control cells (Fig. 6A). In addition, 12 individual clones and a pool of YAP1 clones were generated and further characterised. The pool of YAP1-inducible TREx293 cells displayed a high sensitivity to Dox, which allowed the induction of *YAP1* and its target gene *ANKRD1* even with a low concentration of Dox (Fig. 6B).

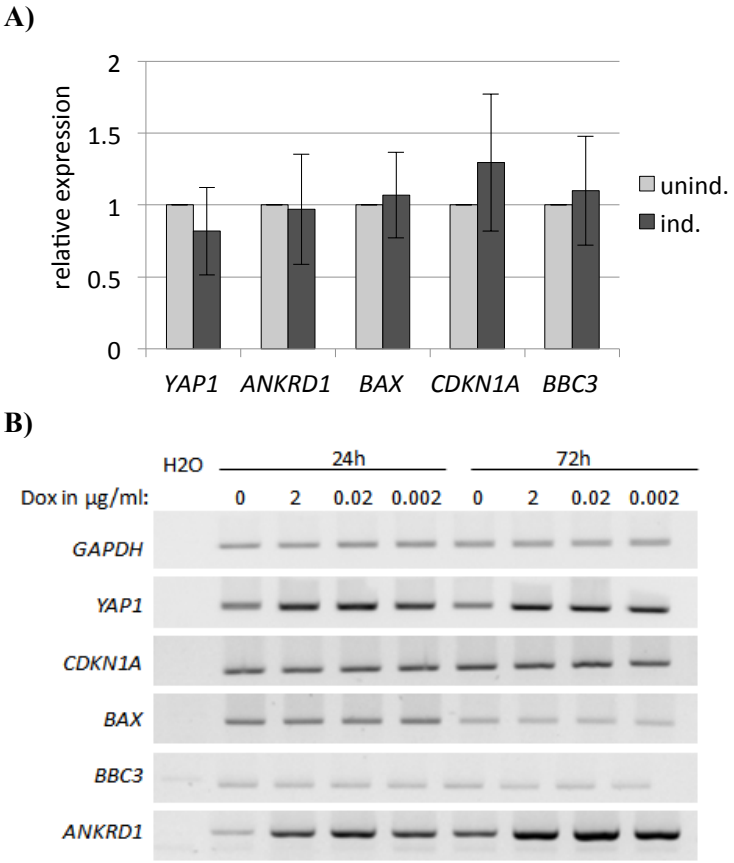

Figure 6: Analyses of expression of *YAP1* and target genes in the control TREx293 cells and in the YAP1-inducible TREx293 cell line pool after induction with Dox. A) Expression of *YAP1, ANKRD1, BAX, CDKN1A* and *BBC3* in control TREx293 cells transfected with control plasmid (pcDNA4TO) 24h after transfection and Dox induction (2 µg/ml). **B)** Induction of YAP1 and upregulation of target genes after YAP1 induction by indicated Dox dilutions in the YAP1-inducible TREx293 pool of clones.

The expression of *YAP1* in the 12 individual clones varied between 5- up to 40-fold after the YAP1 induction with Dox relative to the samples without induction and after normalization to *GAPDH* (Fig. 7A).

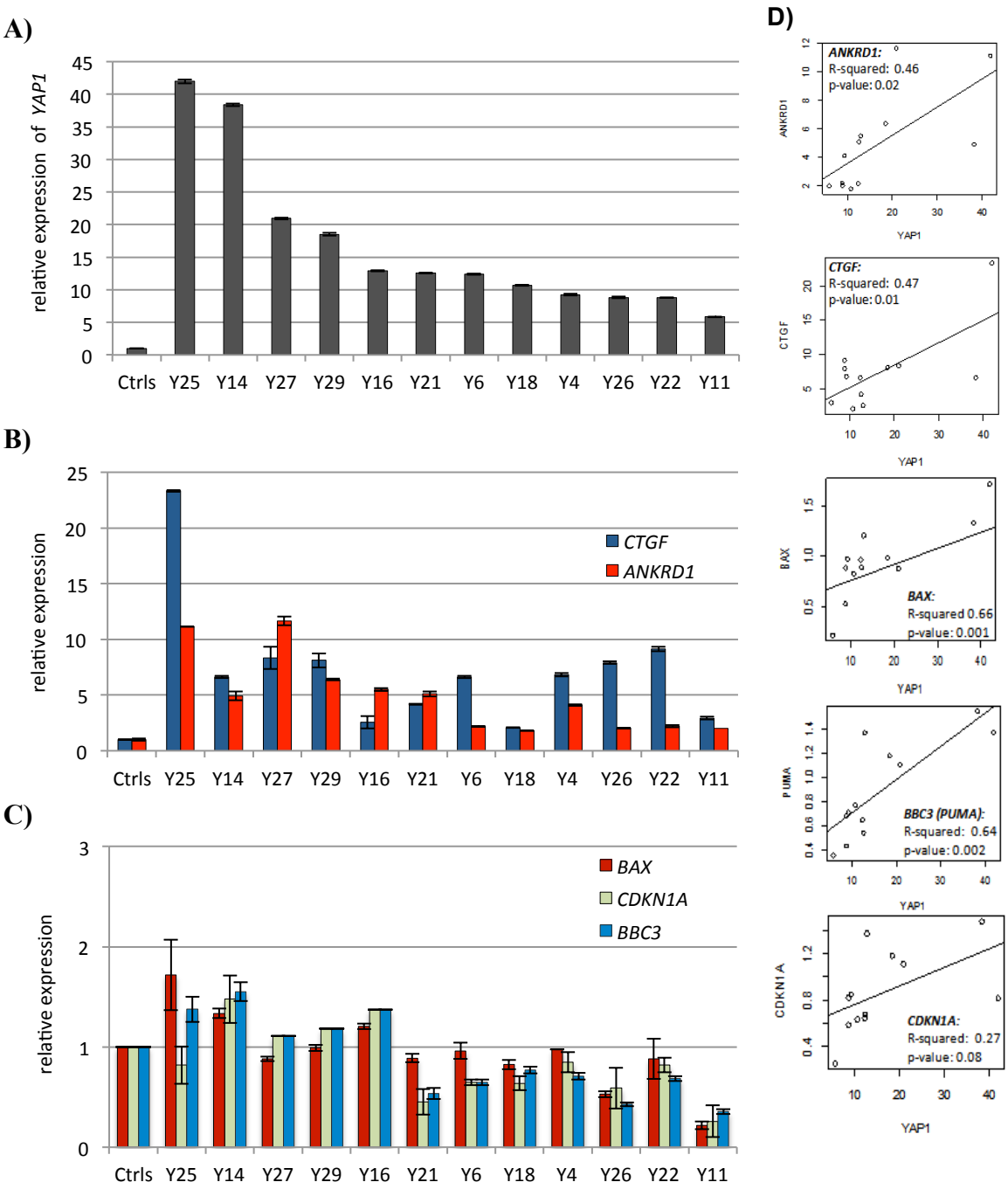

Figure 7: Expression of YAP1 target genes in the individual YAP1-inducible clones. A) Relative *YAP1* level was analysed by qRT-PCR in YAP1-inducible TREx293 individual clones 24h after induction with Dox (2 µg/ml) compared to uninduced cells (Ctrls: set at 1) **B)** Relative expression of *CTGF* and *ANKRD1* after 24h induction of YAP1 compared to uninduced cells. **C)** Relative expression of *BAX, CDKN1A* and *BBC3* 24h after induction of YAP1 compared to uninduced cells. All values are relative to *GAPDH* expression and to the control cells without YAP1 induction (Ctrls=1). **D)** Correlation analysis of the relative *YAP1* expression with *ANKRD1, CTGF, BAX, BBC3* and *CDKN1A* expression of the 12 different YAP1-inducible TREx293 clones and their respective p-values. Analyses performed using the software "R".

All induced clones showed an increase in the expression of *ANKRD1* and *CTGF* after *YAP1* induction (Fig. 7B); furthermore, the expression levels of *BAX, CDKN1A* and *BBC3* correlated with *YAP1* expression (Fig. 7C-D). The clones with higher *YAP1* expression showed an increase in *BAX, CDKN1A* and *BBC3* expression, while, the clones with a 5- to 10-fold *YAP1* induction showed a reduction in the expression of *BAX, CDKN1A* and *BBC3*. The correlation data in figure 7D indicate a significant correlation between *YAP1* expression and *ANKRD1* (p-value 0.02), *CTGF* (p-value 0.01), *BAX* (p-value 0.001), and *BBC3* expression (p-value 0.002). The correlation between *YAP1* and *CDKN1A* is not significant but the expression of *CDKN1A* showed the same tendency as *BAX* and *BBC3* with exception of clone Y25 (Fig. 7C).

The protein level of YAP1 at the individual clones was analysed by western blotting using the lysates from the same cells used for the expression analyses in figure 7. A lysate of the pool of clones was used as control, to compare the protein level of the individual clones (see Fig. 8).

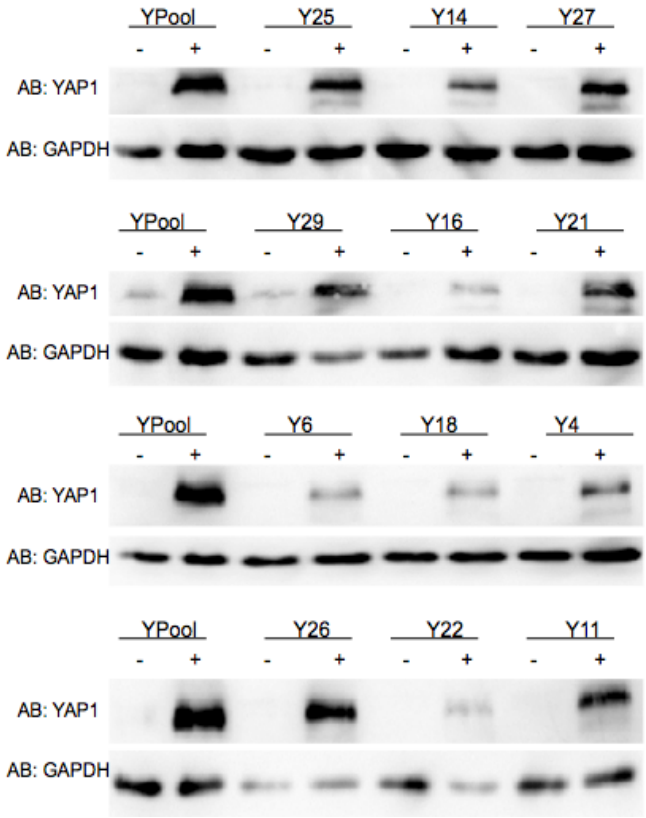

Figure 8: YAP1 protein level in the individual YAP1-inducible TREx293 clones after induction with Dox. Western blot analysis of YAP1 and GAPDH level in the cell lysates from the individual clones and pool of clones (YPool). The expression of YAP1 was induced with Dox (2 µg/ml) (+) for 24h. 10 µg of protein was loaded per lane in a 10% SDS gel, separated by SDS-PAGE and analysed by western blot on PVDF membrane. Experiment performed together with M.Sc. A. Traum.

Figure 8 indicates that the pool of clones expressed the highest protein level of YAP1 compared to the individual clones; interestingly, all four western blots displayed this result. The YAP1 protein level of the individual clones in figure 8 did no correlate with the expression data indicated in figure 7; therefore the subsequent experiments were performed using the pool of clones. The level of endogenous ANKRD1 protein could not be analysed due to the lack of an adequate antibody.

3.1.3 YAP1 downregulates the expression of tumor suppressor genes

To achieve a homogenous effect of YAP1 induction and to avoid clonal differences, the pool of clones was used for the further characterisation. Dox treatment of the YAP1-inducible cells resulted in a 12-fold increase *YAP1* mRNA level (Fig. 9A); furthermore, a significant increase in *CTGF* and *ANKRD1* expression was observed (Fig. 9B; 3.2-fold and 3.3-fold, respectively). Interestingly, the induction of YAP1 also resulted in a significant decrease in the expression of tumor suppressor genes: *RASSF1A* (decreased by 48%), *TP53* (29%), *BAX* (24%), *CDKN1A* (33%) and *BBC3* (27%), as indicated in figure 9B.

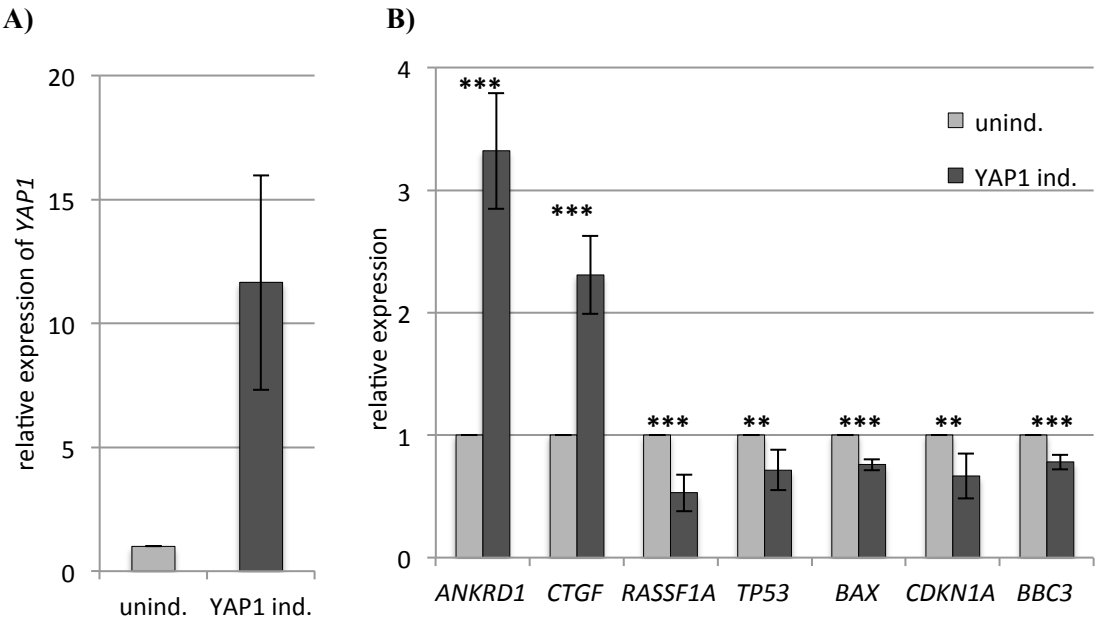

Figure 9: YAP1 induction reduced the expression of tumor suppressor genes. A. Relative expression of *YAP1* in TREx293 pool of clones 24h after induction with Dox (2 µg/ml) (YAP1 ind.) compared to uninduced cells (unind.) **B.** Relative expression of *ANKRD1, CTGF, RASSF1A, TP53, BAX, CDKN1A* and *BBC3* after 24h induction of YAP1 with Dox (YAP1 ind.) compared to uninduced cells (unind.). The data were normalized to *GAPDH* expression. The value for the uninduced cells was set 1. p-values: * $p<0.05$, ** $p<0.01$ and *** $p<0.001$ (t-test).

3.1.4 RASSF1A neutralizes the oncogenic potential of YAP1 and induces cell cycle arrest

To further analyse the effect of RASSF1A on the function of YAP1, the inducible YAP1 TREx293 pool of cells was transfected with GFP or GFP-RASSF1A. The expression of RASSF1A and the induction of YAP1 were confirmed on protein level by western blotting as indicated in figure 10A; in addition, the cell cycle distribution was analysed by flow cytometry 72h after transfection of RASSF1A and induction of YAP1 (Fig. 10B).

The flow cytometry analysis revealed that after 72h, YAP1 (*GFP/YAP1 ind.*) produces a cell accumulation in the S-phase compared to the uninduced cells (*GFP/unind.*; p-value< 0.00001) (Fig. 10B). In contrast, RASSF1A (*RASSF1A/unind.*) produced a cell accumulation in the G0-G1 phase compared to the control uninduced cells (*GFP/unind.*) (Fig. 10B). Moreover, RASSF1A (*RASSF1A/YAP1 ind.*) abolishes the S-phase induction of YAP1 (*GFP/YAP1 ind.)* and increases the cell number in the G0-G1 phase (*Chi*-square test p<0.001) (Fig. 10B).

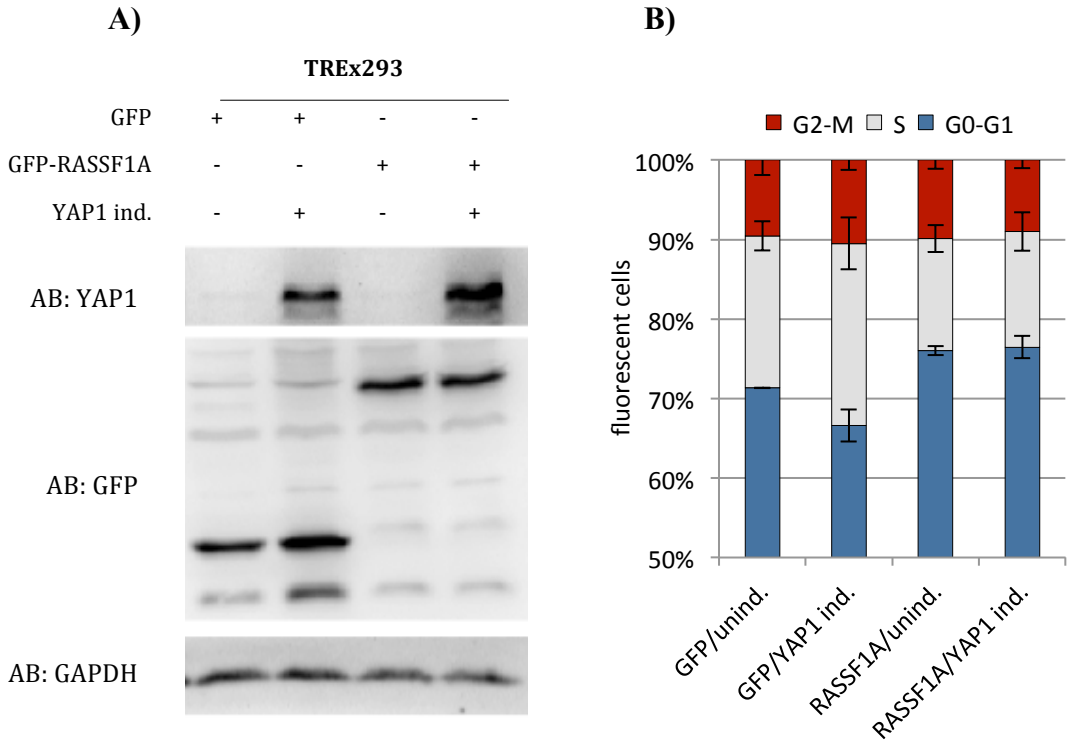

Figure 10: Cell cycle distribution after induction of YAP1 and RASSF1A transfection. A) Western blot of YAP1 in TREx293 cells 72h after transfection of GFP-empty or GFP-RASSF1A with and without induction of YAP1 with Dox (2 µg/ml). 10 µg of protein were loaded per lane and separeted on a 10% SDS gel and afterwards blotted onto PVDF membrane. **B)** Flow cytometry analysis of YAP1-inducible TREx293 cells transfected with GFP-empty or GFP-RASSF1A (10^4 transfected cells) after 72h with or without induction of YAP1. The cell cycle distribution was analysed by flow cytometry using propidium iodide staining.

As previously indicated, YAP1 displays its oncogenic potential by repression of the TP53 target genes and of *RASSF1A* (Fig. 9B) and by induction of the S-phase (Fig. 10B). The suppressive effect of YAP1 on these genes was subsequently validated by promoter assays in HEK293T cells as shown in figure 11. The luciferase constructs with the individual promoter regions of *CDKN1A, BAX, MDM2*, *RASSF1A* and a synthetic vector with 13 TP53 target sites were sequenced and their activity verified after expression of TP53, TP73 and ΔNp73 (Fig. 11A). The activity of the *RASSF1A* promoter was verified after transfection of Myc and Max (Fig. 11C), since both transcription factors bind to the *RASSF1A* promoter (Charlet *et al*., 2014).

In the YAP1-inducible TREx293 cells, the induction of YAP1 resulted in a decrease in the promoter activity of *TP53* target site (28%; p-value < 0.001), *CDKN1A* (18%; p-value <0.0001), *BAX* (7%; p-value 0.02) and *MDM2* (28%; p-value 0.03) (Fig. 11B). The activity of the *RASSF1A* promoter was also significantly reduced (25%; p-value 0.01) after YAP1 transfection in HEK293T cells (Fig. 11C). To characterise the effect of RASSF1A on the YAP1 target genes, further promoter assays were performed in the YAP1-inducible TREx293 cells after expression of RASSF1A with and without induction of YAP1 (Fig. 11B). Here, RASSF1A neutralized the inhibitory effect of YAP1 on the promoters and activated the promoter activity of *TP53 target site* (28% increase; p-value 0.01)*, BAX* (23%; p-value 0.005) and *CDKN1A* (34%; p-value 0.002) compared to the YAP1 induction (Fig. 11B).

To date there is no published indication for the regulation of *RASSF1A* by YAP1. Since YAP1 activates tumor suppressor genes (*BBC3*) together with TP73 (Matallanas *et al*., 2007), the effect of YAP1 and TP73 on the *RASSF1A* promoter was further analysed by promoter assays both in HEK293T cells as well as in the YAP1-inducible TREx293 cells (Fig. 11C). As previously mentioned, the expression of YAP1 significantly repressed the promoter activity of *RASSF1A* in HEK293T cells by 25% (p-value 0.01). The induction of YAP1 in the TREx293 cells also resulted in a decrease of 16% (p-value 0.06) on the promoter activity of *RASSF1A* (Fig. 11C). In contrast to YAP1, TP73 significantly enhanced the promoter activity of *RASSF1A* (1.9-fold; p-value 0.05). The *RASSF1A* repression by YAP1 was also observed after co-expression of YAP1 with RASSF1A (45%; p-value 0.03) as well as after co-expression of YAP1 with TP73 (67%; p-value 0.04). The ΔNp73 isoform did not affect the promoter activity of *RASSF1A* (Fig. 11C).

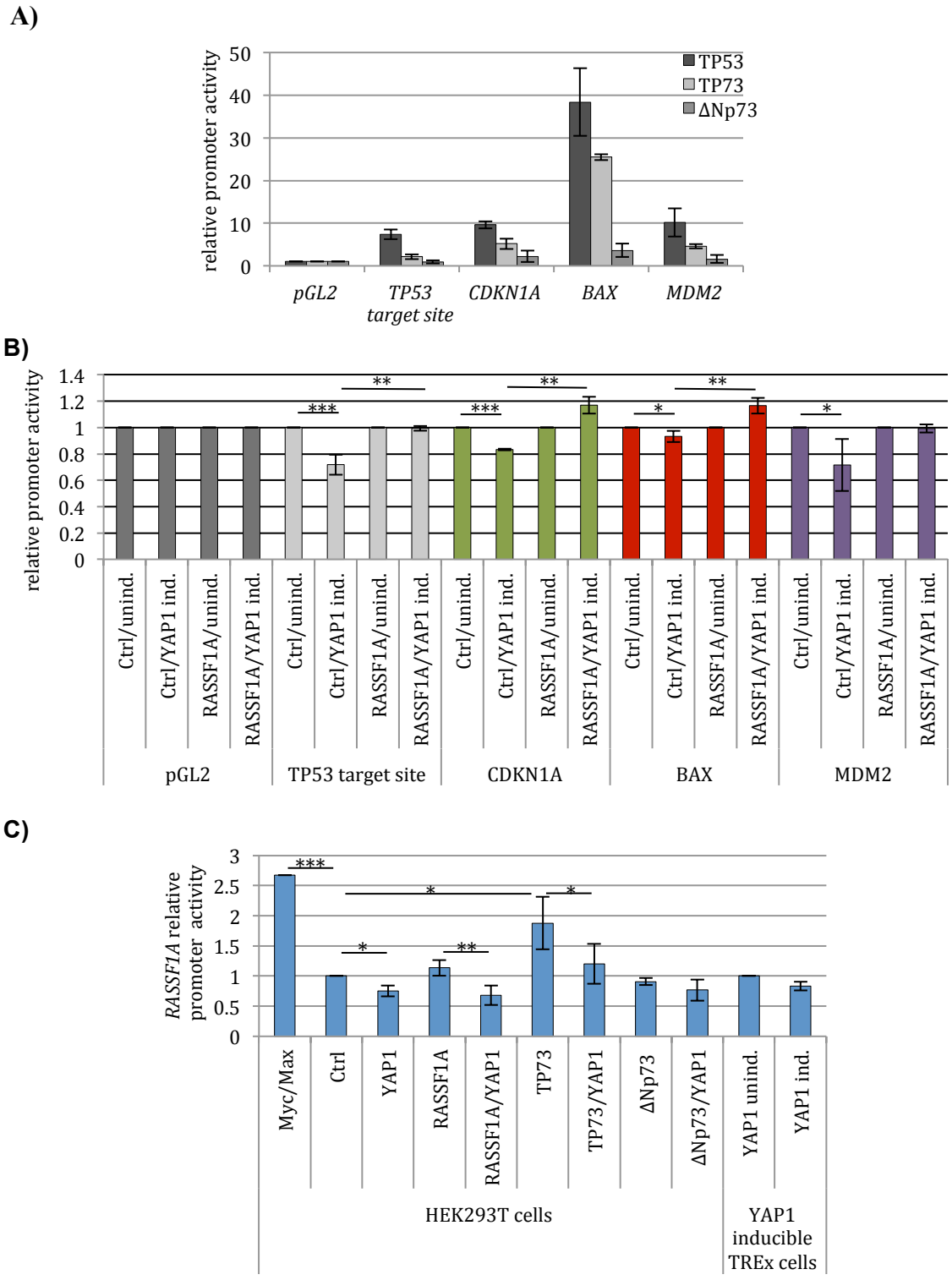

Figure 11: Promoter assays of YAP1 and TP53 target genes. A) Control promoter assays of *BAX, CDKN1A, MDM2* and synthetic *TP53 target sites* after transfection of TP53, TP73 and ΔNp73 in HEK293T cells. **B)** Firefly luciferase activity at the *BAX, CDKN1A, MDM2* and *TP53 target sites* promoters in the YAP1-inducible TREx293 cells after expression of CMV empty vector or RASSF1A and YAP1 induction (YAP1 ind.) or without induction (unind.). Control vector pGL2 empty. **C)** Renilla luciferase activity of *RASSF1A* promoter after transfection of control vector pRL-null empty, RASSF1A, YAP1, TP73 or ΔNp73 and the corresponding co-transfection with YAP1 in HEK293T cells or in TREx293 cells with or without YAP1 induction. Myc and Max were used as positive control (1:1). The data were normalized to the renilla luciferase (B) or firefly luciferase activity (C) and to the empty vector (set to 1). p-values: * $p<0.05$, ** $p<0.01$ and *** $p<0.001$ (t-test).

3.1.5 RASSF1A triggers the translocation of YAP1 into the nucleus

The effect of RASSF1A on the intracellular YAP1 localization is still controversial in the literature. RASSF1A activates the MST/LATS kinase cascade to phosphorylate YAP1 at five serine sites (Zhao *et al*., 2010a). Few reports have demonstrated that the phosphorylation of $YAP1^{S127}$ is involved in nuclear translocation (Matallanas *et al*., 2007). Other authors reported this phosphorylation site as essential for the cytoplasmatic retention and the further degradation of YAP1 (Zhao *et al*., 2007). To further investigate the cellular localization of YAP1 and the effect of RASSF1A on this localization, mCherrry-YAP1 constructs with point mutations at serine 127 (S127A and S127E) were created and compared to YAP1 wild type. For this purpose, the mCherry-YAP1 constructs (wild type or $YAP1^{S127}$ mutants) were co-transfected with GFP-RASSF1A in HEK293T cells and analysed by microscopy after 72h (Fig. 12A). These data are also represented in figure 12B-C after quantification of the YAP1 localization and the nuclear morphology of 100 transfected cells.

Figure 12A indicates that the expression of GFP empty and mCherry empty is distributed all over the cell, both in the nucleus and in the cytosol. RASSF1A was located at the cytoskeleton binding to the microtubules (Fig. 12A). In 74% of the cells, wild type YAP1 was predominantly located in the cytosol. In 26% of the cells, YAP1 was located in both the nucleus and the cytosol (Fig. 12A-B). In contrast to the wild type, both YAP1 mutants were predominantly located in the nucleus, namely in 67% of the cells transfected with the $YAP1^{S127A}$, and 78% of the cells transfected with the $YAP1^{S127E}$ mutant (Fig. 12A-B). The most important observation in this part was that RASSF1A increased the translocation of YAP1 wild type into the nucleus by 37% compared to control cells without RASSF1A (Fig. 12A-B). Moreover, RASSF1A increased the nuclear localization of the YAP1 mutants: 18% increase in translocation in $YAP1^{S127A}$ mutant and 14% increase in $YAP1^{S127E}$ mutant compared to the control cells without RASSF1A. The morphology of the nucleus was also analysed and quantified (Fig. 12C). Here it was observed that the nuclear morphology of the cells with YAP1 wild type was comparable to the mCherry empty control. The YAP1 mutants showed an increased number of deformed nuclei compared to the mCherry control. Also an increase of 5.6% of the mitotic cells was observed in cells with YAP1 wild type and of 4.4% in the cells with $YAP1^{S127A}$. Furthermore, figure 12C indicates that the expression of RASSF1A produced an increase of deformed nuclei and

inhibition of mitosis, especially after co-transfection with YAP1 wild type. In summary, we observed that RASSF1A increased the nuclear translocation of YAP1, repressed mitosis and increased the number of deformed nuclei (Fig. 12A-C). The localization of the phosphorylation mutant YAP1^{S127A} and mimicking mutant YAP1^{S127E} was predominantly nuclear. RASSF1A increased the nuclear localization of both YAP1 mutants and inhibited mitosis (Fig. 12A-C).

A)

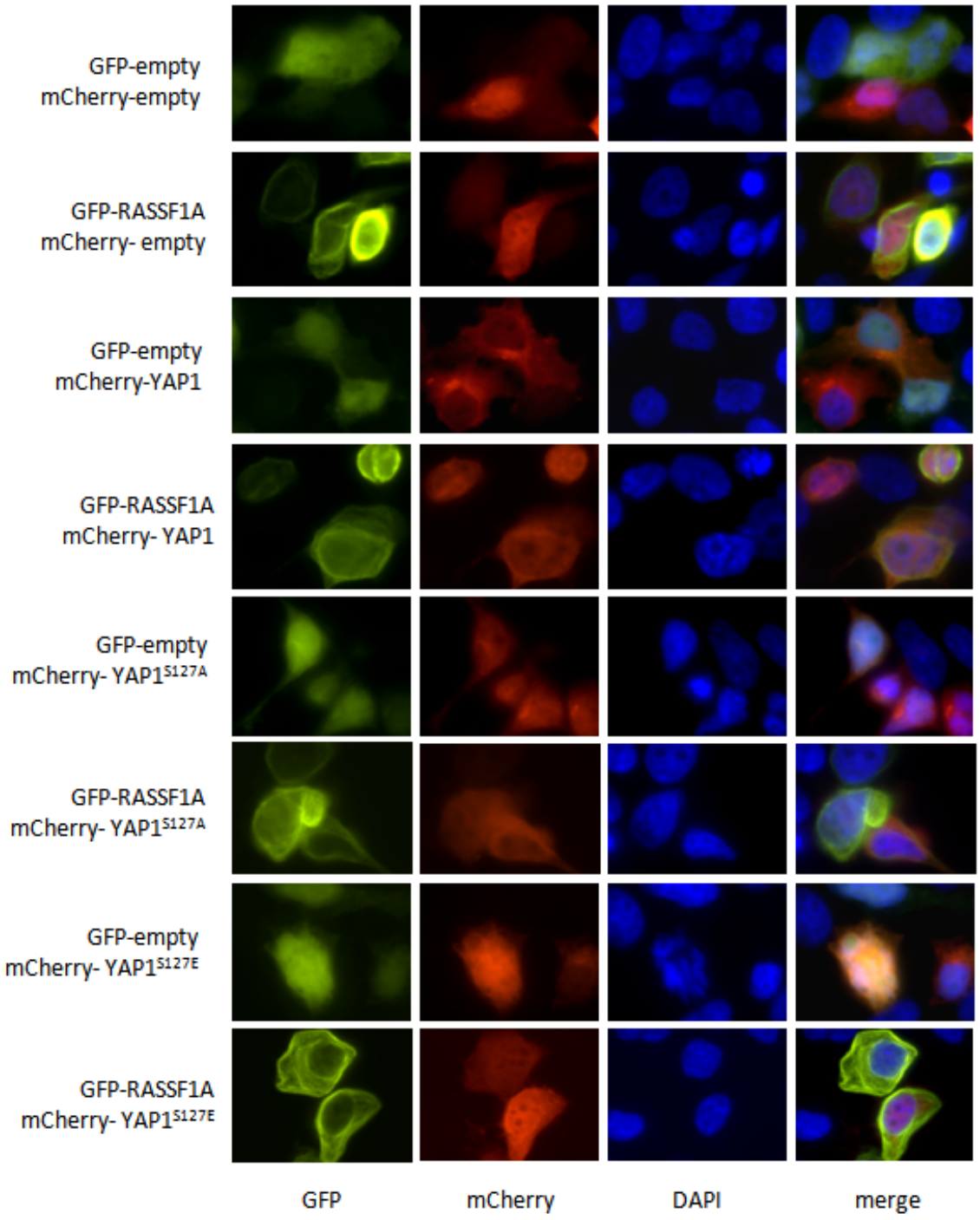

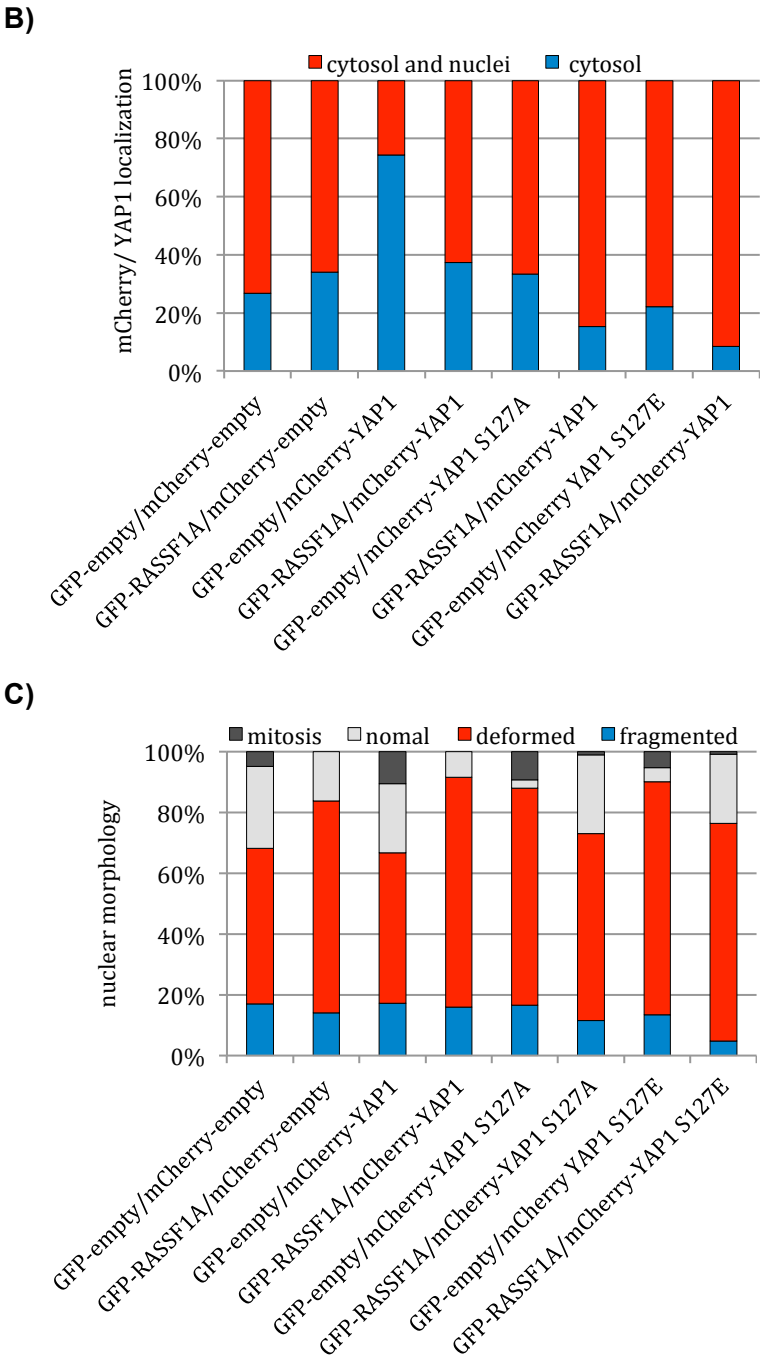

Figure 12: Cellular localization of YAP1 and RASSF1A mediated nuclear translocation. HEK293T cells were co-transfected with mCherry-YAP1 wild type or YAP1^{S127} mutants with GFP-RASSF1A or with the corresponding control plasmids. 72h after transfection, the cells were fixed by formaldehyde and permeabilized using Triton X; the cell nucleus was stained with DAPI and analysed by fluorescence microscopy (magnification of 63X and oil immersion). Via microscopy images, the mCherry localization and nuclear morphology of 100 cells were analysed and quantified using the software Volocity and the inverse microscope Axio Observer.Z1. **A)** Microscopy images of HEK293T cells after co-expression of GFP-empty or GFP-RASSF1A together with mCherry-empty or mCherry-YAP1 wild type or YAP1^{S127} mutants. **B)** Quantification of the cellular localization of mCherry-empty and mCherry-YAP1 wild type or YAP1^{S127} mutants after RASSF1A co-transfection. **C)** Quantification of nuclear morphology after GFP-RASSF1A co-transfection with mCherry-YAP1 wild type or YAP1^{S127} mutants (n=100 cells).

3.1.6 Microarray data confirm the upregulation of *ANKRD1* by YAP1 and RASSF1A and reveal novel target genes

In order to identify novel YAP1 targets, which are regulated by RASSF1A and are involved in the cell cycle arrest or the apoptosis described above, we performed expression analyses by microarrays using the YAP1-inducible TREx293 pool of clones. Therefore, the cells were transfected with GFP or GFP-RASSF1A and with or without YAP1 induction and sorted for GFP positive cells. The RNA from 10^6 million sorted cells was analysed by microarrays (appendix 2). The protein level and expression of YAP1 and RASSF1A in these cells are plotted in figure 13.

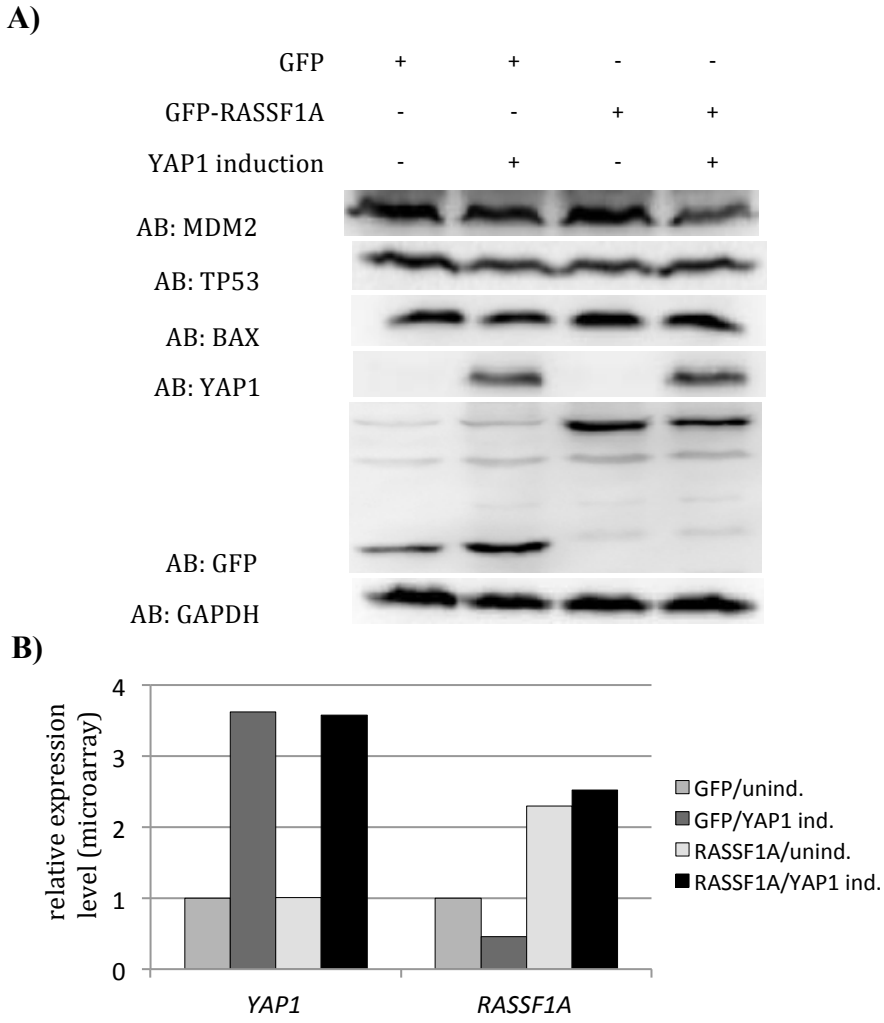

Figure 13: Microarray analysis. The YAP1-inducible TREx293 cells were transfected with GFP-RASSF1A or GFP control plasmid. After 72h, with or without induction of YAP1 by Dox (2 µg/ml), the cells were sorted for GFP positive cells; 250 ng RNA were analysed by microarrays. **A)** Western blot analysis of MDM2, BAX, TP53, YAP1 and GAPDH in the YAP1-inducible TREx293 cells used for the microarrays before sorting by FACS. 10 µg of protein were loaded and separated on a 10% SDS gel and afterwards blotted onto PVDF membrane. **B)** Relative expression of *YAP1* and *RASSF1A* in TREx293 cells obtained by microarrays after normalization to *GAPDH*. The expression levels in control cells (GFP/unind.) were set 1. GFP/unind.: GFP without YAP1 induction; GFP/YAP1 ind.: GFP with YAP1 induction; RASSF1A/unind.: GFP-RASSF1A without YAP1 induction; RASSF1A/YAP1 ind.: GFP-RASSF1A with YAP1 induction.

The protein levels of RASSF1A, YAP1, TP53, BAX and MDM2 in the cells used for the sorting and microarrays were confirmed by western blotting (Fig. 13A). Here, a diminution of the MDM2 level was observed in the cells transfected with RASSF1A and YAP1 induction. Figure 13B shows the expression of *RASSF1A* and *YAP1* in the microarrays on RNA level and the reduction by 50% of *RASSF1A* expression after YAP1 induction.

Subsequently, the results of the microarrays were analysed in further detail and the top up- and downregulated candidate genes were determined (appendix 5 and appendix 6). Table 19 summarizes these top 10 up- and downregulated candidate genes, which were detected in the microarrays to be regulated by RASSF1A and YAP1. The expression levels were normalized to control cells (GFP/unind.) and to the internal microarray controls.

Table 19. Expression of top 10 up- and downregulated genes and selected target genes (bold) after YAP1 induction (YAP1 ind.) and RASSF1A transfection in the YAP1-inducible TREx293 cells.

Gene	GFP/unind.	GFP/YAP1 ind.	RASSF1A/unind.	RASSF1A/YAP1 ind.	
HIF1A-AS2	1,00	7,70	1,16	10,90	Top 10 up-regulated genes
ACTBL2	1,00	2,72	1,16	4,85	
COL12A1	1,00	4,60	1,11	4,41	
CTGF	1,00	2,26	1,34	3,97	
MT-TW	1,00	2,90	2,58	3,64	
ANKRD1	**1,00**	**2,88**	**1,24**	**3,40**	
CYR61	1,00	2,66	1,43	3,26	
CPA4	1,00	2,74	1,24	3,22	
AJUBA	1,00	2,25	1,20	2,77	
SPANXC	1,00	1,69	1,55	2,67	
CDKN1A	**1,00**	**0,64**	**0,84**	**0,91**	
TP53	**1,00**	**0,79**	**0,95**	**0,95**	
BAX	**1,00**	**0,63**	**0,83**	**1,00**	
MDM2	**1,00**	**0,83**	**1,11**	**0,61**	
FOS	1,00	0,92	0,97	0,73	Top 10 down-regulated genes
MAP2K6	1,00	1,15	0,91	0,59	
PINK1	1,00	0,86	0,71	0,56	
TP53I13	1,00	0,81	0,84	0,51	
GDF15	1,00	0,60	0,72	0,46	
FOXD3	1,00	0,74	0,48	0,46	
FGF21	1,00	0,59	0,46	0,45	
ANAPC1P1	1,00	0,65	0,54	0,45	
GH1	1,00	0,57	0,65	0,41	
MAP3K8	1,00	0,40	0,89	0,39	

Table 19 indicates the top ten YAP1 upregulated target genes. The activation of these genes increased further after expression of RASSF1A and YAP1 induction (Table 19). Several candidate genes are already associated with the Hippo pathway and some of them also play

a role in hypoxia, such as *HIF1A-AS2* and *AJUBA*. The Lim domain protein AJUBA has been linked to the Hippo pathway (Das Thakur *et al*., 2010). Other candidates such as *CYR61, ANKRD1* and *CTGF* were previously identified as YAP1 target genes (Li *et al*., 2013; Zhou *et al*., 2016). Other genes like the actin isofom *ACTBL2*, *COL12A1*, which codes for an extracellular matrix protein (Januchowski *et al*., 2014), and the *HIF1A antisense 2*, are not described yet as related to the Hippo pathway and there are only few reports about their functions (Bertozzi *et al*., 2011; Mineo *et al*., 2016).

The expression of the top 10 downregulated genes is repressed by YAP1 alone (see Table 19), but RASSF1A intensified this repression, especially in the genes: *MDM2, FOS, MAP2K6, GDF15, FOXD3* and *FGF21* (Table 19). Other novel candidate genes were also detected; among those genes are regulatory elements such as zinc fingers, microRNAs and other non-coding RNA genes (see Table 21 and Table 22 in appendix 5 and 6).

Additionally, Table 19 shows the expression levels of *ANKRD1, TP53, BAX* and *CDKN1A* according to the microarrays (in bold). The expression of these genes is interesting because *ANKRD1* is a YAP1 target gene, whereas *TP53, BAX* and *CDKN1A* are tumor suppressor genes, which were detected to be repressed by YAP1 as shown in figure 9B. Here, the YAP1 and RASSF1A-induced upregulation of *ANKRD1* (3.4-fold) was verified (Fig. 5C); also the downregulation of *TP53* (0.79-fold), *BAX* (0.63-fold) and *CDKN1A* (0.63-fold) after YAP1 induction was confirmed (Fig. 9B). In addition, the microarrays also suggested that RASSF1A neutralizes the repressive effect of YAP1 on *TP53, BAX* and *CDKN1A* expression (see Table 19).

The microarray data were further validated in three independent biological replicates by qRT-PCR using the YAP1-inducible TREx293 cells (Fig. 14, appendix 7). For this purpose, GFP and GFP-RASSF1A were overexpressed for 72h in the TREx293 cells with and without YAP1 induction. Figure 14 indicates the relative expression of *CTGF, ANKRD1, AJUBA, TP53, BAX* and *CDKN1A* in one representative experiment (Fig. 14). The overexpression of *RASSF1A* and the induction of YAP1 were controlled by semiquantitative PCR as indicated in appendix 7.

Figure 14 indicates that the expression of *CTGF, ANKRD1* and *AJUBA* was significantly enhanced by YAP1: expression increase for *CTGF*: 4.8-fold (p-value< 0.00001); *ANKRD1*:

3.2-fold (p-value< 0.0001) and 2-fold for *AJUBA* (p-value< 0.004). In contrast, the induction of YAP1 repressed the expression of *TP53* by up to 17%; the expression of *BAX* was also reduced by 41% (p-value 0.001), and the expression of *CDKN1A* was repressed by 21% (p-value 0.0004) in comparison to the uninduced cells (Fig 14). The expression of RASSF1A alone did not affect the expression of the candidate genes, but together with YAP1 activated the expression of *ANKRD1* by 70% (p-value 0.02) and the expression of *AJUBA* by 83% (p-value 0.004) (Fig. 14). Moreover, RASSF1A reactivated the expression of the tumor suppressor genes despite of the induction of YAP1. Compared to the YAP1 induced cells, the RASSF1A/YAP1 induced cells showed a significant increase of 17% (p-value 0.01) in *TP53* expression, of 30% in *BAX* expression (p-value 0.007) and of 21% in *CDKN1A* expression (p-value 0.03) (Fig. 14).

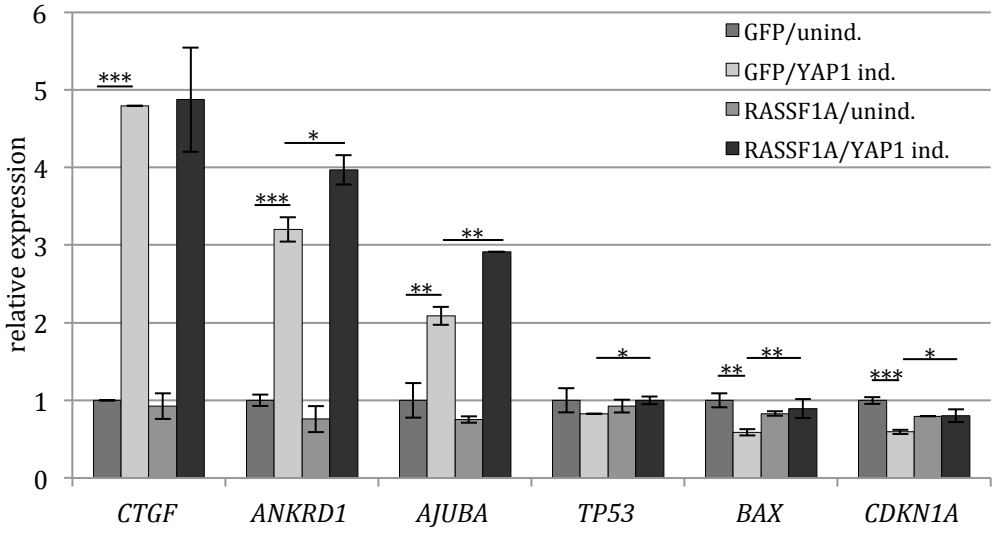

Figure 14: RASSF1A effect on YAP1 target genes. Expression analysis using qRT-PCR of a representative experiment of TREx293 cells after 72h transfection with GFP-RASSF1A or GFP without or with YAP1 induction. Relative expression level of *CTGF, ANKRD1, AJUBA, TP53, BAX* and *CDKN1A* compared to the uninduced control cells (GFP/unind.) and after normalization to *GAPDH*. The standard deviations and p-values were calculated using the technical replicates of the experiment. p-values: * p<0.05, ** p<0.01 and *** p<0.001 (t-test).

The promoter assays plotted in figure 11B-C and the expression data from figure 14 confirmed the data obtained by the microarrays; such as the downregulation by YAP1 of the tumor suppressor genes (*TP53, BAX* and *CDKN1A*) and their reactivation after RASSF1A expression. In addition, figure 5C and figure 14 validated the co-regulation of *ANKRD1* expression by YAP1 and RASSF1A.

3.1.7 The Hippo pathway regulates the expression of *ANKRD1*

As previously indicated, the expression of *ANKRD1* is regulated by YAP1 and RASSF1A. The Hippo pathway is activated by RASSF1A through the SARAH (Sav/Rassf/Hpo) domain, which interacts with MST2 to phosphorylate LATSs and YAP1 (Dittfeld *et al.*, 2012). The focus of this part of our work was to determine if the regulation of *ANKRD1* occurs via the Hippo signalling. For this purpose, expression analyses were performed using HEK293T cells with overexpression of YAP1, RASSF1A wild type and RASSF1A mutant with depletion of the SARAH domain (RASSF1A-ΔSARAH) (Fig. 15A). The obtained results were further validated by promoter assays using the YAP1-inducible TREx293 cells and the promoter of *ANKRD1* in a renilla luciferase vector. The promoter activity was measured after overexpression of RASSF1A wild type or RASSF1A-ΔSARAH mutant and YAP1 induction (Fig. 15B).

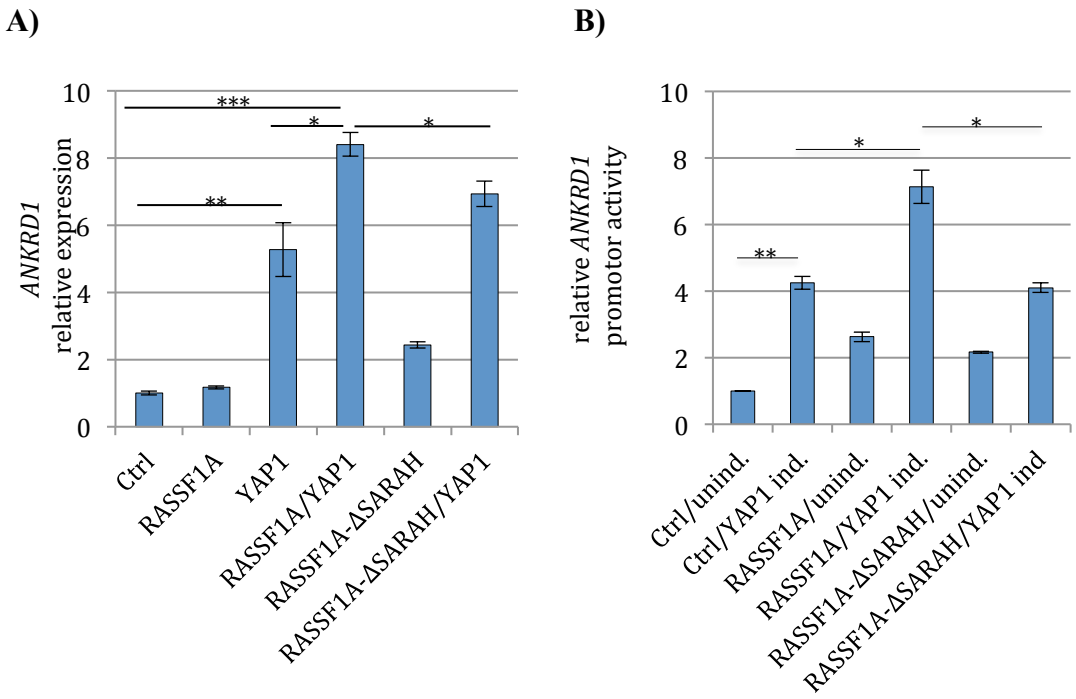

Figure 15: *ANKRD1* expression is regulated via the Hippo pathway. A) Representative figure of the relative *ANKRD1* expression in HEK293T cells 72h after transfection of RASSF1A, RASSF1A-ΔSARAH and/or co-transfected with YAP1. The values were normalized to *GAPDH* expression and to the normalized values for the control cells (empty vector) were set to 1. **B)** Representative figure of the relative *ANKRD1* promoter activity after RASSF1A (wild type or ΔSARAH mutant) and control vector (Ctrl) transfection with and without induction of YAP1 in the YAP1-inducible TREx293 cells. The promoter activity was normalized to the firefly luciferase activity (pGL2) and the control cells (Ctrl/unind.) was set to 1. The standard deviations and p-values were calculated using the technical replicates of the experiment. p-values: * $p<0.05$, ** $p<0.01$ and *** $p<0.001$ (t-test).

Figure 15A shows the relative expression of *ANKRD1* after overexpression of RASSF1A-ΔSARAH mutant in comparison to RASSF1A wild type. As previously demonstrated, YAP1 alone induced the expression of *ANKRD1,* and the co-expression of YAP1 with RASSF1A wild type further increased the expression of *ANKRD1* (Fig. 5, Fig. 14 and Fig. 15A). The RASSF1A-ΔSARAH mutant alone induced the expression of *ANKRD1*. In contrast, RASSF1A-ΔSARAH mutant co-expressed with YAP1 did not increase the expression of *ANKRD1* compared to the co-transfection of YAP1 with the RASSF1A wild type (Fig. 15A).

The data indicated in figure 15A were further validated by promoter assays. For this purpose, 606 bp of the *ANKRD1* promoter region was cloned into a renilla luciferase vector (appendix 1) and analysed in the YAP1-inducible TREx293 cells after YAP1 induction and expression of RASSF1A or RASSF1A-ΔSARAH mutant (Fig. 15B). The induction of YAP1 significantly induced the promoter activity of *ANKRD1* (p-value 0.001). The induction of the *ANKRD1* promoter activity by YAP1 and RASSF1A (p-value 0.01) was also observed (Fig. 15B). RASSF1A-ΔSARAH mutant and the wild type RASSF1A activated the promoter activity of *ANKRD1*; but interestingly, the RASSF1A-ΔSARAH mutant in combination with YAP1 did not affect the promoter activity of *ANKRD1* (Fig. 15B). In comparison to the YAP1/RASSF1A wild type, the RASSF1A-ΔSARAH was unable to further increase the promoter activity of *ANKRD1* (p-value 0.01) (Fig. 15B).

3.1.8 *ANKRD1* is epigenetically silenced in human cancer and represents a potential tumor suppressor gene

To date, ANKRD1 is described as a cardiac protein (Ishiguro *et al*., 2002; Torrado *et al*., 2005). To further characterise the cellular function of *ANKRD1*, its expression level was analysed using RNA from normal tissues samples and from different human cancer cell lines (Fig. 16).

ANKRD1 is highly expressed in heart, 9-fold more than in liver and 5-fold more than in lung, but it is absent in breast tissue (Fig. 16A). The expression of *ANKRD1* and *YAP1* was analysed by qRT-PCR in different human cancer cell lines, including lung cancer (H322, A549 and A427), prostate cancer (LNCaP and PC-3), breast cancer (MCF7 and T47D) and

skin cancer (MeWo and Sk-Mel-28); the expression levels of *YAP1* and *ANKRD1* in the cell lines were plotted relative to those in HEK293T (Fig. 16B). Endogenous *YAP1* expression was observed in all analysed cell lines. In A427 and T47D cells, the expression of *YAP1* was 6-fold and 15-fold higher than in HEK293T cells, respectively (Fig. 16B). This figure also indicated the expression of *ANKRD1* in the cell lines. Interestingly *ANKRD1* was not expressed in LNCaP, MCF7 and in MeWo cells; whereas in T47D it was expressed up to 4-fold higher than in HEK293T cells (Fig. 16B).

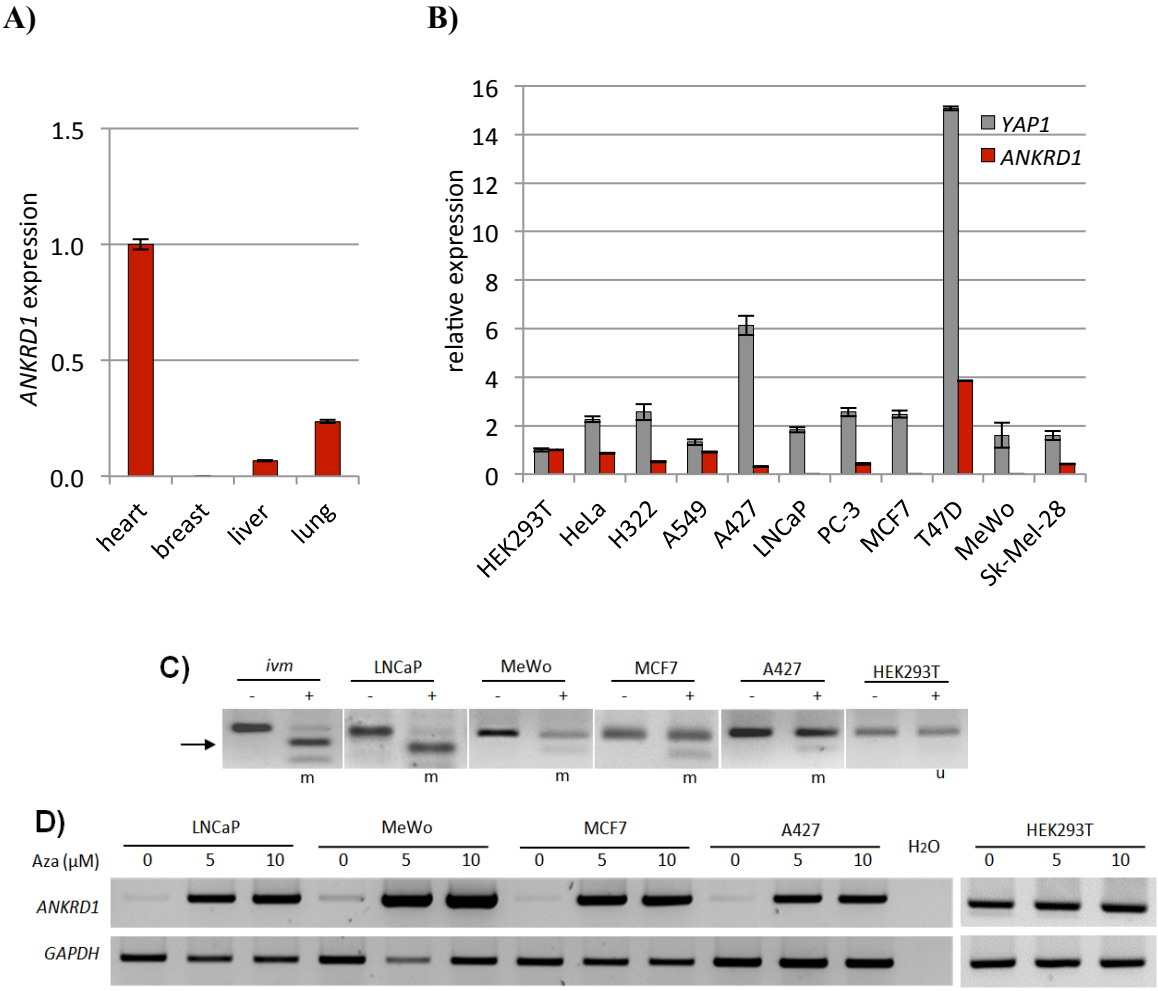

Figure 16: Expression of *ANKRD1* in normal tissue and cancer cell lines. A) Expression of *ANKRD1* was analysed by qRT-PCR in heart, breast, liver and lung tissues. The expression levels were normalized to *GAPDH*. The normalized expression of *ANKRD1* in heart was set to 1. **B)** Expression of *ANKRD1* and *YAP1* in cell lines. The expression analysis was performed by qRT-PCR and normalized to *GAPDH* expression; the normalized expression in HEK293T cells was set to 1. **C)** CoBRA analysis of the methylation status of *ANKRD1* promoter in LNCaP, MeWo, MCF7, A427 and HEK293T cells. A fragment of 139 bp was amplified by PCR using bisulfite converted DNA and subsequently digested with *TaqI* enzyme (+) or without enzyme as control (-). *ivm: in vitro* methylated DNA. m: methylated. u: unmethylated. Arrow: digested fragments. **D)** Semiquantitative PCR of *GAPDH* and *ANKRD1* expression in LNCaP, MeWo, MCF7, A427 and HEK293T cells after 4d of 5-Aza-2'-deoxycytidine (Aza) (0,5,10 µM) treatment.

The inactivation of *ANKRD1* in LNCaP, MeWo, MCF7 and A427 cells was further investigated. For this purpose, the methylation status of the promoter region of *ANKRD1* was analysed by CoBRA in these cell lines (Fig. 16C). The CoBRA analysis in figure 16C indicated that the *ANKRD1* promoter was methylated in LNCaP, MeWo, A427 and MCF7 cells, whereas it was unmethylated in HEK293T (Fig. 16C). The expression analysis shown in figure 16D verified that *ANKRD1* was downregulated in these cell lines, and a reexpression of *ANKRD1* was observed after cell treatment with 5 or 10 µM Aza (Fig. 16D), which indicated that *ANKRD1* was epigenetically silenced in LNCaP, MeWo, A427 and MCF7 cells (Jiménez *et al.* 2017).

To further characterise the function of ANKRD1, colony formation assays were performed by overexpressing ANKRD1 or the respective empty control vector in LNCaP, A427, HEK293T and in T47D cells (Fig. 17A-C). In addition, growth curves of A549 and LNCaP cells were generated to determine the cellular proliferation after expression of ectopic ANKRD1 (Fig. 17D).

Figure 17A and 17C indicate that ANKRD1 expression significantly reduced the number of colonies in LNCaP (42% reduction; $p<0.001$), in A427 (80%; $p<0.001$) and in HEK293T cells (87%; $p<0.0001$) compared to transfected control cells. In contrast, ANKRD1 increased the colony number in T47D cells (p-value< 0.0001) in comparison to the control cells (Fig. 17A-C). The overexpression of ANKRD1 was controlled by semiquantitative PCR as indicated in figure 17B.

In figure 17D, A549 and LNCaP cells were transfected either with ANKRD1 or with the empty control vector and selected for 1 week with G418. Afterwards, 10^5 cells were plated and after 16h the exact number of cells was quantified (day 0 (0d)). Every 24h the cell number was quantified and the growth ratio was determined by normalization to the cell number at 0d. After two and three days, we observed a significant decrease in the growth ratio of the cells transfected with ANKRD1, whereas in cells transfected with the control plasmid, we observed exponential growth in A549 or duplication after 48h in LNCaP cells (Fig. 17D). In A549 cells, the growth ratio of the cells with ANKRD1 decreased significantly after 2d (p-value 0.01) and after 3d (p-value 0.02) compared to the control cells; the cells with ANKRD1 showed a 2-fold reduction of proliferation compared to the control cells (Fig. 17D). In LNCaP cells, the overexpression of ANKRD1 produced

apoptosis. After three days, the control cells triplicated their cell number, whereas in the cells transfected with ANKRD1, the cell number was similar to that of the initial day 0 (0d) (p-value 0.05) (Fig. 17D).

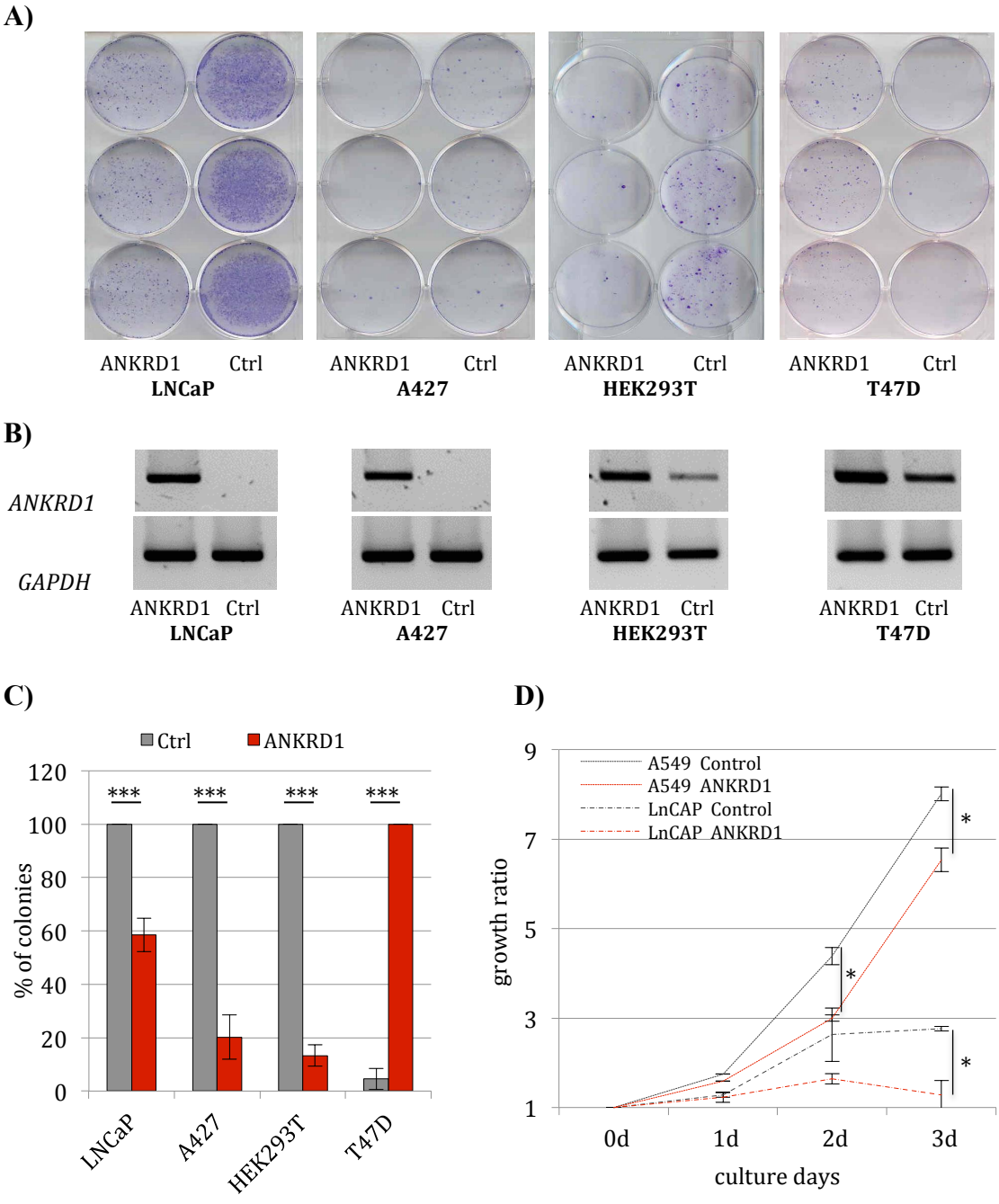

Figure 17: ANKRD1 reduced colony formation and proliferation of cancer cells. A) Colony formation assay. LNCaP, A427 and T47D cells were transfected either with Flag-empty vector (Ctrl) or with Flag-ANKRD1 and further selected with G418 for three weeks. HEK293T cells were transfected with either pCDNA4TO empty vector (Ctrl) or with pCDNA4TO-ANKRD1 and selected with Zeocin for three weeks. The colonies were stained with Giemsa. **B)** Overexpression controls by semiquantitative PCR for *ANKRD1* overexpression and *GAPDH*. **C)** Percentage of colony number of the different cell lines. **D)** Growth curve of A549 und LNCaP pool of cells after stable transfection of Flag-empty vector (Control) or Flag-ANKRD1. 10^5 cells were plated on 0d and after 1d, 2d and 3d the cell growth ratios of three technical triplicates were measured using the Neubauer counting chamber. The measured growth ratio is given relative to day 0 (0d). p-values: * $p<0.05$ and *** $p<0.001$ (t-test).

3.1.9 ANKRD1 activates the expression of *CDKN1A, BAX* and *TP53*

ANKRD1 was demostrated to inhibit colony formation and cell growth (Fig. 18). In 2010 Kojic *et al.* have suggested a role of ANKRD1 as a co-activator of TP53 (Kojic *et al.*, 2010). In this part of the study, the effect of ANKRD1 on the expression of the TP53 target genes was further investigated (Fig. 18). For this purpose, expression analysis and promoter assays were performed in HEK293T cells after transfection of either ANKRD1 or of the control vector (Fig. 18A-B). Furthermore, an inducible ANKRD1 TREx293 cell line was created and the expression of the TP53 target genes was analysed after induction of *ANKRD1* with Dox (Fig. 18C).

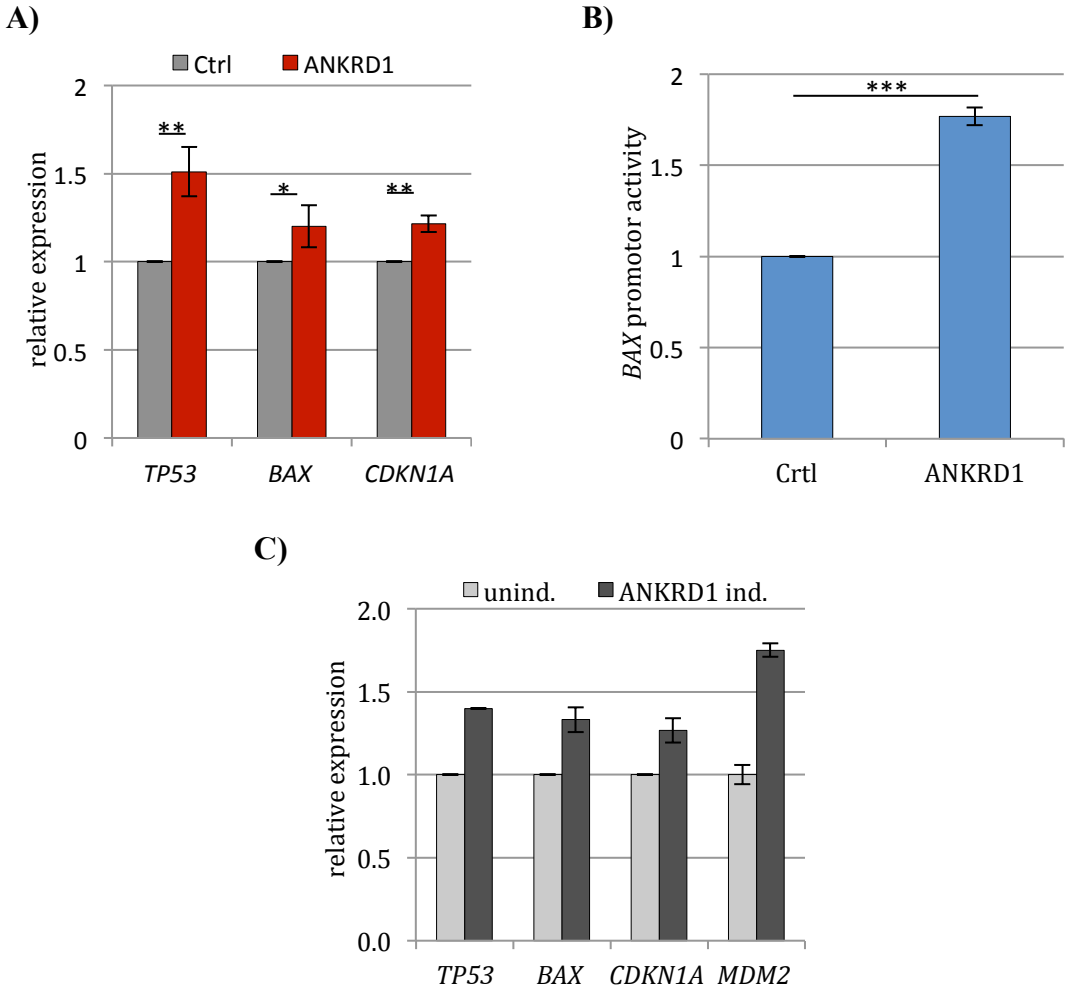

Figure 18: ANKRD1 mediates the activation of *CDKN1A*, *BAX* and *TP53*. **A)** Relative expression of *TP53, BAX* and *CDKN1A* in HEK293T cells 72h after expression of Flag-empty vector (Ctrl) or Flag-ANKRD1. The expression was measured by qRT-PCR and normalized to *GAPDH* and to the control cells (set to 1). **B)** ANKRD1 activates the promoter activity of *BAX*. HEK293T cells were transfected for 24h with Flag-empty vector (Ctrl) or Flag-ANKRD1 and either with pGL2 empty or pGL-BAX vector. pRL-null was used as control for transfection efficiency. The promoter activity was normalized to the renilla luciferase (pRL-null) and the pGL2 empty vector was set to 1. **C)** Relative expression of *TP53, BAX* and *CDKN1A* in ANKRD1-inducible TREx293 cells with and without induction with Dox (2 µg/ml). The expression was measured by qRT-PCR and normalized to *GAPDH* and to the uninduced cells (set to 1). p-values: * $p<0.05$, ** $p<0.01$ and *** $p<0.001$ (t-test).

Figure 18A indicates that in HEK293T cells, the ectopic expression of *ANKRD*1 upregulated the mRNA levels of *TP53* (1.5-fold; p-value 0.003), of *BAX* (1.2-fold; p-value 0.04) and of *CDKN1A* (1.2-fold; p-value 0.002). Furthermore, the promoter assays in figure 18B revealed the significant activation of the *BAX* promoter by ANKRD1 (1.8-fold, $p<0.001$) in comparison to the control cells (Fig. 18B). In the ANKRD1-inducible TREx293 cell line, the induction of ANKRD1 also resulted in the upregulation of *TP53* (1.4-fold), *BAX* (1.3-fold), *MDM2* (1.7-fold) and *CDKN1A* (1.3-fold, Fig. 18C). The overexpression and induction of ANKRD1 were validated by qRT-PCR and western blotting as indicated in appendix 8.

In summary, our data show that *ANKRD1* is silenced by promoter methylation in various cancer cell lines. In addition, ANKRD1 is capable of inhibiting colony formation and cell growth. Further analyses revealed that it significantly activates the expression of *TP53, BAX*, *MDM2* and *CDKN1A*.

3.1.10 RASSF1A-YAP1-ANKRD1 regulates TP53 via MDM2

The previous experiments demonstrated that YAP1/RASSF1A and ANKRD1 modulate the expression of the TP53 target genes *BAX* and *CDKN1A*. The tumor suppressor gene TP53 is known to be regulated by posttranslational modifications, and its major regulator is MDM2 (Kussie *et al*., 1996; Momand *et al*., 1992; Oliner *et al*., 1993). Interestingly, our microarray data displayed a downregulation of *MDM2* mRNA levels (0.61-fold) by RASSF1A expression and YAP1 induction (Table 19). The transcriptional repression of MDM2 by RASSF1A and YAP1 could not be validated, neither by qRT-PCR nor by promoter assay (Fig. 11B). However, at the protein level, a decrease in MDM2 expression was observed in the cell lysates from the YAP1-inducible TREx293 cells, which were sorted and used for the microarrays (Fig. 13A).

In this part of the study, the protein level of YAP1, TP53, BAX and MDM2 were further analysed (Fig. 19). For this purpose, HEK293T cells were co-transfected either with RASSF1A and YAP1 or with ANKRD1 for 72h. Afterwards, the cell lysates were separated by SDS-PAGE and transferred to a PVDF membrane by western blotting (Fig. 19A). The endogenous protein amounts of TP53, BAX, MDM2 and the overexpression of YAP1 were quantified using the ImageJ software and plotted in figure 19B-C.

Figure 19A indicates one representative western blot from five independent biological replicates. After 72h co-transfection of RASSF1A with YAP1, a significant decrease of MDM2 (40% reduction; p-value 0.05) compared to the controls was observed. In addition, an increase in TP53 and BAX (1.4-fold) levels was detected. Interestingly, the overexpression of ANKRD1 also resulted in a decrease of the MDM2 level (0.6-fold, $p<0.001$) and in an increase of TP53 (1.3-fold; p-value 0.03) and BAX level (1.8-fold) (Fig. 19A-B). These results correlated with the measured decrease of MDM2 level detected in the YAP1-inducible TREx293 cells from figure 13A, in which RASSF1A expression and YAP1 induction resulted in a decrease of MDM2 protein level by 30%. Additionally, figure 19C indicates the YAP1 level in the analysed blots. An increase of YAP1 protein level was measured after overexpression of RASSF1A (Fig. 10A and 19C), which suggests that RASSF1A stabilises YAP1 on the protein level and induces its translocation into the nucleus according to the results presented in figure 12.

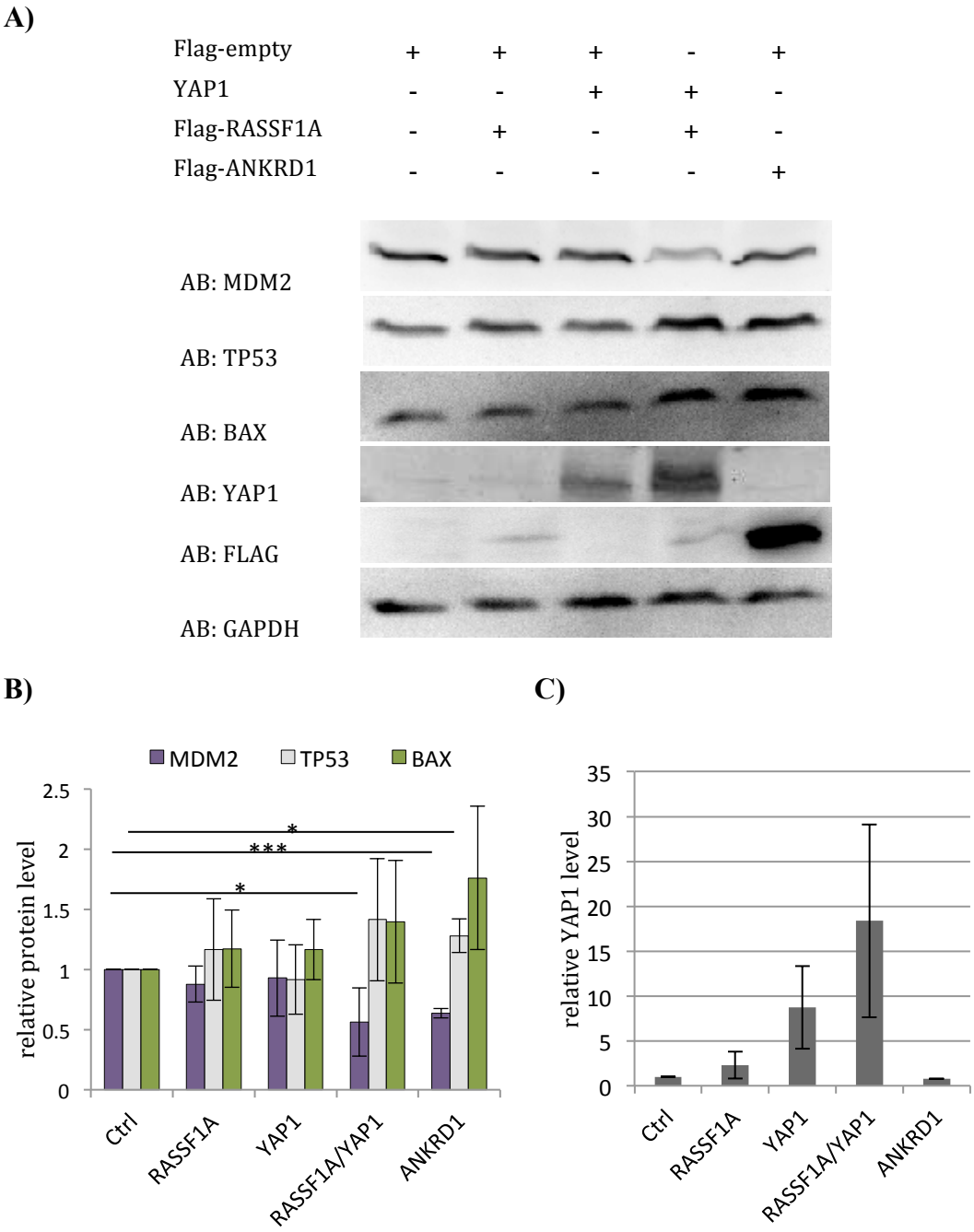

Figure 19: Decrease of MDM2 through the Hippo pathway. A) Representative western blot of overexpression of Flag-empty, Flag-RASSF1A, Flag-YAP1, Flag-ANKRD1 and co-transfection of Flag-RASSF1A with Flag-YAP1 after 72h in HEK293T cells. **B)** Quantification of protein levels of MDM2, TP53, GAPDH and BAX from 5 experiments after overexpression in HEK293T cells. **C)** Quantification of the protein level of YAP1. The protein levels were quantified by ImageJ and normalized to GAPDH and to the control lysates (set to1). p-values: * $p<0.05$, ** $p<0.01$ and *** $p<0.001$ (t-test).

In summary, the co-expression of RASSF1A and YAP1, as well as the expression of ANKRD1 resulted in a decrease of MDM2 at the protein level, whereas the TP53 and BAX levels increased.

3.1.11 ANKRD1 interacts with TP53 and MDM2

To verify the interaction of ANKRD1 with TP53 reported by Kojic *et al.* (2010) and to further investigate a possible protein-protein interaction of ANKRD1 with MDM2, Co-IPs of ectopic ANKRD1 with endogenous TP53 and MDM2 were performed. HEK293T cells were transfected for 72h either with the control empty vector or with a vector containing Flag- or YFP-ANKRD1 (Fig. 20). The Co-IPs were performed using anti Flag-tag- or anti GFP-agarose beads respectively and analysed by western blotting as indicated in figure 20.

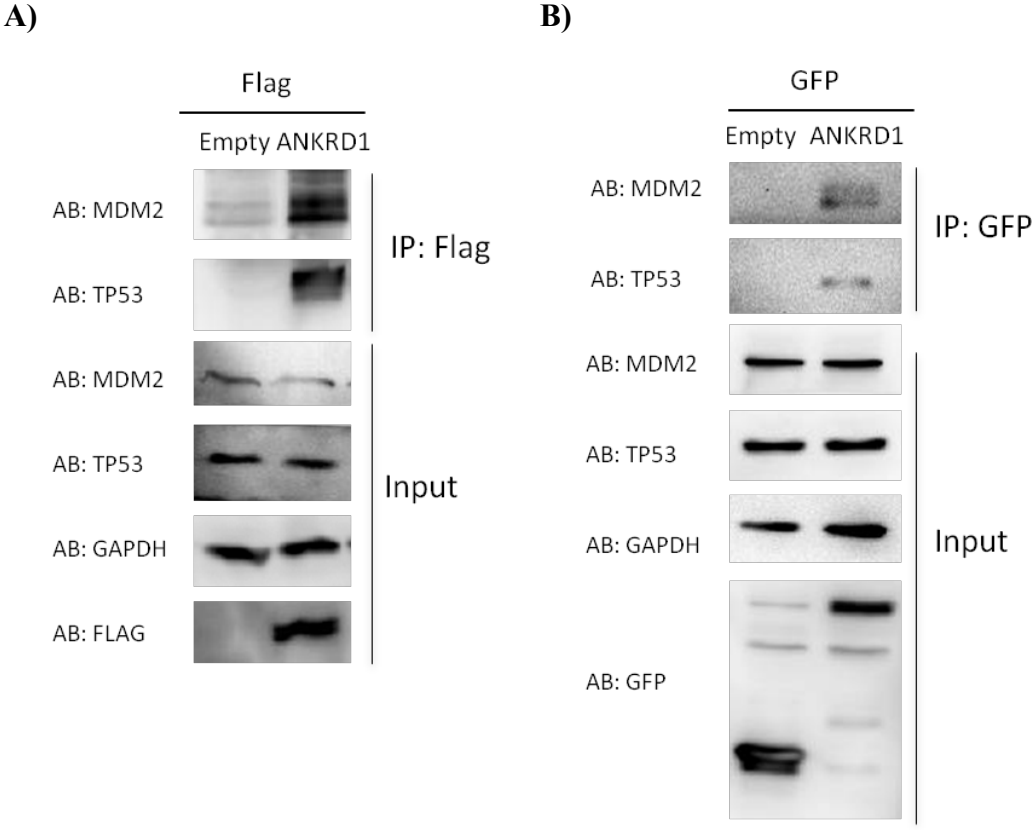

Figure 20: ANKRD1 interacts with TP53 and MDM2. A-B) Co-immunoprecipitation of ANKRD1 with endogenous TP53 and MDM2 from HEK293T cell lysates after 72h transfection of Flag-/YFP-empty vector or Flag-/YFP-ANKRD1. 10 µg of protein lysate before IP were used as input. The IPs were performed using Flag-tag- or anti GFP-agarose beads after ON incubation with the protein lysates. The input and IPs were loaded on a 10% SDS gel and separated by SDS-PAGE and afterwards blotted onto PVDF membrane. The co-immunoprecipitated proteins and the respective controls in the input were detected using the antibodies as indicated in Table 1.

In figure 20, the signal of the input lysates indicates the overexpression of ANKRD1 as demonstrated both with the Flag antibody (Fig. 20A) as well as with the fusion protein with GFP (Fig. 20B). GAPDH was used as loading control. Furthermore, endogenous TP53 and MDM2 were detected both in the cells transfected with the empty vectors as well in the cells with the ANKRD1 overexpression (Fig. 20A-B). It is important to emphasize that the

decrease of MDM2 level was observed in the input after overexpression of Flag-ANKRD1 (Fig. 20A); in the cells with GFP-ANKRD1, we did not directly observe such a decreased MDM2 expression; however, since the GAPDH level between the two samples was apparently different, this effect on MDM2 expression may be occluded by the varying GAPDH level (Fig. 20B).

The interaction of ANKRD1 with TP53 was confirmed both with Flag-ANKRD1 as well as with GFP-ANKRD1 (Fig. 20A-B). Moreover, an interaction of ANKRD1 with endogenous MDM2 was detected with the Flag-ANKRD1 co-IP (Fig. 20A) and further validated with the GFP-ANKRD1 (Fig. 20B). These results suggest that ANKRD1 can interact with MDM2 and with TP53.

3.1.12 ANKRD1 knockdown results in a decreased *TP53*, *BAX*, *CDKN1A* and *MDM2* expression

To verify the involvement of ANKRD1 in the regulation of the TP53 target genes obtained previously, gene-silencing experiments using siRNA against ANKRD1 were performed and analysed by qRT-PCR (Fig. 21). HEK293T cells were transfected with control siRNAs or with siRNAs against human ANKRD1. After 4d transfection, the cells were harvested and the gene expression was further analysed by qRT-PCR as indicated in figure 21.

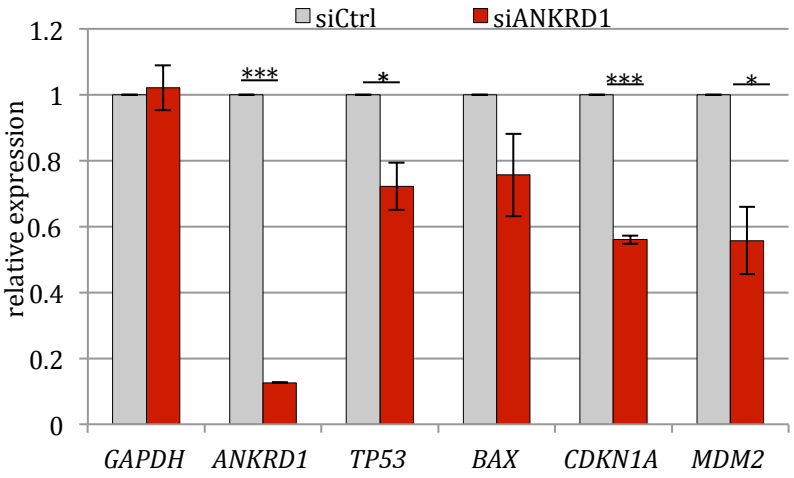

Figure 21: ANKRD1 knockdown represses gene expression of TP53 target genes. HEK293T cells were transfected with a pool of siRNA controls or with a pool of siRNA against ANKRD1. Gene expression of *ANKRD1* and target genes were analysed by qRT-PCR. The expression levels were normalized to *GAPDH* and to the control siRNA (set to 1). p-values: * $p<0.05$, ** $p<0.01$ and *** $p<0.001$ (t-test).

The expression of ANKRD1 was significantly reduced by 80% (p-value<0.001) after the gene-specific knockdown compared to the control siRNA (Fig. 21); furthermore the knockdown of ANKRD1 caused a decrease in the expression of *TP53* (reduction of 28%; p-value 0.03), *BAX* (24%; p-value 0.1), *CDKN1A* (44%; p-value<0.001) and *MDM2* (44%; p-value 0.02), which confirmed the hypothesis that ANKRD1 acts a potential tumor suppressor gene by co-regulation of the TP53 target genes (Fig. 21).

In this part of the study it was demonstrated that RASSF1A and YAP1 co-regulates the expression of *ANKRD1* through the Hippo pathway. In addition, ANKRD1 inhibits colony formation and cell growth by significant activation of *TP53, BAX* and *CDKN1A* and induces the destabilisation of MDM2 levels. Moreover, ANKRD1 interacts with TP53 and MDM2. In addition, the silencing of *ANKRD1* by promoter methylation or its knockdown by siRNA produced a significant decrease in the expression of TP53 target genes.

3.2 Role of the C-terminal members of the RASSF in the Hippo pathway

The RAS association domain family (RASSF) encodes for 10 highly conserved tumor suppressor genes. Six members of the RASSF gene family (RASSF1 to RASSF6) encode a SARAH domain suggesting a possible role in the regulation of the Hippo pathway (Dittfeld *et al*., 2012; Richter *et al*., 2009). To date, there is not much information available on the cellular function of these genes; however, few reports have demonstrated an inactivation of these genes by promoter hypermethylation in some cancer types e.g. *RASSF2* and *RASSF5* are hypermethylated in merkel cell carcinoma and in pheochromocytoma (Richter *et al*., 2013; Richter *et al*., 2015). The aim of this part of the study was the comparative analysis of the effect of the C-terminal RASSF members on the regulation of YAP1 target genes.

3.2.1 Aberrant promoter methylation of C-terminal RASSFs in liver tumors

As indicated in appendix 3 and in Jiménez *et al.* (2017), the promoter methylation status of the Hippo core components (*RASSF1A, MST1, MST2, WW45, LATS1, LATS2* and *YAP1*) was analysed by CoBRA in DNA samples from five primary liver tumors compared to the corresponding matched normal tissues. Here, only *RASSF1A* presented a specific tumor methylation (Jiménez *et al*. 2017, appendix 3). Subsequently, the promoter methylation of the other C-terminal RASSFs was analysed and compared to the methylation status of *RASSF1A* using the same liver cancer and normal samples (Fig. 22).

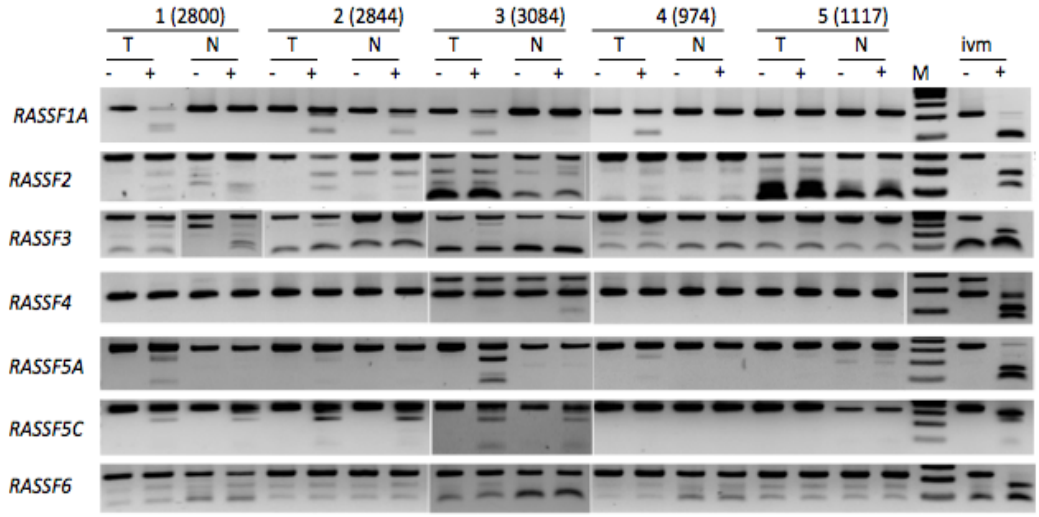

Figure 22: Methylation analysis of the promoter region of C-terminal RASSFs in liver tumors. Combined bisulfite restriction analysis of the promoter region of *RASSF1A, RASSF2, RASSF3, RASSF4*, both isoforms of *RASSF5* (*A* and *C*) and *RASSF6* in liver tumors (T) compared to matched normal samples (N). Positive control: *in vitro* methylated DNA (*ivm*). Mock digest (-); PCR product digested with enzyme (+). Experiment performed by B.Sc. S. Kürschner.

In figure 22, the promotor methylation of *RASSF2, RASSF3, RASSF4, RASSF5A, RASSF5C* and *RASSF6* were analysed by CoBRA and compared to the methylation of *RASSF1A*. *RASSF1A* was found to be methylated in 3 out of 5 liver tumors (patients: 1(2800), 3(3084) and 4(974)). The promoter of *RASSF2* was methylated only in the tumor sample of patient 1(2800). The promoter region of *RASSF3* was tumor-specifically methylated in the sample of patient 2(2844) and patient 3(3084). The promoter of *RASSF5A* was detected as methylated in four DNA tumor samples compared to DNA of the corresponding matched normal tissues (patiente 1(2800), 2 (2844), 3(3084) and 4(974)) (Fig. 22).

In contrast, the promoter region of *RASSF4* was found to be methylated in one normal tissue (patient 3(3084)). *RASSF5C* is methylated both in tumor as well in normal tissue in the patients 1(2800), 2(2844) and 3(3084); the DNA of the other patients was found to be unmethylated, both in tumor as well in normal tissue (Fig. 22). The promoter of *RASSF6* was found to be unmethylated in all patients (Fig. 22). In summary, our data indicated that the methylation status of the C-terminal RASSFs was heterogeneous in the analysed DNA samples, nevertheless RASSF1A, RASSF2, RASSF3 and RASSF5 presented a tumor-specific promoter methylation. This result needs to be confirmed in a larger set of samples.

3.2.2 C-terminal RASSFs affect the cell cycle

The C-terminal RASSF family members encode a SARAH interaction domain, which e.g. interacts with MST2 to activate the Hippo pathway (Cooper *et al*., 2009; Schagdarsurengin *et al*., 2010; Song *et al*., 2010). To further analyse the function of the C-terminal RASSFs regarding the regulation of the Hippo signalling, the YAP1-inducible TREx293 cells were transfected with the respective C-terminal GFP-RASSFs or GFP-MSTs constructs and the cell cycle distribution was analysed by flow cytometry 72h after induction of *YAP1* as described in 3.1.4 (Fig. 23).

Figure 23 indicates the cell cycle distribution of the YAP1-inducible TREx293 cells after transfection of the GFP-RASSF1A, GFP-RASSF2, GFP-RASSF3, GFP-RASSF4, GFP-RASSF5, GFP-RASSF6 and GFP-MST1/MST2 with and without induction of YAP1. The overexpression of GFP-RASSF1A and GFP-empty vector were used as controls. As described in figure 10, YAP1 leads the cells into the S-phase and RASSF1A arrests the

cells in the G0-G1 phase and inhibits the proliferative effect of YAP1 (Fig. 10B). In this additional experiment, the YAP1 and RASSF1A transfected cells exhibited the same pattern as in figure 10B (Fig. 23). Interestingly, the co-expression of MST1 and MST2 showed the same effect as that of YAP1, namely a significant increase of cells in the S-phase (*chi*-square test; p-value< 0.0001) (Fig. 23). In contrast, the C-terminal RASSFs, with exception of RASSF2, counteract the S-phase induction by YAP1 thus accumulating the cells in the G0-G1 phase (p-values< 0.0001) as compared to the control cells and to the cells transfected with RASSF1A (Fig. 23). In contrast, the expression of RASSF2 alone and together with YAP1 resulted in a cell accumulation in the G2-M phase (p-value< 0.0001, Fig. 23).

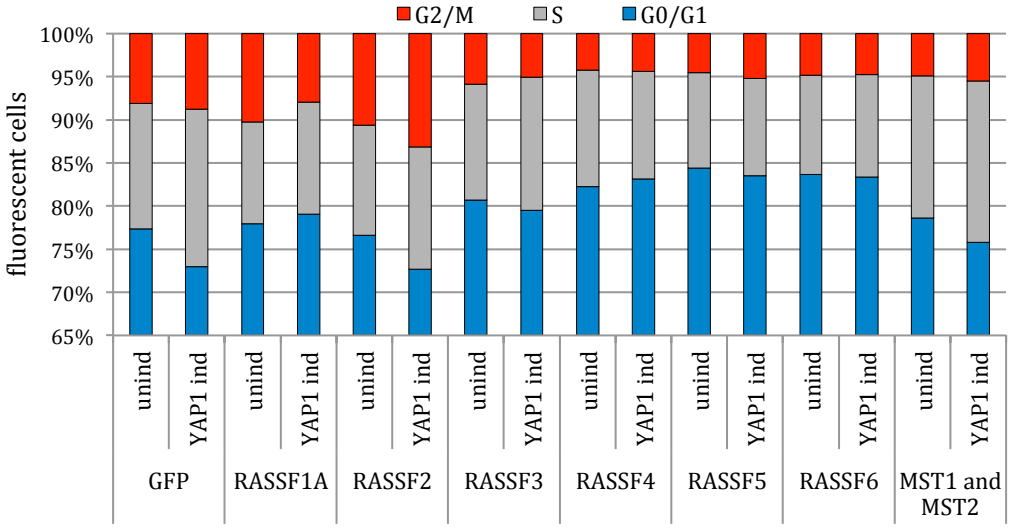

Figure 23: Cell cycle distribution of YAP1-inducible TREx293 cells after transfection of the C-terminal RASSFs or co-transfection of MST1 and MST2. Flow cytometry analysis of YAP1-inducible TREx293 cells transfected with GFP-empty, GFP-RASSF1A, GFP-RASSF2, GFP-RASSF3, GFP-RASSF4, GFP-RASSF5, GFP-RASSF6 or GFP-MST1 and GFP-MST2 (1:1) with or without induction of YAP1 (72h). The cell cycle of 10^4 transfected cells was analysed by flow cytometry using propidium iodide staining.

The induction of YAP1 and the co-expression of MST1 and MST2 resulted in an increase in cell proliferation (S-phase). Every C-terminal RASSF family member affected the progression of the cell cycle. RASSF2 lead to the accumulation of the cells in the G2-M phase, whereas RASSF1A, RASSF3, RASSF4, RASSF5 and RASSF6 counteracted the proliferative effect of YAP1 arresting the cells in the G0-G1 phase.

3.2.3 Effect of RASSFs on YAP1 target genes

The SARAH domain of the C-terminal RASSFs mediates the activation the Hippo pathway (Cooper *et al*., 2009; Song *et al*., 2010). To understand the role of the C-terminal RASSFs

in the regulation of the YAP1 target genes, the YAP1-inducible TREx293 cells were transfected with the respective Flag-RASSFs or with the corresponding empty vector and, after 72h induction of YAP1, were further analysed by qRT-PCR. Also HEK293T cells were co-transfected with the Flag-RASSFs and YAP1 and further analysed by qRT-PCR (Fig. 24 and Fig. 25). In addition, TP73 and ΔNp73 were overexpressed in both cell lines and used as positive control for the expression of *BAX*, *CDKN1A* and *BAX*. Since the C-terminal RASSFs affected the cell cycle (Fig. 23), the expression of *p16 (CDKN2A)* was determined and used as indicator for cell cycle arrest. The overexpression was controlled by semiquantitative PCR as shown in appendix 9. The expression of *ANKRD1* is plotted in figure 24; the expression levels of *BAX, BBC3, CDKN1A, TP53* and *p16* are plotted in figure 25.

A)

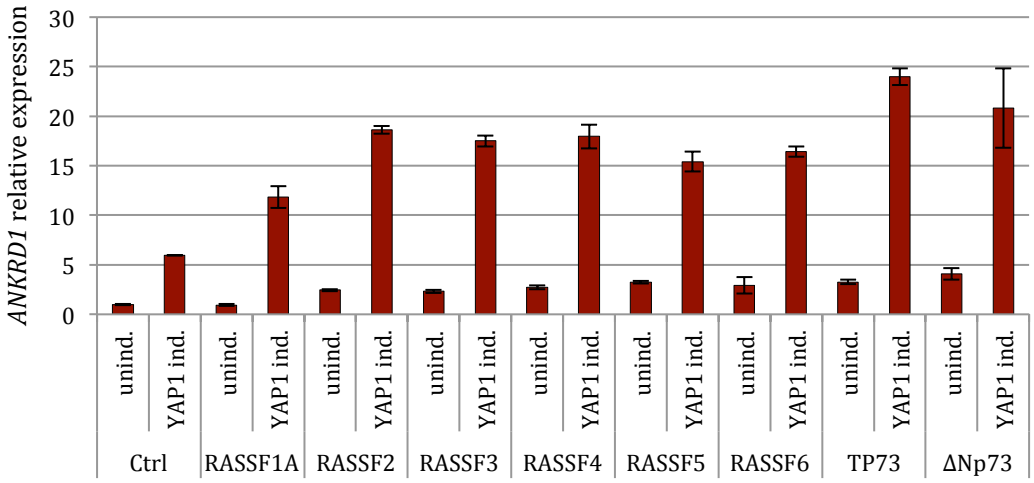

B)

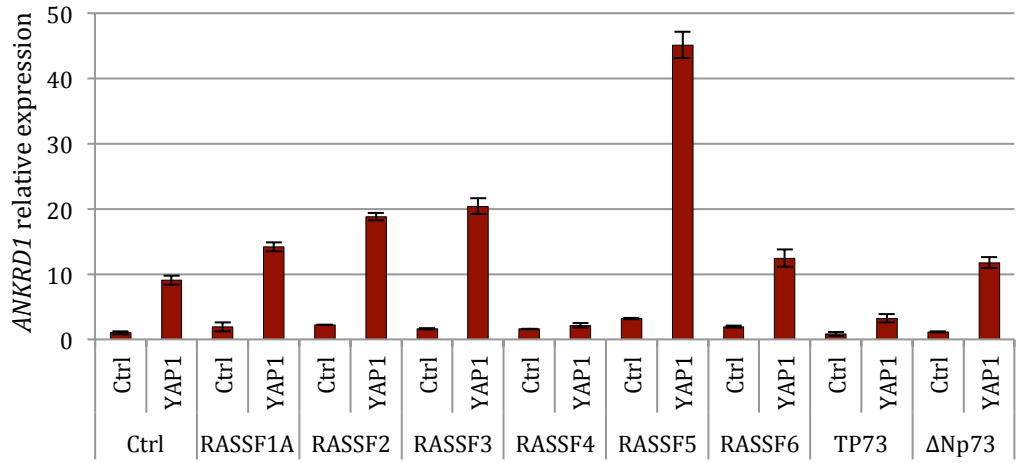

Figure 24: C-terminal RASSFs regulate the expression of *ANKRD1*. Representative graph of *ANKRD1* expression analysed by qRT-PCR 72h after transfection of Flag-empty, -RASSF1A, -RASSF2, -RASSF3, -RASSF4, -RASSF5, -RASSF6, -TP73, -ΔNp73 and the respective induction or co-transfection of YAP1 in: **A)** YAP1-inducible TREx293 cells with or without induction **B)** HEK293T cells. The expression levels were normalized to *GAPDH* and to the controls cells (set to1). SD from technical replicates.

Figure 24 indicates that C-terminal RASSFs and the TP73 isoforms together with YAP1 were able to regulate the expression of *ANKRD1* both in the TREx293 cells after induction of YAP1 (Fig. 24A) as well as after co-transfection with YAP1 in the HEK293T cells (Fig. 24B). The co-expression of the RASSFs with YAP1 resulted in a significant increase of *ANKRD1* expression in a range of 13- to 45-fold compared to the controls cells and of 4- to 5-fold compared to YAP1-overexpressing cells (Fig. 24). The observed expression changes were significant relative to the control cells and to the cells with an overexpression of YAP1 and even to the cells with the co-expression of RASSF1A and YAP1 (the p-values are listed in Table 23 in appendix 10). The regulation of *ANKRD1* expression by RASSF4 and TP73 could not be reproduced (Fig. 24).

Figure 25 indicates the expression of *BAX, BBC3, CDKN1A, TP53* and *p16* after transfection of the C-terminal RASSFs both in the TREx293 cells after induction of YAP1 (Fig. 25A) as well as in the HEK293T cells (Fig. 25B). In the YAP1-inducible TREx293 cells (Fig. 25A), the induction of YAP1 repressed the expression of *BAX*, *BBC3* and *CDKN1A* as previously observed in figure 9. Ectopic RASSF1A expression significantly increased the expression of *BAX* and *TP53* whereas the expression of *BBC3*, *CDKN1A* returned almost to the normal level (Fig. 25A). The other C-terminal RASSFs together with YAP1 caused a significant increase of up to 2-fold in the expression of *TP53, BAX* and *p16* expression compared to the uninduced cells and control cells. Moreover, both TP73 isoforms together with YAP1 showed an additional increase in the gene expression of the target genes, except for *p16* (Fig. 25A; the p-values are listed in Table 23 in appendix 10).

The data presented in figure 25A were further validated in a biological replicate in HEK293T cells (Fig. 25B). Here, the transfection of the C-terminal RASSFs, TP73 and ΔNp73 also resulted in a significant increase of the *TP53* expression (Fig. 25B). The increase of the *BAX* expression was observed after transfection of RASSF1A and RASSF5 compared to the control cells. The co-transfection of RASSFs with YAP1, with exception of RASSF4, resulted in an increase in the expression of all analysed genes compared to the controls without YAP1. (Fig. 25B, the p-values are listed in Table 23 in appendix 10).

The C-terminal RASSFs and YAP1 alone induced the expression levels of *p16* in a range between 10% up to 60% (Fig. 25). The co-transfection of RASSFs with YAP1 or the

induction of YAP1 in the TREx293 cells significantly increased the expression of *p16* by up to 72% compared to the respective controls cells (Fig. 25A). Moreover, TP73 and ΔNp73 affected the *p16* expression independent of YAP1. These preliminary data suggest that the C-terminal RASSFs together with YAP1 could be involved in the regulation of *p16* expression levels, which in turn might explain the cell cycle arrest observed in 3.2.2.

A)

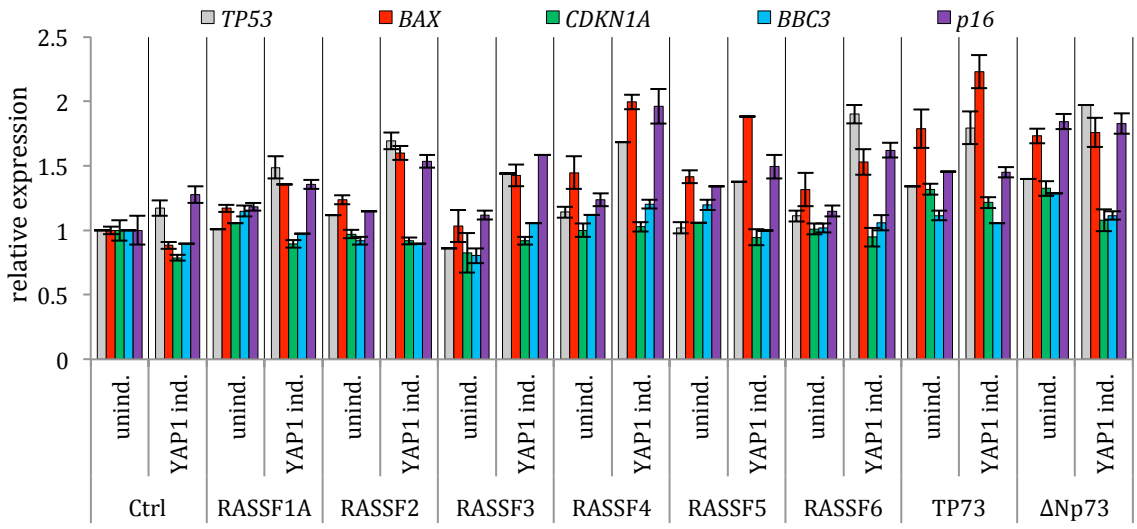

B)

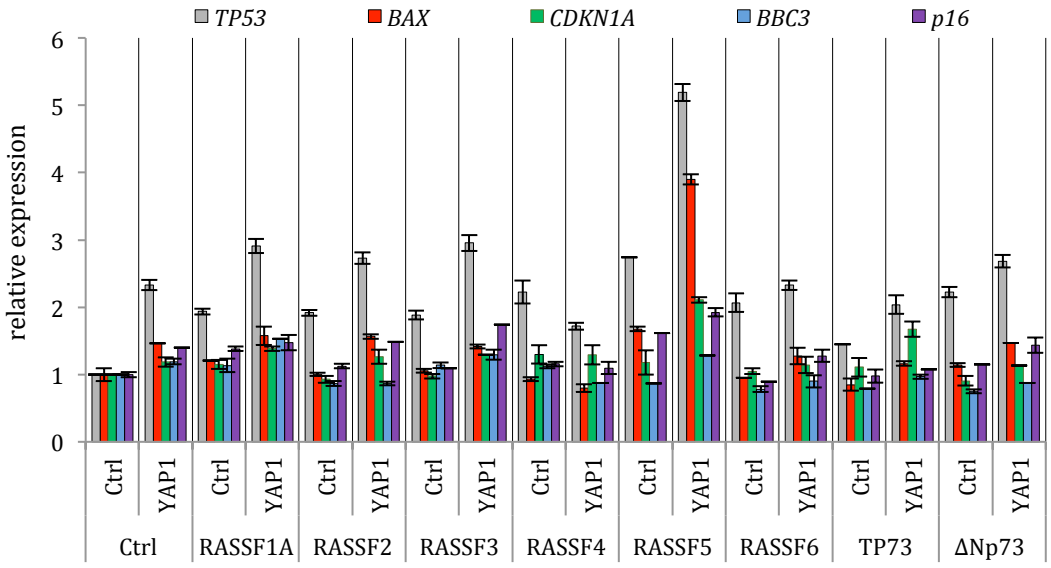

Figure 25: C-terminal RASSFs regulate the expression of YAP1 target genes and of *p16*. Representative graph of the expression of *TP53, BAX, CDKN1A, BBC3* and *p16* after 72h transfection of Flag-empty, -RASSF1A, -RASSF2, -RASSF3, -RASSF4, -RASSF5, -RASSF6, -TP73, -ΔNp73 and the respective co-transfection with YAP1 in: **A)** YAP1-inducible TREx293 cells with or without induction of YAP1. **B)** HEK293T cells. The expression levels were normalized to *GAPDH* and to the control cells (set to 1). SD from technical replicates.

3.2.4 Effects of RASSFs on MDM2 level

RASSF1A, RASSF2 and RASSF5 are the best characterised C-terminal RASSF members. In our study, RASSF1A, RASSF2, RASSF3 and RASSF5 showed tumor-specific methylation (Fig. 22) and activated the expression of *ANKRD1* (Fig. 24). RASSF1A and RASSF5 arrested the cells in the G0-G1 phase, whereas RASSF2 is the only C-terminal RASSF members that arrested the cells in the G2-M phase (Fig. 23). Kudo *et al.* (2012) and Iwasa *et al.* (2013) reported the inhibitory effect of RASSF3 and RASSF6 on MDM2 level independent of the Hippo pathway; therefore, the effect of RASSF2 and RASSF5 on MDM2 was further investigated. The protein levels of MDM2 after 72h expression of RASSF1A, RASSF2 and RASSF5 were further analysed by western blotting using the YAP1-inducible TREx293 cells with and without YAP1 induction (Fig. 26).

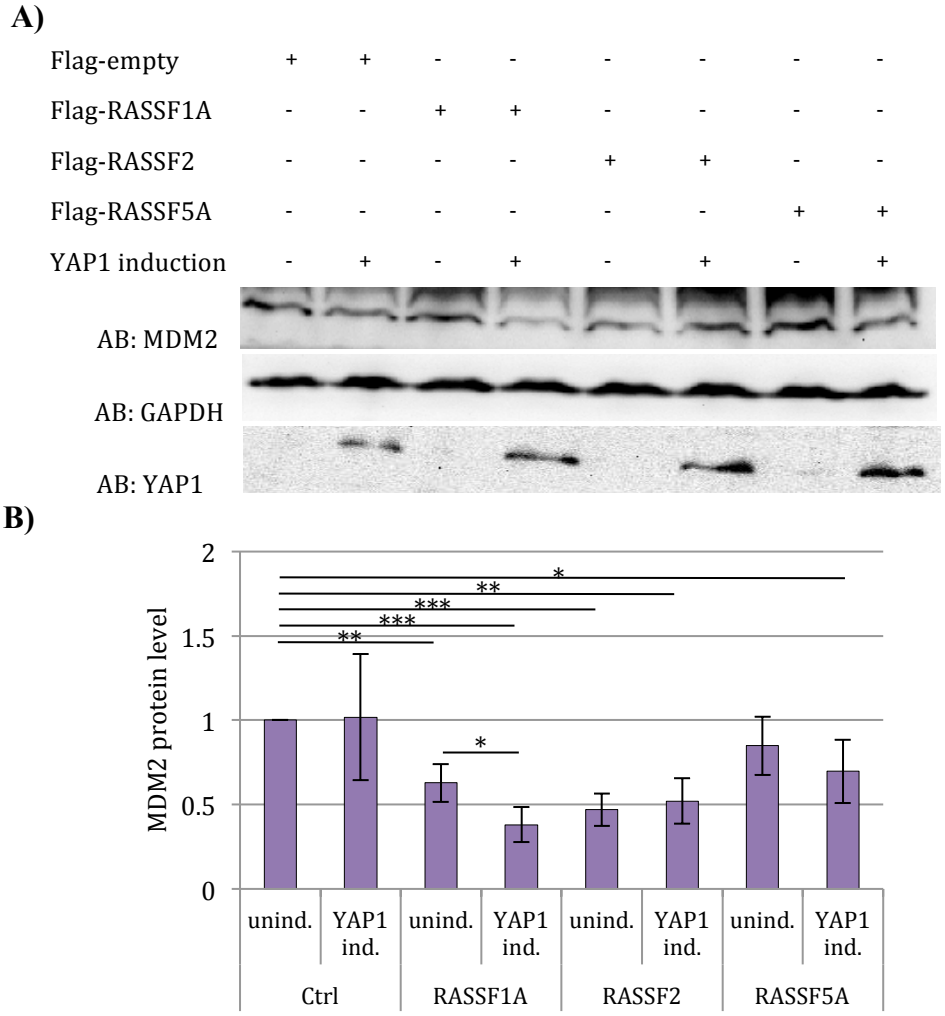

Figure 26: Destabilisation of MDM2 by the C-terminal RASSFs. A) Representative western blot of 72h overexpression of Flag-empty, Flag-RASSF1A, Flag-RASSF2 and Flag-RASSF5A in TREx293 cells with and without induction of YAP1. **B)** Quantification of protein levels of MDM2 from three biological replicates. The protein levels were quantified by ImageJ and normalized to GAPDH and to the control lysates (unind.). p-values: * $p<0.05$, ** $p<0.01$ and *** $p<0.001$ (t-test).

Figure 26A indicates a representative western blot of the YAP1-inducible TREx293 cells transfected with RASSF1A, RASSF2 and RASSF5 with and without YAP1 induction. The control blot for the overexpression is shown in appendix 11. The respective quantification of three biological replicates is plotted in figure 26B. Here we observed, that the expression of RASSF1A and RASSF2 alone significantly reduced the level of MDM2 by up to 37% (p-value 0.005) and up to 53% (p-value<0.001), respectively, in comparison to the control cells without the RASSFs and YAP1. In combination with YAP1, only RASSF1A resulted in a significant decrease of MDM2 (reduction of 25%; p-value 0.05) in comparison to the uninduced cells transfected with RASSF1A (Fig. 26). Compared to the control uninduced cells, RASSF1A and YAP1 reduced the protein level of MDM2 by up to 62% (p-value<0.001) (Fig. 26B). RASSF2 and RASSF5A in combination with the induction of YAP1 did not reduce the MDM2 level.

Table 20 summarizes the obtained data of the potential role of the C-terminal RASSFs in the regulation of the Hippo pathway. The promoter methylation of C-terminal RASSFs is described in this work using DNA from liver tumors compared to DNA from matched normal tissues. In comparison to YAP1 and to the control cells, the expression of the C-terminal RASSFs resulted in cell cycle arrest in the G0-G1 phase or G2-M phase. The expression the YAP1 target genes and of *p16* is regulated by the C-terminal RASSFs. From the literature, and from this work, it is known that C-terminal RASSFs diminish the protein level of MDM2. RASSF1A in association with YAP1 also reduced the MDM2 level.

Table 20. Summary of the potential function of C-terminal RASSFs

Factor	Tumor-specific promoter methylation	cell cycle accumulation	transcriptional co-regulation together with YAP1				decrease of MDM2 level	
			ANKRD1	*TP53*	*P16*	*BAX*	alone	with YAP1
YAP1	um	S	+	-	+	-	-	-
RASSF1A	m	G0-G1	+	+	+	+	+	+
RASSF2	m	G2-M	+	+	+	+	+	-
RASSF3	m	G0-G1	+	+	+	+	+	NA
RASSF4	um	G0-G1	+	+	+	+	NA	NA
RASSF5A	m	G0-G1	+	+	+	+	+	-
RASSF6	um	G0-G1	+	+	+	+	+	NA

Not analysed (**NA**). Unmethylated (um). Methylated (m). No regulation (-). Significant regulation (+).

4. DISCUSSION

4.1 The Hippo pathway and cancer

The precise balance between cell growth and death is essential for the maintenance of tissues, and the deregulation of this homeostasis results in cancer. Cancer cells inactivate the function of tumor suppressor genes by several mechanisms, e.g. by deletion of genomic loci, mutations or gene silencing via promoter methylation (Feinberg *et al*., 2016; Risch and Plass, 2008). In contrast, oncogenes like *MDM2* or *MYC* are activated in the genome e.g. by amplification (Hanahan and Weinberg, 2011)

The Hippo pathway is a kinase cascade that plays a crucial role in organ size regulation, carcinogenesis and apoptosis (Edgar, 2006; Harvey *et al*., 2013). The cellular localization of the Hippo components can be divided into two groups, a junctional localization group and a cytoskeleton interaction group (Yu and Guan, 2013). RASSF1A is an important regulator of the Hippo kinases MST1/2 and the large tumor suppressor kinases LATS1/2 (Dittfeld *et al*., 2012; O'Neill *et al*., 2004; Praskova *et al*., 2004). RASSF1A disrupts the Raf1-MST2 complex and interacts with MST2 via the SARAH domain hereby activating the kinase cascade (Hwang *et al*., 2007; Matallanas *et al*., 2007). In turn, MST1/2 phosphorylate LATS1/2. The active LATS1/2 phosphorylate YAP1, but the function of the phosphorylation is still discussed controversially in the literature. Various authors have reported that the phosphorylation is necessary for the cytoplasmic retention and subsequent degradation of YAP1 (Basu *et al*., 2003), but other authors have suggested that phosphorylated YAP1 translocates into the nucleus and acts as a co-activator (Matallanas *et al*., 2007; Strano *et al*., 2001; Wang *et al*., 2016).

The downstream transcriptional activator of the Hippo pathway is YAP1, which is mostly described as an oncogenic factor (Kang *et al*., 2011; Mizuno *et al*., 2012; Steinhardt *et al*., 2008). YAP1 is highly expressed in cancer cells and involved in tumorigenesis, cell proliferation and metastasis interacting as co-factor with TEADs, SMADs and ß-catenin (Kim *et al*., 2015; Silvis *et al*., 2011). However, YAP1 can also interact with the tumor suppressor TP73 and regulates the transcription of pro-apoptotic genes (Levy *et al*., 2008b;

Strano *et al*., 2001). These reports suggest that YAP1 acts as an oncogenic factor and as a co-regulator of the tumor suppressor activity of the Hippo pathway as well.

Matallanas *et al.* (2007) have shown that RASSF1A induces apoptosis through the Hippo pathway and YAP1 by activating the transcription of the pro-apoptotic gene *BBC3* and the stabilisation of the tumor suppressor protein TP73 (Matallanas *et al*., 2007). In A549 lung cancer cells, our group has observed the upregulation of *CDKN1A* and *BAX* after overexpression of RASSF1A confirming the apoptotic functions of RASSF1A (Richter *et al*., 2010). However, several reports have shown that *RASSF1A* is one of the most frequently epigenetically inactivated genes in different types of human cancer and acts as a prominent tumor suppressor (Dammann *et al*., 2000; Richter *et al*., 2009; Schagdarsurengin *et al*., 2003). As indicated in Jiménez *et al.* (2017), the promoter methylation status of the Hippo core components (*RASSF1A, MST1, MST2, WW45, LATS1, LATS2* and *YAP1*) was analysed using liver tumor samples compared to the matched normal tissues (see appendix 3). Only RASSF1A showed a tumor-specific methylation in primary liver cancer (Jiménez *et al*. 2017). The inactivation of the key regulator *RASSF1A* produces an imbalance in the pathway, which may alter the pro-apoptotic effect of the Hippo pathway switching into the oncogenic function (Yu and Guan, 2013).

From the literature we know that the cellular function of YAP1 depends on its phosphorylation status (Basu *et al*., 2003; Zhao *et al*., 2010b) and on the binding of YAP1 to transcription factors (Strano *et al*., 2001; Sudol *et al*., 2012), but the mechanism underlying the regulation of the YAP1 activity is still unclear. Furthermore, the Hippo cascade is activated by RASSF1A; however, RASSF1A is frequently silenced in cancer cells (Dammann *et al*., 2000). For this reason, the aim of this study was to analyse the effect of RASSF1A on the regulation of YAP1 and on the expression of the YAP1 target genes.

4.2 The oncogenic function of YAP1

The amplification of *YAP1* is commonly observed in tumors e.g. in oral squamous carcinoma, medulloblastoma and in glioblastoma (Fernandez *et al*., 2009; Modena *et al*., 2006; Orr *et al*., 2011). The increased level of YAP1 drives oncogenesis in human HCC

and ovarian cancer (Moran-Jones *et al*., 2015; Xu *et al*., 2013). In murine HCC, the *Yap* gene locus is mutated and amplified; Yap1 cooperates with Myc favoring tumor transformation (Zender *et al*., 2006). To understand the role of the amplification of *YAP1* in cancer cells, a YAP1-inducible system was created using the TREx293 cells and it was further characterised as individual clones and as a pool of clones. Compared to the control cell line (Fig. 6A) and to the uninduced cells, the mRNA and protein levels of YAP1 vary between the individual clones (Fig. 7, Fig. 8); nevertheless, there is a significant correlation between the expression of *YAP1* and the expression of *BAX, BBC3*, *CTGF* and *ANKRD1* (Fig. 7D). To avoid this clonal variability and to obtain a homogeneous expression of YAP1, a pool of clones was used for the further analysis.

The induction of YAP1 with Dox (Doxycycline) in the pool of clones was very sensitive (Fig. 6B) and resulted in a 12-fold expression increase compared to the uninduced cells (Fig. 9A). The induction of YAP1 occurred even with a low concentration of Dox and resulted in the upregulation of the YAP1 target genes *ankyrin repeat domain 1* (*ANKRD1)* (Fig. 6B, Fig. 7B) and *connective tissue growth factor* (*CTGF)* (Fig. 7B). YAP1 together with TEAD regulate the expression of *Cyr61, CTGF* and *AREG* (Li *et al*., 2013; Zhou *et al*., 2016). CTGF is a growth factor, which is associated with the oncogenic properties of YAP1 e.g. in non-small cell lung cancer (Hsu *et al*., 2016; Zhao *et al*., 2008). In ovarian cancer, *YAP1* and *CTGF* are overexpressed and associated with poor prognosis and metastasis (Moran-Jones *et al*., 2015). The function of *ANKRD1* will be explained below in more detail in a RASSF1A and TP53 context.

In this study, YAP1 also displays its oncogenic potential by transcriptional repression of following tumor suppressor genes: *RASSF1A, TP53, BAX, BBC3* and *CDKN1A* (Fig. 9B). The transcriptional downregulation of these tumor suppressor genes by YAP1 was observed in the microarrays (Table 19) and further validated by qRT-PCR (Fig. 14) and by promoter assays (Fig. 11B). In normal cells, TP53 is the major regulator of the cell cycle, senescence and apoptosis (Levine, 1997). Since *CDKN1A, BBC3* and *BAX* are target genes of both TP73 and TP53 (Levine, 1997), their downregulation by YAP1 resulted in a shift in the cell cycle distribution of the cells into the S-phase (Fig. 10B). These results together with the correlation data from the YAP1 individual clones (Fig. 7D) suggest a modulation of the expression of *RASSF1A* and TP53 target genes by YAP1 and by the Hippo pathway (see Fig. 27).

CDKN1A is an important regulator of the cell cycle progression in G1/S and G2/M transition by inhibiting CDKs and the phosphorylation of RB (Harper *et al*., 1993; Xiong *et al*., 1993). The down-regulation of *CDKN1A* by YAP1 observed in this study correlates with the findings in the literature. Hsueh *et al*. (2015) demonstrated the proliferative effect of YAP1 in human corneal endothelial cells through reduction of *CDKN1A* levels and the transition of the cells into the G1/S phase (Hsueh *et al*., 2015). Also, Muramatsu et al. (2011) suggested YAP1 as putative oncogene in esophageal squamous cell carcinoma (Muramatsu *et al*., 2011). This group indicated that the knockdown for YAP1 by siRNA reactivates the expression of *CDKN1A* and inhibits the expression of *survivin* in KYSE170 cells (Muramatsu *et al*., 2011). BAX, in association with voltage-dependent anion channels, induces the mitochondrial dependent apoptosis by formation of pores in the mitochondrial outer membrane, which allows the release of cytochrome c (Shimizu *et al*., 1999). The transcriptional repression of *BAX* and *BBC3* by YAP1 observed in this work has not been reported in the literature. The transcriptional regulation of *BAX* by YAP1 was previously reported by Basu *et al.* (2003) and by Zagurovskaya *et al*. (2009), but only as co-factor together with TP73 or ERG1, respectively (Basu *et al*., 2003; Zagurovskaya *et al*., 2009). The regulation of *BBC3* by YAP1 is linked to RASSF1A and TP73 (Matallanas *et al*., 2007).

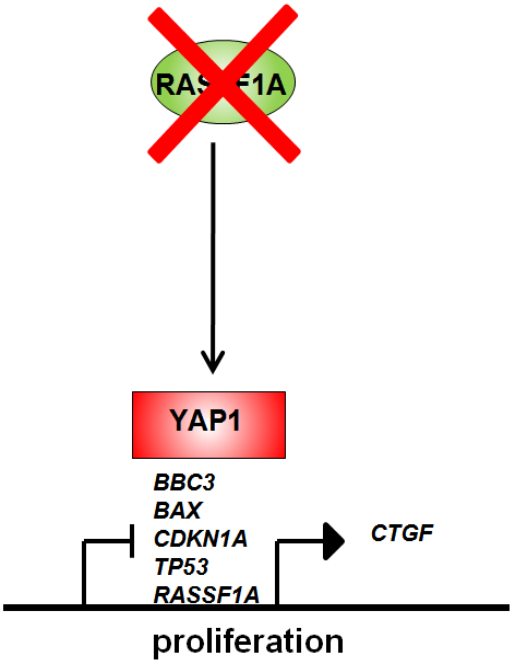

Figure 27: Hippo pathway in cancer cells after silencing of *RASSF1A*. YAP1 displays its oncogenic potential by repressing tumor suppressor genes and the activation of growth factors such as *CTGF*.

To date there is a big discrepancy about the connection of YAP1 with TP53. YAP1 can interact with the TP53 family members TP73 and TP63, but not with TP53 (Levy *et al*., 2008a; Strano *et al*., 2001; Tomlinson *et al*., 2010). Recently, *YAP1* was identified as a novel potential TP53 target gene by genome-wide analysis of TP53 response elements (Tebaldi *et al*., 2015). Bai *et al*. (2013) demonstrated that the YAP1/TEAD complex activates the expression of *TP53* during chemotherapy in HCC; furthermore by ChIP assays, they detected that YAP1 could directly bind to the *TP53* promoter suggesting a TP53-YAP1 feedback (Bai *et al*., 2013). However, in this work YAP1 induction represses the expression of *TP53,* which might also explain the repression of *BAX, BBC3* and *CDKN1A*. Other reports also showed an association between amplification of YAP1 and TP53 deficiency e.g. in mice models of mammary carcinoma (Cheng *et al*., 2010). Sugawara *et al*. (2011) demonstrated a correlation of the TP53 missense mutation ($TP53^{R273H}$) with the amplification of YAP1 in tumors from patients with Li-Fraumeni syndrome (Sugawara *et al*., 2011). Moreover, YAP1 can inhibit cellular senescence in a RB-TP53-p16 dependent manner by the regulation of *CDK6* expression (Xie *et al*., 2013).

RASSF1A is frequently silenced in cancer cells by promoter hypermethylation; however, there are few reports about the transcriptional regulation of *RASSF1A*. HDAC6 and MYC together with PRC2 and DNMT3B are involved in the epigenetic inactivation of *RASSF1A* (Charlet *et al*., 2014; Tao *et al*., 2016). Furthermore, Beckedorff *et al*. (2013) described a novel mechanism of inactivation by an antisense noncoding RNA (*ANRASSF1*) that also recruits PRC2 to the *RASSF1A* promoter region (Beckedorff *et al*., 2013). To date it is known that the transcription factors Sp1 and Sp3 bind to the GC-boxes and activate the *RASSF1A* promoter (Strunnikova *et al*., 2005). In the literature, there is no data that indicates a regulation of *RASSF1A* expression by TP73 or YAP1. In this study, we observed a possible novel mechanism of regulation in which TP73 activates the promoter activity of *RASSF1A,* while YAP1 represses it and abrogates the effect of TP73 (Fig. 11C). In addition, Tian *et al.* (2011) demonstrated that TP53 could regulate the expression of *RASSF1A* by direct binding to the promoter and create a negative autoregulatory feedback loop between RASSF1A and TP53 (Tian *et al*., 2011). However, the data obtained in this study suggest a positive feedback between RASSF1A with TP53 via YAP1, since the inactivation of *RASSF1A* results in transcriptional repression of *TP53* and its target genes by YAP1 (Fig. 9B, Fig. 11B, see Fig. 27).

In summary, the induction of YAP1 results in the upregulation of the oncogenic *CTGF* and the repression of the expression of *TP53, BAX, CDKN1A, BBC3* and *RASSF1A*. These results corroborate the data from the literature, which suggest YAP1 as an oncogenic factor. In addition, the literature and the results from this work suggest a regulatory loop between YAP1 and TP53 (Bai *et al*., 2013; Tebaldi *et al*., 2015) as well as between RASSF1A and TP53 (Tian *et al*., 2011).

4.3 RASSF1A regulates the expression of the YAP1 target genes and counteracts the oncogenic function of YAP1

RASSF1A is epigenetically silenced in cancer cells (Dammann *et al*., 2000). The tumor suppressive function of the Hippo pathway has been described in association with RASSF1A and TP73 (Levy *et al*., 2008a; Matallanas *et al*., 2007; Strano *et al*., 2001). *RASSF1A* is methylated in the YAP1-inducible TREx293 cells (appendix 4); therefore, to analyse both the effect of RASSF1A on the expression of the YAP1 target genes, as well as to identify novel potential target genes of the Hippo pathway, RASSF1A was overexpressed in HEK293T cells and in the YAP1-inducible TREx293 cells for further investigation.

The obtained results from the microarrays and the further validation (Table 19, Fig. 14) demonstrated that RASSF1A promotes its tumor suppressive function through the activation of pro-apoptotic and anti-proliferative YAP1 target genes such as *ANKRD1*, *BAX* and *CDKN1A* (Table 19, Fig. 11B, Fig. 14). In addition, RASSF1A counteracts the oncogenic properties of YAP1 by neutralizing the YAP1-induced downregulation of *BAX* and *CDKN1A* (Table 19, Fig. 11B, Fig. 14, see Fig. 28). These data and the flow cytometry data suggest that RASSF1A and YAP1 regulate the cell cycle by the transcriptional regulation of *CDKN1A* and *BAX,* which results in accumulation or cell arrest either in the S-phase after induction of YAP1 or in the G0/G1 phase by co-expression of RASSF1A with YAP1 (Fig. 10B). RASSF1A regulates the cell cycle by several mechanisms, for example the G1/S transition by transcriptional repression of cyclin A2 and the inhibition of cyclin D1 (Ahmed-Choudhury *et al*., 2005; Shivakumar *et al*., 2002). RASSF1A interacts with and stabilises the microtubules, and its depletion affects the mitotic checkpoint (G2/M) and chromatid segregation (Dallol *et al*., 2004; Rong *et al*., 2004). Moreover,

Aurora A, together with RASSF1A, modulates the CDC20/anaphase-promoting complex and the anaphase phase progression (Song *et al*., 2009b). Aurora A and Aurora B kinases phosphorylate RASSF1A and induce mitotic arrest by modulating the ability of RASSF1A to bind to the microtubules (Rong *et al*., 2007; Song *et al*., 2009a).

Interestingly, the microarrays revealed that the co-expression of RASSF1A and YAP1 repressed the mRNA expression of *MDM2* (Table 19). This finding could not be validated either by qRT-PCR or by promoter assays (Fig. 11). However, the western blots indicated that the co-expression of RASSF1A and YAP1 significantly reduces the protein level of MDM2, which produces an increase of TP53 and BAX level (Fig. 13A, Fig. 19A, see Fig. 28). *MDM2* is a TP53 target gene, which encodes for an E3 ubiquitin ligase (Momand *et al*., 1992). TP53 is negatively regulated by MDM2 via ubiquitination of the transactivation domain, which leads to the subsequent proteasomal degradation (Kussie *et al*., 1996; Momand *et al*., 1992; Oliner *et al*., 1993). Song *et al*. (2008) had reported that RASSF1A negatively regulates MDM2 by disrupting the MDM2-DAXX-HAUSP complex by inducing the self-ubiquitination of MDM2 (Song *et al*., 2008). Other reports have indicated the inhibitory effects of RASSF3 and RASSF6 on MDM2 independent of Hippo signalling (Iwasa *et al*., 2013; Kudo *et al*., 2012). Furthermore, it has also been reported that the LATS2 kinase binds MDM2 and thereby inhibits its E3 ligase function and activates TP53 (Aylon *et al*., 2006).

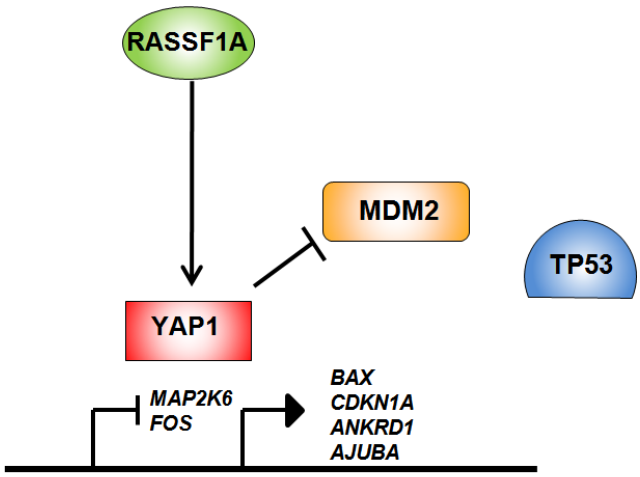

Figure 28: Effect of RASSF1A on the Hippo pathway. RASSF1A activates the expression of the YAP1 target genes such as *BAX*, *ANKRD1*, *CDKN1A* and *AJUBA*. YAP1 and RASSF1A reduce the MDM2 level.

From the microarray data, it is also interesting to note that the co-expression RASSF1A and YAP1 repressed the expression of other growth-associated genes including transcription factors (*FOS* and *FOXD3*), mitogen-activated protein kinases (*MAP2K6* and *MAP3K8*) and growth factors (*FGF21, GH1* and *GDF15*) (Table 19, see Fig. 28, appendix 5 and 6). Of these genes, only *FOS* has been described in association with the oncogenic YAP1. Recent data have shown that YAP1 and FOS compensate the loss of K-Ras signalling by activating the epithelial-mesenchymal transition (Shao *et al*., 2014). Zanconato *et al.* (2015) also demonstrated that YAP1 and TEAD could form a complex with the AP-1 proto-oncoproteins JUN and FOS, to regulate the expression of *CTGF, AJUBA* and *ANKRD1* in breast cancer cells (Zanconato *et al*., 2015). There is no data in the literature on the transcriptional repression of *FOS, FOXD3, MAP2K6*, *MAP3K8, FGF21, GH1* and *GDF15* by RASSF1A and YAP1; hence they could represent novel potential target genes of the Hippo pathway.

Additionally, it was observed that RASSF1A induced the expression of the YAP1 target genes such as *ANKRD1, CYR61*, *AJUBA* (Fig. 5, Fig. 14, see Fig. 28) and the expression of other novel target genes like *HIF1A-antisense 2*, *ACTBL2*, *CPA4* and *COL12A1* (see Table 19 and appendix 5). The gene regulation of the remaining novel target genes by YAP1 and RASSF1A needs to be further validated, since this work is focused on the regulation and function of *ANKRD1*. The precise tumor-related function of some YAP1 targets is still under investigation and may depend on expression level, cell origin or the genetic and epigenetic background. For example, in this study the expression of *AJUBA* is activated by YAP1 and RASSF1A, but the function of the gene in this context needs to be investigated (Fig. 14). Some authors have proposed AJUBA as a potential tumor suppressor gene (Foxler *et al*., 2012; Tanaka *et al*., 2015). In 2012, Foxler *et al*. demonstrated that AJUBA, in complex with PHD and VHL, regulates HIF-1α degradation and thus its oncogenic activity (Foxler *et al*., 2012). Further, AJUBA has been shown to suppress the proliferation of malignant mesothelioma, and its expression is reduced in lung cancer by promoter hypermethylation and genomic instability (Sharp *et al*., 2008; Tanaka *et al*., 2015). However, AJUBA has also been described as a negative regulator of the Hippo signalling and as the link for the regulation of YAP1 by other cellular pathways, since AJUBA can interact with LATS1/2 and inhibit the phosphorylation of $YAP1^{S127}$ (Das Thakur *et al*., 2010). The JNK signalling promotes the activity of YAP1 by regulating the phosphorylation of AJUBA and the binding to LATS1/2 or SAV1, respectively (Reddy and

Irvine, 2013; Sun and Irvine, 2013). Similar to RASSF1A, AJUBA is located at the microtubules and can interact with Aurora A and Aurora B (Ferrand *et al*., 2009). The interactions of AJUBA with Aurora and with LATS proteins are essential for the mitotic spindle formation and the centrosomal localization of Aurora-A and γ-tubulin (Abe *et al*., 2006; Ferrand *et al*., 2009; Hirota *et al*., 2003). To understand the regulatory function of RASSF1A on YAP1, it may be important to analyse the expression changes of *ANKRD1, AJUBA* and *HIF-1AS* by different stimuli such as UV stress, hypoxia or serum starvation. Since RASSF1A controls the cell cycle by microtubule stabilisation, it would be interesting to also analyse the effect of nocodazole on the expression of *ANKRD1* or *AJUBA* and on the cell cycle in the YAP1-inducible system.

In summary, in this work it was observed that RASSF1A activates the expression of YAP1 target genes (*ANKRD1*, *BAX* and *CDKN1A)*. Moreover, RASSF1A and YAP1 cause a decrease of the MDM2 level, which in turn results in an increase in TP53 and BAX (Fig. 28). These data suggest a mechanism of RASSF1A together with YAP1 in regulating TP53 and the G1/S transition of the cell cycle. The microarray data suggest that RASSF1A restrains the cell proliferation and cancer stemness by direct transcriptional repression of growth factors (*MDM2*, *CTGF*, *FOS* and *GH1)* and of factors involved in stem cell maintenance (*FOXD3* and *FGF21*). RASSF1A induced the expression of the YAP1 target genes *CYR61, ANKRD1* and *AJUBA,* which are regulated by the binding of YAP1 to TEAD (Li *et al*., 2013; Zanconato *et al*., 2015; Zhou *et al*., 2016). These data suggest that RASSF1A regulates the binding of YAP1 to TP73 (Matallanas *et al*., 2007) and the binding of YAP1 to the TEAD transcription factors; thus it will be interesting to further dissect the exact mechanism in more detail.

4.3 RASSF1A triggers the nuclear localization of YAP1

The post-transcriptional modifications of YAP1 are under investigation and their function is not fully understood. In part, the phosphorylation of YAP1 is responsible for its protein stability, cellular localization and enhances the interactions with binding partners (Basu *et al*., 2003; Oka *et al*., 2010; Sudol *et al*., 1995). YAP1 has over 20 different sites that could be phosphorylated by several kinases such as: LATS1/2, MAPK9, MAPK8, CK1 and ABL1 (Levy *et al*., 2008a; Tomlinson *et al*., 2010; Zhao *et al*., 2010b; Zhao *et al*., 2007).

The nuclear translocation of YAP1 and its regulation is controversial in the literature. It has been demonstrated that the phosphorylation of $YAP1^{S127}$ is involved in both the nuclear translocation and as well as in the binding of YAP1 to 14-3-3 for cytoplasmatic retention and degradation (Matallanas *et al*., 2007; Zhao *et al*., 2007). LATS1/2 can phosphorylate YAP1 on five HXRXXS consensus motifs (S61, S109, S127, S164 and S381) (Zhao *et al*., 2010a; Zhao *et al*., 2007). The deletion of all five LATS1/2 phosphorylation sites promoted the oncogenic potential of YAP1, but after restoration of S127 and S381 the transformation potential of YAP1 was suppressed (Zhao *et al*., 2010a). Moreover, YAP1 is phosphorylated by c-Abl on Y357 in response to DNA damage thereby increasing the affinity of YAP1 to TP73 (Keshet *et al*., 2015; Levy *et al*., 2008a).

In this study, RASSF1A triggered the protein stabilisation (Fig. 10A, Fig. 19A and 19C) and the nuclear translocation of YAP1 (Fig. 12A-B). The translocation of YAP1 induced nucleus deformation and apoptosis (Fig. 12C). These data corroborated the hypothesis that RASSF1A regulates the translocation of YAP1 into the nucleus, which is necessary for inducing transcription of YAP1 target genes and cell death (Fig. 12) (Matallanas *et al*., 2007; Wang *et al*., 2016). In this work $YAP1^{S127A/E}$ mutants were also created. Both YAP1 mutants showed a nuclear and cytoplasmic localization and an increase in the nuclear localization after expression of RASSF1A (Fig. 12B). The results did not reveal a possible regulatory mechanism for how RASSF1A induces the nuclear translocation of YAP1. In contrast, they suggested that the regulation of YAP1 depends on several factors and not only on one phosphorylation site ($YAP1^{S127}$). Further experiments should focus on the mutation of the five LATS phosphorylation sites and the location of these mutants after RASSF1, LATSs and MSTs expression or in response to cellular stress.

4.4 ANKRD1 is a potential tumor suppressor gene

ANKRD1 has been described as a cardiac protein, which is involved in heart development and failure (Ishiguro *et al*., 2002; Torrado *et al*., 2005). However, in this study it was demonstrated that *ANKRD1* is also expressed in liver and lung tissue but is silenced in breast tissue (Almodovar-Garcia *et al*., 2014). The function of ANKRD1 in cardiac cells varies according to its localization; in the cytosol, in complex with titin, ANKRD1 plays a role in sarcomere stability, whereas in the nucleus it can act as transcriptional co-regulator

with YB1 and nucleolin e.g. by repression of *MMP13* expression (Almodovar-Garcia *et al*., 2014; Mikhailov and Torrado, 2008). Recent reports indicated the potential role of ANKRD1 in cancer, for example by interaction with TP53 and its involvement in the Hippo, Wnt and TGF-β pathways (Kojic *et al*., 2010; Labbe *et al*., 2007).

An important observation in this study was the significant co-regulation of *ANKRD1* expression by YAP1 and RASSF1A via activation of the Hippo pathway (Fig. 5, Fig. 14, Fig. 15). The transcriptional activation of *ANKRD1* by YAP1 and RASSF1A was measured by qRT-PCR in HEK293T cells (Fig. 5C) and in the YAP1-inducible TREx293 cells (see Fig. 14); it was also detected by microarrays (Table 19) and validated e.g. by promoter assays (Fig. 15B). In this work, the expression changes were observed after 72h expression of RASSF1A and induction of YAP1. It will be interesting to elucidate if cell density or hypoxic condition also play a role in this regulation. To date, there is no data in the literature that support the hypothesis of regulation of *ANKRD1* by RASSF1A. The YAP1-dependent regulation of *ANKRD1* has been described previously in association with proliferation or apoptosis depending on the cellular context, e.g. as oncogene in the arsenic-induced carcinogenesis in skin (Li *et al*., 2013), in glioblastoma by amplification of the *YAP1* locus (Stein *et al*., 2015) and in ovarian cancer (Scurr *et al*., 2008). In contrast, ANKRD1 is described as a potential tumor supressor gene in HCC (Park *et al*., 2005), in cardiomyocytes (Shen *et al*., 2015) and in rhabdomyosarcomas (Ishiguro *et al*., 2002). However, it is still unclear if the anti-proliferative function of ANKRD1 is due to a dosage dependent effect or only functional in association with the regulation by RASSF1A and YAP1. Additionally, this work confirmed that the regulation of the expression of *ANKRD1* occurs via the Hippo pathway, since the truncation of the SARAH domain of RASSF1A abolished the induction of *ANKRD1* expression compared to the effect of RASSF1A wild type (Fig. 15). As previously described, YAP1 and TEAD are responsible for the transcription of *ANKRD1* (Li *et al*., 2013; Stein *et al*., 2015; Zanconato *et al*., 2015). However, according to the results presented in this study, TP73 and ΔNp73 also induced the expression of *ANKRD1* (Fig. 24). There is no evidence in the literature for an interaction of YAP1 with ΔNp73 and therefore it needs to be investigated in further detail.

The promoter region of *ANKRD1* contains only few CpGs sites and therefore they are not defined as a CpG island. Breitling *et al*. (2011) demonstrated the effect of methylation of a single CpG site on the gene expression (Breitling *et al*., 2011). An important finding in this

work was the epigenetic inactivation of *ANKRD1* by methylation of a CpG site (cg01262952) at the promoter region (Fig. 16C, appendix 1). The silencing of *ANKRD1* was observed in several cancer cells including lung (A427) and prostate cancer cells (LNCaP) (Fig. 16B). The obtained methylation data correlated with the expression analysis (Fig. 16B-C). Additionally a re-expression of *ANKRD1* was observed after 4d Aza treatment of the cells, which confirmed the epigenetic regulation of *ANKRD1* expression (Fig. 16D). The ectopic expression of ANKRD1 results in a significant reduction of the colony formation and cell proliferation in lung and prostate cancer cells by inducing e.g. the expression of *TP53, CDKN1A* and *BAX* (Fig. 17A-C, Fig. 18, see Fig. 29). These results are consistent with the observation of Park *et al*. (2005), which demonstrated the apoptotic function of ANKRD1 in human hepatic cancer cells (Hep3B and SK-HEP-1 cells) (Park *et al*., 2005). In contrast, in breast cells (T47D), the expression of ANKRD1 showed a proliferative effect (Fig. 17A-C), supporting the hypothesis that ANKRD1 could have a tissue-specific oncogenic or tumor suppressive role (Kojic *et al*., 2010; Lei *et al*., 2015; Shen *et al*., 2015). Here, it was demonstrated that *ANKRD1* is expressed in a cell type-dependent manner and its function should be analysed in other cell lines and in response to cellular and chemical stress.

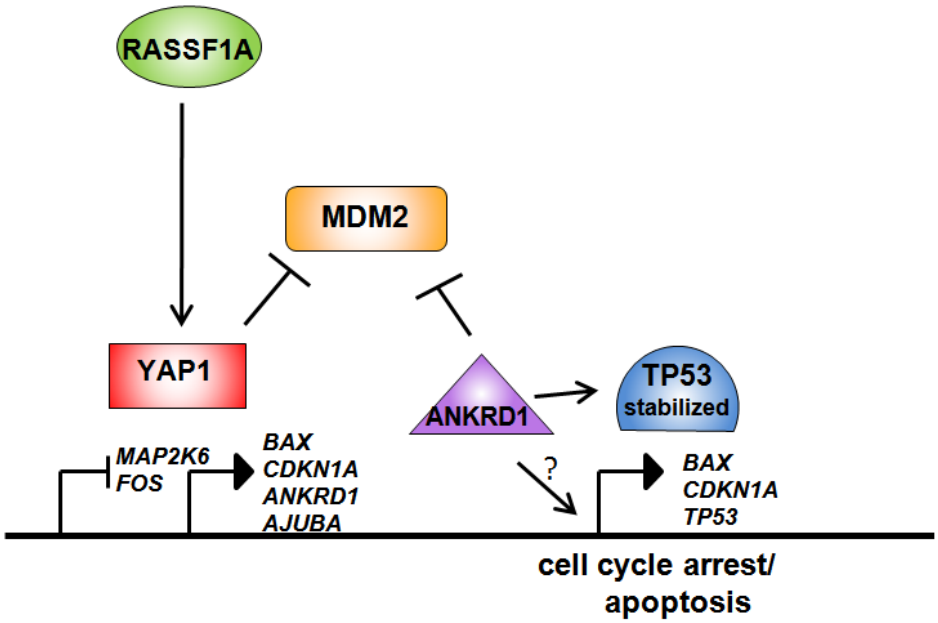

Figure 29: Model of RASSF1A-YAP1-ANKRD1 regulatory loop. RASSF1A induces cell cycle arrest and apoptosis through activation of specific YAP1 target genes (e.g. *ANKRD1*). RASSF1A and YAP1 as well as ANKRD1 increase TP53 and BAX levels by destabilisation or reduction of MDM2 protein level.

Interestingly, it has been suggested that ANKRD1 is a co-activator of TP53 (Kojic *et al*., 2010). Recently it has been reported that ANKRD1 contributes to apoptosis in cardiomyocytes by mitochondrial translocation of BAX and TP53 phosphorylation (Shen *et al*., 2015). In addition, the interaction of ANKRD1 with TP53 and the transcriptional activation of *CDKN1A* and *MDM2* by ANKRD1 were demonstrated *in vitro* and *in vivo* (Kojic *et al*., 2010). In our study, the interaction of ANKRD1 with TP53 was confirmed and it was extended by the detection of the interaction between ANKRD1 and MDM2 (Fig. 20). Moreover, it was found that ANKRD1 induces the expression of *TP53, BAX, MDM2* and *CDKN1A* (Fig. 18), which supports the hypothesis and data of Kojic *et al.* (2010) that suggested ANKRD1 as a possible co-activator of TP53 (Kojic *et al*., 2010). The knockdown of ANKRD1 by siRNA also corroborated these findings, since the silencing of ANKRD1 resulted in a transcriptional repression of TP53 target genes (Fig. 21). Similar to the effect observed by the co-expression of YAP1 and RASSF1A (Fig. 13A, Fig. 19), ANKRD1 overexpression reduced the protein level of MDM2, which allows the stabilisation of TP53 and an increase of BAX level (see Fig. 29, Fig. 19A-B). In this study, it was observed that the transcriptional regulation of MDM2 depends on ANKRD1 and TP53; however, the reduction of the protein level of MDM2 by ANKRD1 overexpression or by co-expression of RASSF1A and YAP1 needs to be further investigated.

There is no data on a possible kinase activity of ANKRD1, but somehow the level of TP53 is stabilised after expression of ANKRD1 and after expression of RASSF1A and YAP1. This effect on TP53 might occur by direct phosphorylation of TP53 or indirectly e.g. by binding competition of ANKRD1 with MDM2 or TP53, which prevents the interaction of TP53 with MDM2 and the subsequent ubiquitinylation of TP53 (Fig. 19A-B, Fig. 20). The regulation of MDM2 and TP53 by ANKRD1 should be characterised in further detail, for example by competition assays or by using ANKRD1 depletion mutants. In the future, it also needs to be elucidated which ANKRD1 domain is responsible for the interaction with MDM2 and with TP53. The ankyrin repeat domains of ANKRD1 are among the most abundant motifs for protein-protein interactions, e.g. the INK4 tumor suppressors and the TP53 binding protein 2 contain several ankyrin repeats (Mosavi *et al*., 2004). Furthermore, ANKRD1 has been described as a potential transcription factor and as co-activator of TP53 (Kojic *et al*., 2010; Liu *et al*., 2015), but there is no information on putative binding sites or novel potential target genes beside *TP53, BAX* and *CDKN1A*. It would be interesting to do microarrays or RNA-seq and ChIP analysis of ANKRD1 to further investigate its function

at the transcriptional level. *ANKRD1* silencing by CRISPR-Cas should also be performed to confirm the findings of this work.

Figure 29 summarizes the obtained data of this project and suggests a hypothetical model of the pro-apoptotic signalling of the Hippo pathway. In this study, RASSF1A, ANKRD1, MDM2 are the key players involved in the pro-apoptotic function of the Hippo pathway. RASSF1A stabilises YAP1 thereby increasing its translocation into the nucleus; once there, YAP1 induces a higher expression of *ANKRD*1, whereas MDM2 is destabilised, and TP53 and BAX protein levels increase (Fig. 29). ANKRD1 showed a tumor suppressive function by interaction and activation of TP53, which induces *BAX, CDKN1A* and *TP53* expression. Furthermore, ANKRD1 can interact and decrease the protein level of MDM2, suggesting that ANKRD1 could be responsible for the MDM2 destabilisation and the subsequent TP53 stabilisation and BAX induction (see Fig. 29). Since *RASSF1A* and *ANKRD1* show an aberrant promoter methylation and the resulting gene silencing, the pro-apoptotic signal of the Hippo pathway is disturbed and the oncogenic function of YAP1 cannot be counteracted. Subsequently, YAP1 represses the expression of the tumor suppressor genes and promotes cell proliferation.

4.5 Effect of the other C-terminal RASSFs on the Hippo pathway

Six members of the RAS association domain family (RASSF1 to RASSF6) have a SARAH interaction domain, which suggests a role in the regulation of the Hippo pathway. Through the SARAH domain, they are capable to interact with the MSTs, WW45 and with each other (Schagdarsurengin *et al*., 2010). In the literature RASSF1A, RASSF2 and RASSF5 are directly associated with the regulation of both MSTs and the Hippo pathway (Cooper *et al*., 2009; Ni *et al*., 2013; Praskova *et al*., 2004; Song *et al*., 2010). Therefore in this study, the function of the other C-terminal RASSFs on the regulation of the YAP1 target genes was further characterised and compared to the previous results for RASSF1A.

In contrast to RASSF1A, there are only few data available concerning the cellular function of the other RASSF genes. Few reports have demonstrated that they are also inactivated by promoter hypermethylation for example in thyroid cancer, Merkel cell carcinoma, and in pheochromocytoma (Richter *et al*., 2013; Richter *et al*., 2015; Schagdarsurengin *et al*.,

2010). Also in this work we observed a tumor-specific methylation of *RASSF2, RASSF3* and *RASSF5*A isoform in HCC (Fig. 22). To date, there is no data on the methylation status of *RASSF2, RASSF3* and *RASSF6* in liver tumors. However, previous reports demonstrated that the *RASSF5A* and *RASSF5B* isoforms are inactivated by promoter methylation and their expression is reduced in HCC, which corroborated with our findings on RASSF5A (Liu *et al*., 2014; Macheiner *et al*., 2006).

The data displayed in this study demonstrated that all C-terminal RASSFs induce the expression of the YAP1 target genes: *ANKRD1*, *TP53* and *BAX* (Fig. 24, Fig. 25). Moreover, it was observed that YAP1 together with the C-terminal RASSFs, with exception of RASSF1A, induced the expression of *p16* (Fig. 25), which resulted in cell cycle arrest in the G0-G1 phase (Fig. 23). p16 is the inhibitor of CDK4/CDK6 in association with the RB-E2F pathway inducing cellular senescence and cell cycle arrest in the G0-G1 phase (Ragione *et al*., 1996). There are two possible explanations for these observations; the first one is that YAP1 and the RASSFs could directly regulate the expression of *p16*, but there is no data in the literature supporting this hypothesis. The other explanation could be that the increase of *p16* expression is a response to a pro-proliferative factor or a response to a highly expressed interaction partner like *CDK6*, which is interestingly also a YAP1 target gene (Xie *et al*., 2013). In the future, both hypotheses should be further analysed in further detail. It would also be important to analyse the expression of the other INK4 tumor suppressors after expression of YAP1 and the C-terminal RASSFs, since *p14* and *p15* are located in the same genomic locus as *p16*. Moreover, it may be worthwhile to investigate a possible interaction of YAP1 with the transcription factors, which modulate the expression of *p16*.

As previously indicated, the co-expression of RASSF1A with YAP1 and the overexpression of ANKRD1 reduce the MDM2 protein level (Fig. 19A-B). Since the other C-terminal RASSFs also induced the expression of *ANKRD1* (Fig. 24), the protein level of MDM2 was further analysed after expression of RASSF2 and RASSF5 in the YAP1-inducible cells. RASSF2 and RASSF5 are the best-characterised C-terminal RASSF members after RASSF1A. RASSF2 is located in the nucleus and its activation by p300 is associated with apoptosis (Liu *et al*., 2010; Schagdarsurengin *et al*., 2010). RASSF3 and RASSF6 regulate the MDM2 levels independent of the Hippo pathway (Iwasa *et al*., 2013; Kudo *et al*., 2012). In addition, RASSF5 and RASSF6 interact with MDM2 and regulate

TP53 expression (Donninger *et al*., 2015; Iwasa *et al*., 2013). In this study, it was observed that RASSF1A, RASSF2 and RASSF5 overexpression are capable to decrease the protein level of MDM2. At present, there is no data in the literature on RASSF2 regulation or interaction with MDM2 or TP53 regulation. The decrease of MDM2 by RASSF5 was recently published by Schmidt *et al*. (2016) in association with β-TrCP (Schmidt *et al*., 2016). Only the expression of RASSF1A with YAP1 resulted in a significant decrease of MDM2 (Fig. 26), which may suggest that only RASSF1A is able to induce the repression of MDM2 via Hippo signalling. Here RASSF2 and RASSF5A did not reduce the MDM2 level after induction of YAP1, suggesting that they may reduce MDM2 independently of the Hippo pathway, similar to RASSF3 and RASSF6.

This study arises new questions involving the role of C-terminal RASSFs in the regulation of the Hippo pathway. For example; which are the regulatory upstream events that induce the apoptosis signalling through RASSF1A and YAP1. Another major point that needs to be investigated is how MDM2 is destabilised by RASSF1A and YAP1 or by ANKRD1. Other reports and this work demonstrated that the C-terminal RASSFs regulated the level of MDM2 and TP53. Here the mechanism needs to be elucidated, how RASSF1A together with YAP1 and RASSF2 modulate the protein level of MDM2.

APPENDIX 1

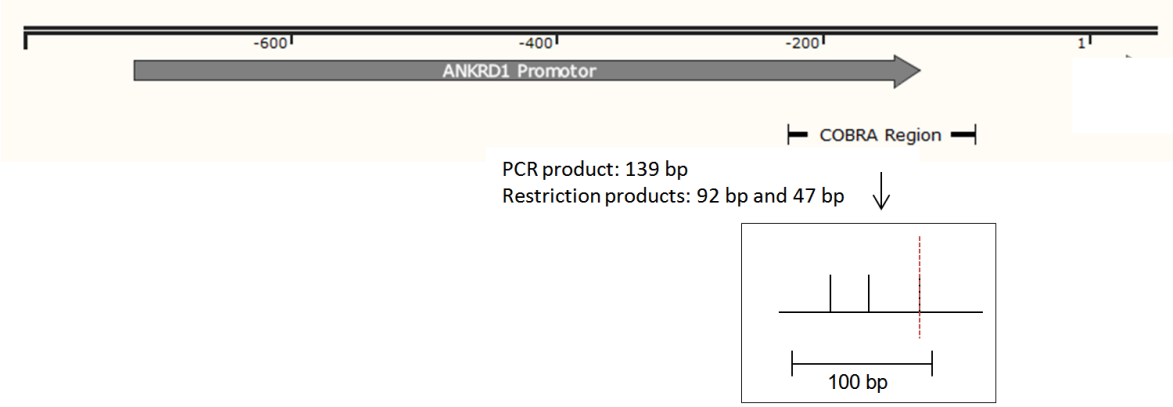

Appendix 1: The promoter region of *ANKRD1* (606 bp) was cloned into the pRL-NULL reporter vector for the subsequent promoter assays. For the methylation analysis, a region of 139 bp of the *ANKRD1* promoter was amplified by PCR using bisulfite DNA and further analysed by CoBRA (panel). The blackvertical bars represent single CpG sites. The analysed CpG (cg01262952) site is represented with the dotted red line.

APPENDIX 2

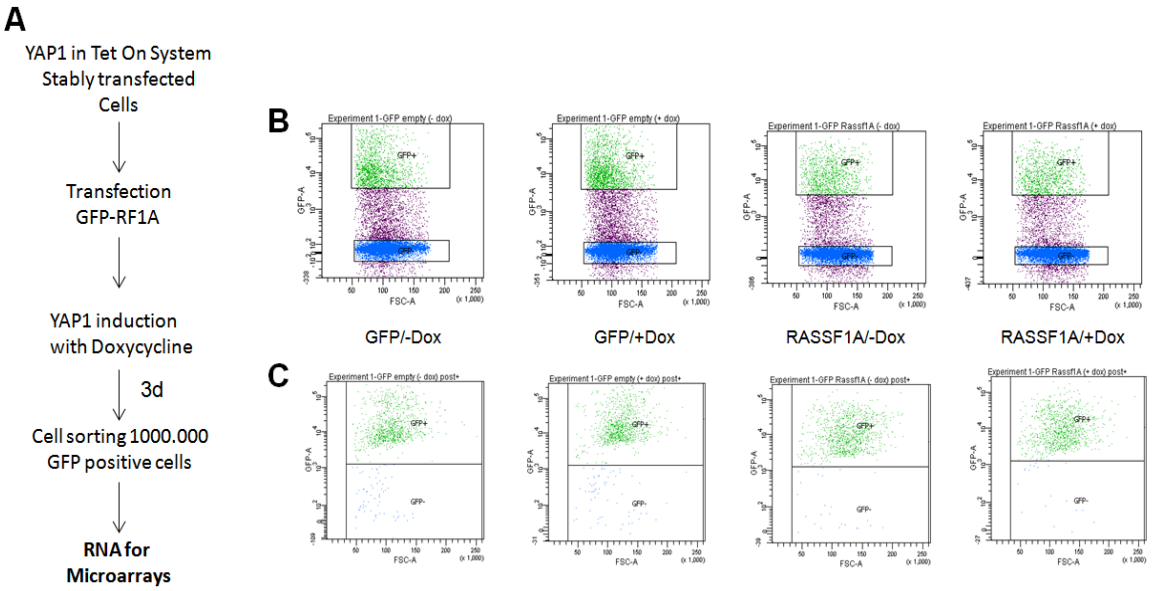

Appendix 2: **Experimental design for expression analysis by microarrays. A.** Outline **B**. Sorted cells in green. **C.** Purity control of sorted cells; green spots: sorted cells with GFP signal.

APPENDIX 3

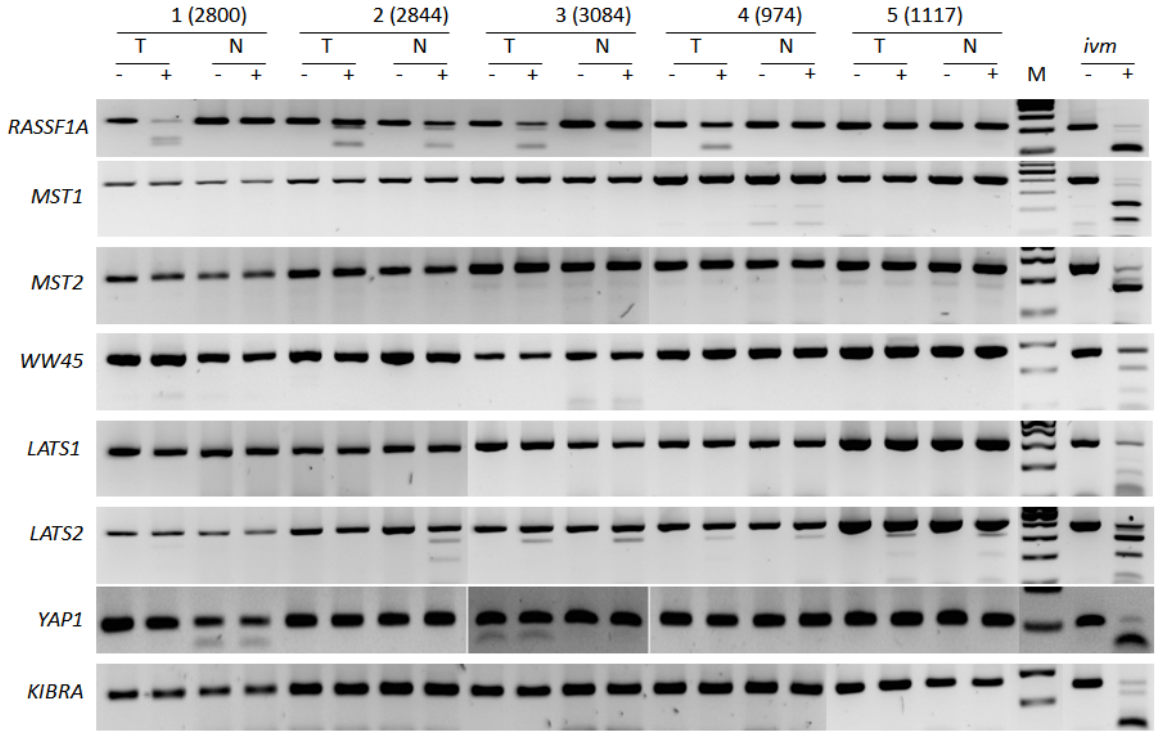

Appendix 3: Methylation analysis of the promoter region of core components of the Hippo pathway. Combined bisulfite restriction analysis of the promoter region of *RASSF1A, MST1, MST2, WW45, LATS1, LATS2, YAP1* and *KIBRA* in liver tumors (T) compared to matched normal samples (N). Positive control: *in vitro* methylated DNA (*ivm*). Mock digest (-); PCR product digested with respective enzyme (+), and further analysed by AGE in a 2% TBE gel. Experiment perfomed by Dr. Richter.

APPENDIX 4

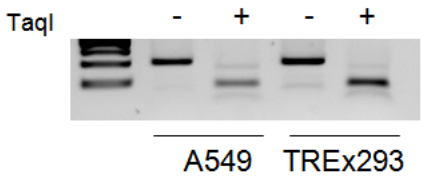

Appendix 4: Methylation analysis of the promoter region of *RASSF1A* in TREx293 cells. Combined bisulfite restriction analysis of the promoter region of *RASSF1A*. A fragment of 205 bp of the promoter region of *RASSF1A* was amplified by seminested PCR using bisulfite converted DNA from TREx293 cells and A549 cells as positive control. The PCR product was subsequently digested with *TaqI* (+) or with water (-) and further analysed by AGE in a 2% TBE gel.

APPENDIX 5

Table 21. List of potential upregulated candidate genes (at least 2.5-fold) obtained after the unbiased analysis of the microarrays of the YAP1-inducible TREx293 cells. The genes were sorted in descending order by the relative measured expression of the samples with an overexpression of RASSF1A and YAP1 induction. The expression level is relative to the control uninduced cells (GFP/unind.).

Gene name	GFP/unind.	GFP/YAP1 ind.	RASSF1A/unind.	RASSF1A/YAP1 ind.
HIF1A-AS2	1.00	7.70	1.16	10.90
MIR3665	1.00	0.52	1.68	5.39
ACTBL2	1.00	2.72	1.16	4.85
COL12A1	1.00	4.60	1.11	4.41
RNU6-1284P	1.00	2.49	5.85	4.37
RNU6-135P	1.00	3.09	1.90	4.02
CTGF	1.00	2.26	1.34	3.97
MT-TW	1.00	2.90	2.58	3.64
YAP1	1.00	3.62	1.01	3.58
RNA5SP253	1.00	7.42	5.05	3.44
RNA5SP253	1.00	7.42	5.05	3.44
RNA5SP253	1.00	7.42	5.05	3.44
ANKRD1	1.00	2.88	1.24	3.40
HIF1A-AS2	1.00	3.69	0.73	3.26
CYR61	1.00	2.66	1.43	3.26
CPA4	1.00	2.74	1.24	3.22
RNU6-470P	1.00	1.62	1.55	3.09
RNU6-96P	1.00	1.38	1.90	2.94
RNU4ATAC16P	1.00	5.14	5.15	2.85
MIR634	1.00	1.74	1.50	2.83
MIR4441	1.00	2.37	1.80	2.80
AJUBA	1.00	2.25	1.20	2.77
MIR1321	1.00	3.17	2.04	2.76
MIR329-1	1.00	1.55	1.62	2.74
RNU6-1318P	1.00	4.05	4.05	2.69
SNAPC1	1.00	2.02	1.20	2.69
SPANXC	1.00	1.69	1.55	2.67
RNA5SP222	1.00	1.05	1.24	2.67
MIR378H	1.00	2.33	2.05	2.60
SPATA31D4	1.00	1.56	0.83	2.56
MYOF	1.00	1.81	1.34	2.55
MIR4731	1.00	2.91	1.88	2.53
RASSF1	1.00	0.46	2.30	2.52
PRAMEF2	1.00	1.82	1.67	2.51
RNU6-604P	1.00	2.41	1.32	2.50

APPENDIX 6

Table 22. List of potential downregulated candidate genes (from 0.5-fold) obtained after the unbiased analysis of the microarrays of the YAP1-inducible TREx293 cells. The genes were sorted in descending order by the relative measured expression of the samples with an overexpression of RASSF1A and YAP1 induction. The expression level is relative to the control uninduced cells (GFP/unind.).

Gene name	GFP/unind.	GFP/YAP1 ind.	RASSF1A/unind.	RASSF1A/YAP1 ind.
AC100802.3	1.00	0.48	0.56	0.50
AF196970.3	1.00	0.65	0.75	0.50
LINC00346	1.00	0.63	0.59	0.50
AC073218.1	1.00	0.65	0.64	0.50
TRIM48	1.00	0.51	0.78	0.50
RP11-313D6.3	1.00	0.57	0.41	0.50
RNA5SP207	1.00	0.85	0.78	0.50
RP11-475I24.3	1.00	0.75	0.58	0.50
ZNF280D	1.00	0.62	0.70	0.50
RNU6-457P	1.00	0.84	0.55	0.50
RNU6-487P	1.00	0.48	0.37	0.49
SNORD115-32	1.00	1.09	0.75	0.49
RNU6-646P	1.00	0.44	0.53	0.49
SPRR2A	1.00	0.92	0.78	0.49
HIST1H2BH	1.00	0.52	0.73	0.49
PYDC2	1.00	0.99	0.64	0.49
RNU6-271P	1.00	0.51	0.54	0.49
OR2A14	1.00	0.88	0.61	0.48
RNA5SP133	1.00	0.61	0.61	0.48
SNORD23	1.00	0.79	0.77	0.48
RNU6-971P	1.00	0.63	0.50	0.47
CCL4	1.00	0.39	0.63	0.47
RNA5SP230	1.00	0.72	0.54	0.47
RNU6-218P	1.00	0.48	0.61	0.47
RPLP0P2	1.00	0.51	0.55	0.47
GDF15	1.00	0.60	0.72	0.46
FOXD3	1.00	0.74	0.48	0.46
MIR376B	1.00	0.69	0.64	0.46
TREML5P	1.00	1.11	0.56	0.46
IGHV3-15	1.00	0.67	0.72	0.46
FGF21	1.00	0.59	0.46	0.45
RNU6-659P	1.00	0.53	0.47	0.45
ANAPC1P1	1.00	0.65	0.54	0.45
RP11-166D18.1	1.00	0.50	0.48	0.45
TRBJ2-4	1.00	0.83	0.76	0.45
C6orf47	1.00	0.55	0.82	0.45
MIR3189	1.00	0.72	0.44	0.45
ARL14EPL	1.00	0.65	0.53	0.44
ULBP2	1.00	0.49	0.46	0.44

RNA5SP302	1.00	0.42	0.92	0.44
CLEC4M	1.00	0.34	0.35	0.44
RPL23AP82	1.00	0.86	0.77	0.44
MIR1184-1	1.00	0.44	0.54	0.43
MIR1184-1	1.00	0.44	0.54	0.43
MIR1184-1	1.00	0.44	0.54	0.43
VTRNA2-2P	1.00	0.81	0.70	0.43
LOC101927703	1.00	0.38	0.92	0.43
RNU2-24P	1.00	1.64	1.28	0.42
MIR548H3	1.00	1.08	0.72	0.42
RNU1-92P	1.00	0.57	0.37	0.41
ALPPL2	1.00	0.57	0.38	0.41
MIR4710	1.00	0.72	0.76	0.41
TRIM49	1.00	0.70	0.72	0.41
GH1	1.00	0.57	0.65	0.41
RNU2-71P	1.00	0.38	0.50	0.40
RP11-203M5.8	1.00	0.43	0.49	0.40
MIR601	1.00	0.51	0.71	0.40
MAP3K8	1.00	0.40	0.89	0.39
RNF216P1	1.00	0.49	0.85	0.39
MIR4503	1.00	0.63	0.34	0.39
RNA5SP241	1.00	1.05	0.56	0.39
FAM66A	1.00	0.49	0.38	0.38
RNU6-1295P	1.00	0.54	0.94	0.37
MIR1324	1.00	0.99	0.49	0.35
MIR3163	1.00	1.01	0.47	0.35
KRT18P39	1.00	0.83	0.33	0.34
RNY1P8	1.00	0.55	1.07	0.34
RNU6-361P	1.00	0.96	0.41	0.33
HIST1H3H	1.00	0.49	0.48	0.32
RNU6ATAC25P	1.00	0.80	0.45	0.32
RNU6-612P	1.00	0.81	0.26	0.31
MIR501	1.00	0.63	0.47	0.15

APPENDIX 7

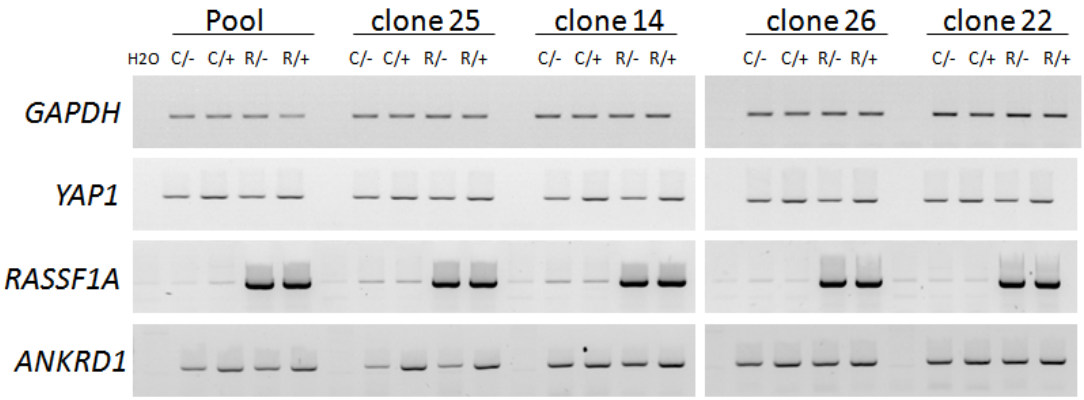

Appendix 7: Semiquantitative PCR to control the overexpression of RASSF1A and YAP1 induction in the clones used for the validation of the microarrays. The individual YAP1-inducible TREx293 clones were tranfected with Flag-empty vector or with Flag-RASSF1A respectively. The PCR products were analysed by AGE. After 72h induction of YAP1 (- unind.; + YAP1 induced), the expressions of the candidates target genes were further analysed by qRT-PCR. The gene expression of the target genes of clone 14 was displayed in figure 14. C: Overexpression of control empty vector. R: overexpression of RASSF1A.

APPENDIX 8

A)

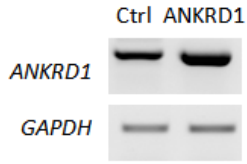

B)

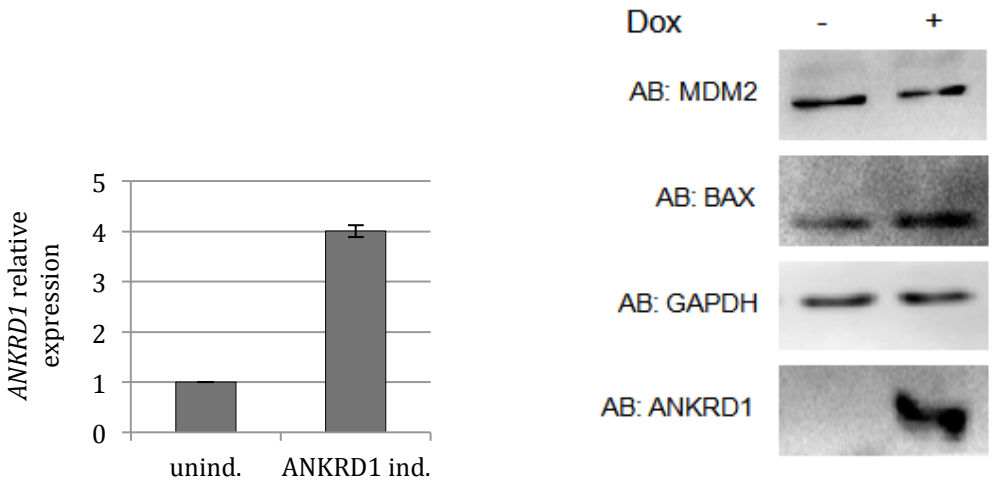

Appendix 8: Controls corresponding to figure 18. A) Semiquantitative PCR to control the overexpression of *ANKRD1* in HEK293T cells. The expressions of the target genes were further analysed by qRT-PCR and displayed in figure 18A. **B)** Western blot analysis and qRT-PCR to control the induction *ANKRD1* in the ANKRD1-inducible TREx293 cells and the protein level of the target genes MDM2, GAPDH and BAX.

APPENDIX 9

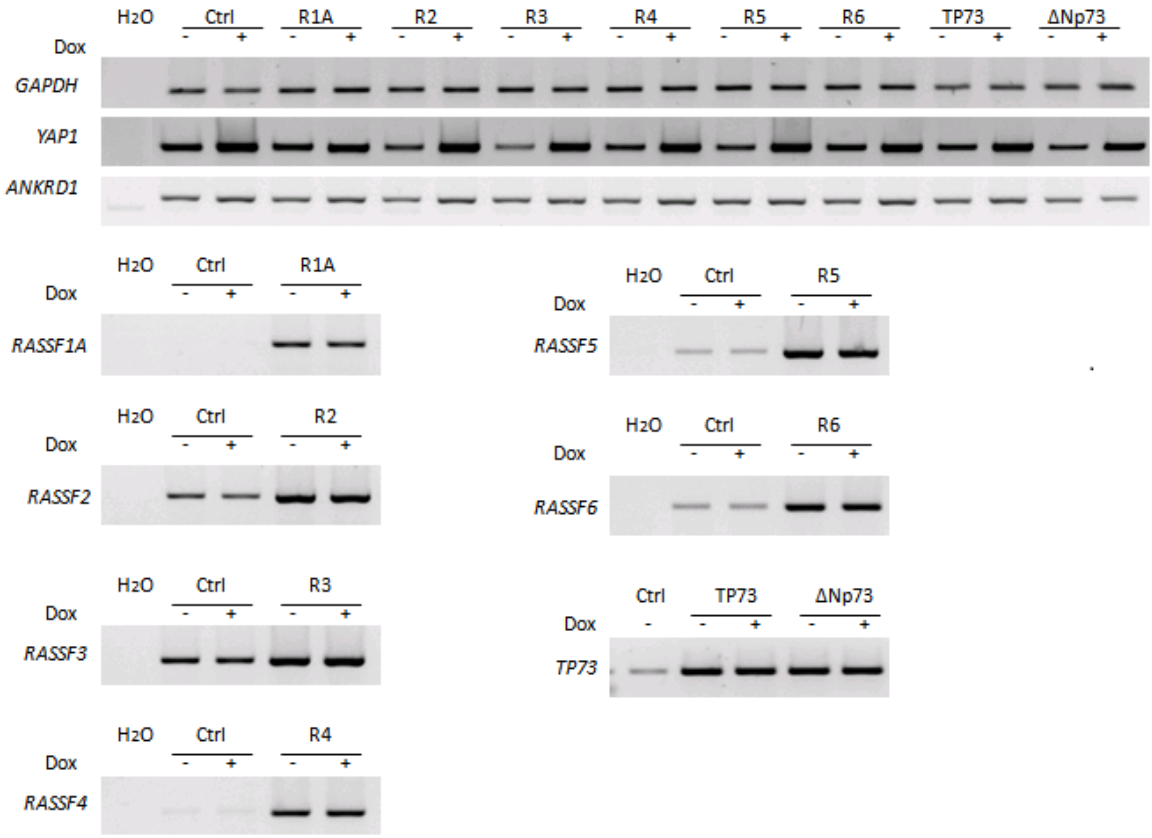

Appendix 9: Exemplary semiquantitative PCR to control the overexpression of the C-terminal RASSFs, TP73, ΔNp73 and the YAP1 induction in the YAP1-inducible TREx293 cells. The individual constructs were overexpressed in the YAP1-inducible TREx293 pool of clones. After 72h induction of YAP1 (- unind.; + YAP1 induced), the expression of the candidates target genes were further analysed by qRT-PCR. R1A: overexpression of RASSF1A, R2: overexpression of RASSF2, R3: overexpression of RASSF3, R4: overexpression of RASSF4, R5: overexpression of RASSF5, R6: overexpression of RASSF6, TP73: overexpression of TP73, ΔNp73: overexpression of ΔNp73). The measured expression of the target genes was displayed in figures 24 and 25.

APPENDIX 10

Table 23. p-values corresponding to figure 24 and figure 25.

YAP1 TREx cells	Non significant	p-values <0.05	p-values <0.01	p-values <0.001

p-values for ANKRD1	relative to Ctrl	relative to YAP1	relative to RASSF1A/YAP1
Ctrl/unind.			
Ctrl/YAP1 ind.	0.0001		
RASSF1A/unind.	0.182	0.0002	
RASSF1A/YAP1 ind.	0.008	0.033	
RASSF2/unind.	0.012	0.001	0.010
RASSF2/YAP1 ind.	0.0007	0.002	0.037
RASSF3/unind.	0.011	0.001	0.011
RASSF3/YAP1 ind.	0.0008	0.002	0.022
RASSF4/unind.	0.008	0.002	0.012
RASSF4/YAP1 ind.	0.003	0.006	0.032
RASSF5/unind.	0.002	0.002	0.015
RASSF5/YAP1 ind.	0.003	0.009	0.089
RASSF6/unind.	0.005	0.010	0.017
RASSF6/YAP1 ind.	0.00001	0.00001	0.015
TP73/unind.	0.007	0.003	0.013
TP73/YAP1 ind.	0.0009	0.001	0.007
ΔNp73/unind.	0.010	0.129	0.027
ΔNp73/YAP1 ind.	0.019	0.030	0.057

p-values for TP53	relative to Ctrl	relative to YAP1	relative to RASSF1A/YAP1	relative to RASSFs controls
Ctrl/unind.				
Ctrl/YAP1 ind.	0.047			0.047
RASSF1A/unind.	0.000001	0.000015		
RASSF1A/YAP1 ind.	0.065	0.312		0.0001
RASSF2/unind.	0.000001	0.000013	0.0001	
RASSF2/YAP1 ind.	0.012	0.057	0.305	0.00002
RASSF3/unind.	0.065	0.067	0.069	
RASSF3/YAP1 ind.	0.0006	0.041	0.457	0.070
RASSF4/unind.	0.133	0.293	0.155	
RASSF4/YAP1 ind.	0.0001	0.007	0.043	0.005
RASSF5/unind.	0.133	0.293	0.155	
RASSF5/YAP1 ind.	0.0009	0.423	0.423	0.095
RASSF6/unind.	0.023	0.293	0.699	
RASSF6/YAP1 ind.	0.003	0.006	0.013	0.007
TP73/unind.	0.0009	0.423	0.423	
TP73/YAP1 ind.	0.016	0.027	0.051	0.027
ΔNp73/unind.	0.0001	0.007	0.043	
ΔNp73/YAP1 ind.	0.00002	0.001	0.005	0.0001

p-values for BAX	relative to Ctrl	relative to YAP1	relative to RASSF1A/YAP1	relative to RASSFs controls
Ctrl/unind.				
Ctrl/YAP1 ind.	0.028			0.028
RASSF1A/unind.	0.077	0.006		
RASSF1A/YAP1 ind.	0.028	0.004		0.0082
RASSF2/unind.	0.294	0.022	0.088	
RASSF2/YAP1 ind.	0.021	0.007	0.054	0.034
RASSF3/unind.	0.868	0.247	0.246	
RASSF3/YAP1 ind.	0.048	0.019	0.124	0.108
RASSF4/unind.	0.057	0.028	0.113	
RASSF4/YAP1 ind.	0.003	0.002	0.004	0.051
RASSF5/unind.	0.007	0.004	0.009	
RASSF5/YAP1 ind.	0.001	0.0006	0.0001	0.095
RASSF6/unind.	0.085	0.046	0.155	
RASSF6/YAP1 ind.	0.018	0.011	0.029	0.475
TP73/unind.	0.034	0.021	0.053	
TP73/YAP1 ind.	0.008	0.006	0.010	0.088
ΔNp73/unind.	0.003	0.002	0.003	
ΔNp73/YAP1 ind.	0.010	0.007	0.013	0.699

p-values for p16	relative to Ctrl	relative to YAP1	relative to RASSF1A/YAP1	relative to RASSFs controls
Ctrl/unind.				
Ctrl/YAP1 ind.	0.105			0.105
RASSF1A/unind.	0.411	0.035		
RASSF1A/YAP1 ind.	0.232	0.075		0.011
RASSF2/unind.	0.755	0.012	0.001	
RASSF2/YAP1 ind.	0.181	0.294	0.375	0.029
RASSF3/unind.	0.583	0.042	0.088	
RASSF3/YAP1 ind.	0.033	0.026	0.0004	0.005
RASSF4/unind.	0.181	0.294	0.375	
RASSF4/YAP1 ind.	0.026	0.035	0.023	0.029
RASSF5/unind.	0.033	0.026	0.0004	
RASSF5/YAP1 ind.	0.115	0.673	0.165	0.152
RASSF6/unind.	0.105	1.000	0.0746	
RASSF6/YAP1 ind.	0.020	0.017	0.007	0.017
TP73/unind.	0.076	0.416	0.001	
TP73/YAP1 ind.	0.076	0.416	0.001	1.000
ΔNp73/unind.	0.008	0.006	0.003	
ΔNp73/YAP1 ind.	0.011	0.009	0.005	0.290

HEK293T cells	Non significant	p-values <0.05	p-values <0.01	p-values <0.001

p-values for ANKRD1	relative to Ctrl	relative to YAP1	relative to RASSF1A/YAP1
Ctrl			
YAP1	0.004		
RASSF1A	0.451	0.008	
RASSF1A/YAP1	0.001	0.024	
RASSF2	0.048	0.004	0.0009
RASSF2/YAP1	0.001	0.014	0.112
RASSF3	0.061	0.004	0.001
RASSF3/YAP1	0.004	0.028	0.175
RASSF4	0.075	0.004	0.0009
RASSF4/YAP1	0.049	0.006	0.001
RASSF5	0.010	0.006	0.001
RASSF5/YAP1	0.003	0.007	0.011
RASSF6	0.034	0.005	0.001
RASSF6/YAP1	0.008	0.139	0.328
TP73	0.974	0.004	0.001
TP73/YAP1	0.060	0.011	0.003
ΔNp73	0.317	0.004	0.0009
ΔNp73 /YAP1	0.004	0.174	0.084

p-values for TP53	relative to Ctrl	relative to YAP1	relative to RASSF1A/YAP1	relative to RASSFs controls
Ctrl				
YAP1	0.002			0.002
RASSF1A	0.006	0.008		
RASSF1A/YAP1	0.002	0.113		0.006
RASSF2	0.009	0.007	0.005	
RASSF2/YAP1	0.003	0.109	0.033	0.011
RASSF3	0.003	0.052	0.021	
RASSF3/YAP1	0.002	0.293	0.054	0.102
RASSF4	0.010	0.308	0.085	
RASSF4/YAP1	0.003	0.019	0.011	0.095
RASSF5	0.00005	0.423	0.047	
RASSF5/YAP1	0.002	0.021	0.056	0.012
RASSF6	0.00002	0.044	0.017	
RASSF6/YAP1	0.000005	0.107	0.026	0.002
TP73	0.0000005	0.011	0.007	
TP73/YAP1	0.014	0.050	0.024	0.425
ΔNp73	0.0000002	0.426	0.047	
ΔNp73 /YAP1	0.002	0.293	0.294	0.096

p-values for BAX	relative to Ctrl	relative to YAP1	relative to RASSF1A/YAP1	relative to RASSFs controls
Ctrl				
YAP1	0.020			0.020
RASSF1A	0.437	0.0001		
RASSF1A/YAP1	0.038	0.950		0.015
RASSF2	0.077	0.0007	0.010	
RASSF2/YAP1	0.110	0.008	0.062	0.005
RASSF3	0.330	0.004	0.034	
RASSF3/YAP1	0.788	0.0001	0.022	0.099
RASSF4	0.352	0.002	0.016	
RASSF4/YAP1	0.202	0.004	0.015	0.306
RASSF5	0.027	0.006	0.425	
RASSF5/YAP1	0.004	0.004	0.011	0.004
RASSF6	0.774	0.0001	0.018	
RASSF6/YAP1	0.204	0.081	0.123	0.116
TP73	0.501	0.014	0.039	
TP73/YAP1	0.607	0.003	0.027	0.699
ΔNp73	0.110	0.008	0.062	
ΔNp73 /YAP1	0.036	0.002	0.206	0.025

p-values for p16	relative to Ctrl	relative to YAP1	relative to RASSF1A/YAP1	relative to RASSFs controls
Ctrl				
YAP1	0.012			0.012
RASSF1A	0.172	0.0002		
RASSF1A/YAP1	0.107	0.421		0.166
RASSF2	0.140	0.002	0.052	
RASSF2/YAP1	0.076	0.00001	0.263	0.006
RASSF3	0.076	0.00001	0.263	
RASSF3/YAP1	0.027	0.00002	0.754	0.00003
RASSF4	0.076	0.00001	0.263	
RASSF4/YAP1	0.076	0.014	0.344	0.429
RASSF5	0.018	0.0001	0.808	
RASSF5/YAP1	0.076	0.014	0.344	0.030
RASSF6	0.356	0.000002	0.068	
RASSF6/YAP1	0.103	0.080	0.498	0.045
TP73	0.103	0.080	0.498	
TP73/YAP1	0.902	0.000001	0.088	0.065
ΔNp73	0.044	0.00001	0.424	
ΔNp73 /YAP1	0.024	0.418	0.611	0.046

APPENDIX 11

Flag-empty	+	+	-	-	-	-	-	-
Flag-RASSF1A	-	-	+	+	-	-	-	-
Flag-RASSF2	-	-	-	-	+	+	-	-
Flag-RASSF5A	-	-	-	-	-	-	+	+
YAP1 induction	-	+	-	+	-	+	-	+

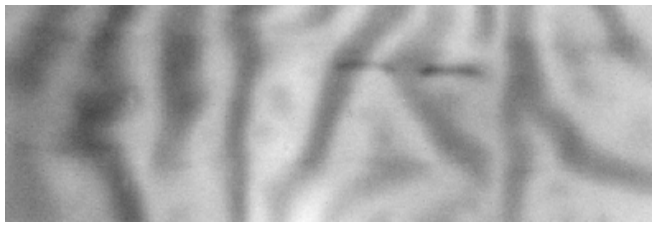

AB: FLAG

Appendix 11: Control western blot for the overepression of Flag empty, Flag-RASSF1A, Flag-RASSF2 and Flag-RASSF5. The induction of YAP1 and the protein level of GAPDH and MDM2 are indicated in figure 26. The anti-FLAG antibody showed the overexpression of RASSF2 (40 kDa). Since the FLAG and the RASSF1A antibodies do not showed the overepression as expected, the overexpressions of RASSF1A, RASSF2 and RASSF5 were confimed in the biological replicates by semiquantitative PCR as indicated in appendix 9.

APPENDIX 12

Additionally in this work, several potential binding partners of YAP1 were detected by mass spectrometry. In this appendix, the detected proteins with a mascot score higher than 62 are listed in Table 24. Interestingly, it was found that YAP1 might interact with Lamin B1 and voltage-dependent anion channels. The interaction of YAP1 with Lamin B1 was further analysed but could not be validated. The possible interaction of YAP1 with voltage-dependent anion channels may be associated with the apoptotic function of BAX and need to be analysed in more detail. With the exception of Lamin B1 and CENPF, the other identified proteins are cytoplasmic and related to cell-cell junctions, intermediate filaments or have been previously described with the Hippo pathway. In the future, it should be interesting to validate the interaction of those candidate interaction partners with YAP1 and the conditions that promote those interactions such as phosphorylation, conformational changes or localization. In addition, the mass spectrometry data should be repeated after cell fractionation, in order to find out novel YAP1 interaction partners in the nucleus.

Table 24. Mass spectrometry results with the potential binding partners of YAP1 and the respective mascot score.

Name	Mascot Score
Angiomotin	403.0
Heat shock 70 kDa protein 1A/1B	354.0
Vimentin	252.0
78 kDa glucose-regulated protein	227.0
YAP1	208.0
Pyrroline-5-carboxylate reductase 2	128.0
Voltage-dependent anion-selective channel protein 1	116.0
14-3-3 protein epsilon	108.0
Heat shock 70 kDa protein 6	104.0
Heat shock 70 kDa protein 1-like	100.0
Heat shock cognate 71 kDa protein	96.6
Polyadenylate-binding protein 1	96.0
Voltage-dependent anion-selective channel protein 3	88.2
60S ribosomal protein L5	88.0
Voltage-dependent anion-selective channel protein 2	86.0
A-kinase anchor protein 9	81.6
WW domain-binding protein 2	81.3
Actin, cytoplasmic 2	78.8
Golgin subfamily A member 4	78.6
40S ribosomal protein S4	78.4
Golgin subfamily A member 4	74.6
Heterogeneous nuclear ribonucleoproteins A2/B1	73.2
Vinculin	69.4
Tropomyosin beta chain	68.3
Dystonin	68.0
Lamin-B1	67.5
Centromere protein F	67.4
Plectin	65.8
Hemoglobin subunit epsilon	64.4
Uncharacterised protein	64.0
Regulating synaptic membrane exocytosis protein 1	63.7
Plectin	63.2
Glutathione S-transferase Mu 1	62.9
Prohibitin-2	62.8
Spectrin alpha chain	62.0

REFERENCES

Abe, Y., Ohsugi, M., Haraguchi, K., Fujimoto, J., and Yamamoto, T. (2006). LATS2-Ajuba complex regulates gamma-tubulin recruitment to centrosomes and spindle organization during mitosis. FEBS letters *580*, 782-788.

Agathanggelou, A., Bieche, I., Ahmed-Choudhury, J., Nicke, B., Dammann, R., Baksh, S., Gao, B., Minna, J.D., Downward, J., Maher, E.R.*, et al.* (2003). Identification of novel gene expression targets for the Ras association domain family 1 (RASSF1A) tumor suppressor gene in non-small cell lung cancer and neuroblastoma. Cancer research *63*, 5344-5351.

Ahmed-Choudhury, J., Agathanggelou, A., Fenton, S.L., Ricketts, C., Clark, G.J., Maher, E.R., and Latif, F. (2005). Transcriptional regulation of cyclin A2 by RASSF1A through the enhanced binding of p120E4F to the cyclin A2 promoter. Cancer research *65*, 2690-2697.

Almodovar-Garcia, K., Kwon, M., Samaras, S.E., and Davidson, J.M. (2014). ANKRD1 acts as a transcriptional repressor of MMP13 via the AP-1 site. Molecular and cellular biology *34*, 1500-1511.

Amaar, Y.G., Minera, M.G., Hatran, L.K., Strong, D.D., Mohan, S., and Reeves, M.E. (2006). Ras association domain family 1C protein stimulates human lung cancer cell proliferation. American journal of physiology Lung cellular and molecular physiology *291*, L1185-1190.

Arimura, T., Bos, J.M., Sato, A., Kubo, T., Okamoto, H., Nishi, H., Harada, H., Koga, Y., Moulik, M., Doi, Y.L.*, et al.* (2009). Cardiac ankyrin repeat protein gene (ANKRD1) mutations in hypertrophic cardiomyopathy. Journal of the American College of Cardiology *54*, 334-342.

Aylon, Y., Michael, D., Shmueli, A., Yabuta, N., Nojima, H., and Oren, M. (2006). A positive feedback loop between the p53 and Lats2 tumor suppressors prevents tetraploidization. Genes & development *20*, 2687-2700.

Badi, I., Cinquetti, R., Frascoli, M., Parolini, C., Chiesa, G., Taramelli, R., and Acquati, F. (2009). Intracellular ANKRD1 protein levels are regulated by 26S proteasome-mediated degradation. FEBS letters *583*, 2486-2492.

Bai, N., Zhang, C., Liang, N., Zhang, Z., Chang, A., Yin, J., Li, Z., Luo, N., Tan, X., Luo, N.*, et al.* (2013). Yes-associated protein (YAP) increases chemosensitivity of hepatocellular carcinoma cells by modulation of p53. Cancer biology & therapy *14*, 511-520.

Barash, I.A., Bang, M.L., Mathew, L., Greaser, M.L., Chen, J., and Lieber, R.L. (2007). Structural and regulatory roles of muscle ankyrin repeat protein family in skeletal muscle. American journal of physiology Cell physiology *293*, C218-227.

Basu, S., Totty, N.F., Irwin, M.S., Sudol, M., and Downward, J. (2003). Akt phosphorylates the Yes-associated protein, YAP, to induce interaction with 14-3-3 and attenuation of p73-mediated apoptosis. Molecular cell *11*, 11-23.

Beckedorff, F.C., Ayupe, A.C., Crocci-Souza, R., Amaral, M.S., Nakaya, H.I., Soltys, D.T., Menck, C.F., Reis, E.M., and Verjovski-Almeida, S. (2013). The intronic long noncoding RNA ANRASSF1 recruits PRC2 to the RASSF1A promoter, reducing the expression of RASSF1A and increasing cell proliferation. PLoS genetics *9*, e1003705.

Bertozzi, D., Iurlaro, R., Sordet, O., Marinello, J., Zaffaroni, N., and Capranico, G. (2011). Characterization of novel antisense HIF-1alpha transcripts in human cancers. Cell Cycle *10*, 3189-3197.

Bogomolovas, J., Brohm, K., Celutkiene, J., Balciunaite, G., Bironaite, D., Bukelskiene, V., Daunoravicus, D., Witt, C.C., Fielitz, J., Grabauskiene, V.*, et al.* (2015). Induction of Ankrd1 in Dilated Cardiomyopathy Correlates with the Heart Failure Progression. BioMed research international *2015*, 273936.

Breitling, L.P., Yang, R., Korn, B., Burwinkel, B., and Brenner, H. (2011). Tobacco-smoking-related differential DNA methylation: 27K discovery and replication. American journal of human genetics *88*, 450-457.

Calvisi, D.F., Donninger, H., Vos, M.D., Birrer, M.J., Gordon, L., Leaner, V., and Clark, G.J. (2009). NORE1A tumor suppressor candidate modulates p21CIP1 via p53. Cancer research *69*, 4629-4637.

Chan, E.H., Nousiainen, M., Chalamalasetty, R.B., Schafer, A., Nigg, E.A., and Sillje, H.H. (2005). The Ste20-like kinase Mst2 activates the human large tumor suppressor kinase Lats1. Oncogene *24*, 2076-2086.

Charlet, J., Szemes, M., Malik, K.T., and Brown, K.W. (2014). MYCN is recruited to the RASSF1A promoter but is not critical for DNA hypermethylation in neuroblastoma. Molecular carcinogenesis *53*, 413-420.

Chen, B., Zhong, L., Roush, S.F., Pentassuglia, L., Peng, X., Samaras, S., Davidson, J.M., Sawyer, D.B., and Lim, C.C. (2012). Disruption of a GATA4/Ankrd1 signaling axis in cardiomyocytes leads to sarcomere disarray: implications for anthracycline cardiomyopathy. PloS one *7*, e35743.

Cheng, L., Zhou, Z., Flesken-Nikitin, A., Toshkov, I.A., Wang, W., Camps, J., Ried, T., and Nikitin, A.Y. (2010). Rb inactivation accelerates neoplastic growth and substitutes for recurrent amplification of cIAP1, cIAP2 and Yap1 in sporadic mammary carcinoma associated with p53 deficiency. Oncogene *29*, 5700-5711.

Cinquetti, R., Badi, I., Campione, M., Bortoletto, E., Chiesa, G., Parolini, C., Camesasca, C., Russo, A., Taramelli, R., and Acquati, F. (2008). Transcriptional deregulation and a missense mutation define ANKRD1 as a candidate gene for total anomalous pulmonary venous return. Human mutation *29*, 468-474.

Cooper, W.N., Hesson, L.B., Matallanas, D., Dallol, A., von Kriegsheim, A., Ward, R., Kolch, W., and Latif, F. (2009). RASSF2 associates with and stabilizes the proapoptotic kinase MST2. Oncogene *28*, 2988-2998.

Crocini, C., Arimura, T., Reischmann, S., Eder, A., Braren, I., Hansen, A., Eschenhagen, T., Kimura, A., and Carrier, L. (2013). Impact of ANKRD1 mutations associated with hypertrophic cardiomyopathy on contraction parameters of engineered heart tissue. Basic research in cardiology *108*, 349.

Dallol, A., Agathanggelou, A., Fenton, S.L., Ahmed-Choudhury, J., Hesson, L., Vos, M.D., Clark, G.J., Downward, J., Maher, E.R., and Latif, F. (2004). RASSF1A interacts with microtubule-associated proteins and modulates microtubule dynamics. Cancer research *64*, 4112-4116.

Dallol, A., Hesson, L.B., Matallanas, D., Cooper, W.N., O'Neill, E., Maher, E.R., Kolch, W., and Latif, F. (2009). RAN GTPase is a RASSF1A effector involved in controlling microtubule organization. Current biology : CB *19*, 1227-1232.

Dammann, R., Li, C., Yoon, J.H., Chin, P.L., Bates, S., and Pfeifer, G.P. (2000). Epigenetic inactivation of a RAS association domain family protein from the lung tumour suppressor locus 3p21.3. Nature genetics *25*, 315-319.

Dammann, R., Schagdarsurengin, U., Liu, L., Otto, N., Gimm, O., Dralle, H., Boehm, B.O., Pfeifer, G.P., and Hoang-Vu, C. (2003). Frequent RASSF1A promoter hypermethylation and K-ras mutations in pancreatic carcinoma. Oncogene *22*, 3806-3812.

Dammann, R., Yang, G., and Pfeifer, G.P. (2001). Hypermethylation of the cpG island of Ras association domain family 1A (RASSF1A), a putative tumor suppressor gene from the 3p21.3 locus, occurs in a large percentage of human breast cancers. Cancer research *61*, 3105-3109.

Das Thakur, M., Feng, Y., Jagannathan, R., Seppa, M.J., Skeath, J.B., and Longmore, G.D. (2010). Ajuba LIM proteins are negative regulators of the Hippo signaling pathway. Current biology : CB *20*, 657-662.

Dittfeld, C., Richter, A.M., Steinmann, K., Klagge-Ulonska, A., and Dammann, R.H. (2012). The SARAH Domain of RASSF1A and Its Tumor Suppressor Function. Molecular biology international *2012*, 196715.

Donninger, H., Calvisi, D.F., Barnoud, T., Clark, J., Schmidt, M.L., Vos, M.D., and Clark, G.J. (2015). NORE1A is a Ras senescence effector that controls the apoptotic/senescent balance of p53 via HIPK2. The Journal of cell biology *208*, 777-789.

Duboscq-Bidot, L., Charron, P., Ruppert, V., Fauchier, L., Richter, A., Tavazzi, L., Arbustini, E., Wichter, T., Maisch, B., Komajda, M.*, et al.* (2009). Mutations in the ANKRD1 gene encoding CARP are responsible for human dilated cardiomyopathy. European heart journal *30*, 2128-2136.

Edgar, B.A. (2006). From cell structure to transcription: Hippo forges a new path. Cell *124*, 267-273.

Elbediwy, A., Vincent-Mistiaen, Z.I., and Thompson, B.J. (2016). YAP and TAZ in epithelial stem cells: A sensor for cell polarity, mechanical forces and tissue damage. BioEssays : news and reviews in molecular, cellular and developmental biology *38*, 644-653.

Esteller, M. (2011). Non-coding RNAs in human disease. Nature reviews Genetics *12*, 861-874.

Fausti, F., Di Agostino, S., Sacconi, A., Strano, S., and Blandino, G. (2012). Hippo and rassf1a Pathways: A Growing Affair. Molecular biology international *2012*, 307628.

Feinberg, A.P., Koldobskiy, M.A., and Gondor, A. (2016). Epigenetic modulators, modifiers and mediators in cancer aetiology and progression. Nature reviews Genetics *17*, 284-299.

Fernandez, L.A., Northcott, P.A., Dalton, J., Fraga, C., Ellison, D., Angers, S., Taylor, M.D., and Kenney, A.M. (2009). YAP1 is amplified and up-regulated in hedgehog-associated medulloblastomas and mediates Sonic hedgehog-driven neural precursor proliferation. Genes & development *23*, 2729-2741.

Ferrand, A., Chevrier, V., Chauvin, J.P., and Birnbaum, D. (2009). Ajuba: a new microtubule-associated protein that interacts with BUBR1 and Aurora B at kinetochores in metaphase. Biology of the cell *101*, 221-235.

Fire, A., Xu, S., Montgomery, M.K., Kostas, S.A., Driver, S.E., and Mello, C.C. (1998). Potent and specific genetic interference by double-stranded RNA in Caenorhabditis elegans. Nature *391*, 806-811.

Foley, C.J., Freedman, H., Choo, S.L., Onyskiw, C., Fu, N.Y., Yu, V.C., Tuszynski, J., Pratt, J.C., and Baksh, S. (2008). Dynamics of RASSF1A/MOAP-1 association with death receptors. Molecular and cellular biology *28*, 4520-4535.

Foxler, D.E., Bridge, K.S., James, V., Webb, T.M., Mee, M., Wong, S.C., Feng, Y., Constantin-Teodosiu, D., Petursdottir, T.E., Bjornsson, J.*, et al.* (2012). The LIMD1 protein bridges an association between the prolyl hydroxylases and VHL to repress HIF-1 activity. Nature cell biology *14*, 201-208.

Furth, N., Bossel Ben-Moshe, N., Pozniak, Y., Porat, Z., Geiger, T., Domany, E., Aylon, Y., and Oren, M. (2015). Down-regulation of LATS kinases alters p53 to promote cell migration. Genes & development *29*, 2325-2330.

Gaffney, C.J., Oka, T., Mazack, V., Hilman, D., Gat, U., Muramatsu, T., Inazawa, J., Golden, A., Carey, D.J., Farooq, A.*, et al.* (2012). Identification, basic characterization and evolutionary analysis of differentially spliced mRNA isoforms of human YAP1 gene. Gene *509*, 215-222.

Grannas, K., Arngarden, L., Lonn, P., Mazurkiewicz, M., Blokzijl, A., Zieba, A., and Soderberg, O. (2015). Crosstalk between Hippo and TGFbeta: Subcellular Localization of YAP/TAZ/Smad Complexes. J Mol Biol *427*, 3407-3415.

Gutmann, D.H. (1997). Molecular insights into neurofibromatosis 2. Neurobiology of disease *3*, 247-261.
Han, X.J., Chae, J.K., Lee, M.J., You, K.R., Lee, B.H., and Kim, D.G. (2005). Involvement of GADD153 and cardiac ankyrin repeat protein in hypoxia-induced apoptosis of H9c2 cells. The Journal of biological chemistry *280*, 23122-23129.

Hanahan, D., and Weinberg, R.A. (2011). Hallmarks of cancer: the next generation. Cell *144*, 646-674.

Hao, Y., Chun, A., Cheung, K., Rashidi, B., and Yang, X. (2008). Tumor suppressor LATS1 is a negative regulator of oncogene YAP. The Journal of biological chemistry *283*, 5496-5509.

Harper, J.W., Adami, G.R., Wei, N., Keyomarsi, K., and Elledge, S.J. (1993). The p21 Cdk-interacting protein Cip1 is a potent inhibitor of G1 cyclin-dependent kinases. Cell *75*, 805-816.

Harvey, K.F., Zhang, X., and Thomas, D.M. (2013). The Hippo pathway and human cancer. Nat Rev Cancer *13*, 246-257.

Helmbold, P., Lahtz, C., Enk, A., Herrmann-Trost, P., Marsch, W., Kutzner, H., and Dammann, R.H. (2009). Frequent occurrence of RASSF1A promoter hypermethylation and Merkel cell polyomavirus in Merkel cell carcinoma. Molecular carcinogenesis *48*, 903-909.

Hirota, T., Kunitoku, N., Sasayama, T., Marumoto, T., Zhang, D., Nitta, M., Hatakeyama, K., and Saya, H. (2003). Aurora-A and an Interacting Activator, the LIM Protein Ajuba, Are Required for Mitotic Commitment in Human Cells. Cell *114*, 585-598.

Hsu, P.C., You, B., Yang, Y.L., Zhang, W.Q., Wang, Y.C., Xu, Z., Dai, Y., Liu, S., Yang, C.T., Li, H.*, et al.* (2016). YAP promotes erlotinib resistance in human non-small cell lung cancer cells. Oncotarget *7*, 51922-51933.

Hsueh, Y.J., Chen, H.C., Wu, S.E., Wang, T.K., Chen, J.K., and Ma, D.H. (2015). Lysophosphatidic acid induces YAP-promoted proliferation of human corneal endothelial cells via PI3K and ROCK pathways. Molecular therapy Methods & clinical development *2*, 15014.

Huo, X., Zhang, Q., Liu, A.M., Tang, C., Gong, Y., Bian, J., Luk, J.M., Xu, Z., and Chen, J. (2013). Overexpression of Yes-associated protein confers doxorubicin resistance in hepatocellullar carcinoma. Oncology reports *29*, 840-846.

Hwang, E., Ryu, K.S., Paakkonen, K., Guntert, P., Cheong, H.K., Lim, D.S., Lee, J.O., Jeon, Y.H., and Cheong, C. (2007). Structural insight into dimeric interaction of the SARAH domains from Mst1 and RASSF family proteins in the apoptosis pathway. Proceedings of the National Academy of Sciences of the United States of America *104*, 9236-9241.

Ishiguro, N., Baba, T., Ishida, T., Takeuchi, K., Osaki, M., Araki, N., Okada, E., Takahashi, S., Saito, M., Watanabe, M.*, et al.* (2002). Carp, a cardiac ankyrin-repeated protein, and its new homologue, Arpp, are differentially expressed in heart, skeletal muscle, and rhabdomyosarcomas. The American journal of pathology *160*, 1767-1778.

Ishizaki, K., Fujimoto, J., Kumimoto, H., Nishimoto, Y., Shimada, Y., Shinoda, M., and Yamamoto, T. (2002). Frequent polymorphic changes but rare tumor specific mutations of the LATS2 gene on 13q11-12 in esophageal squamous cell carcinoma. International journal of oncology *21*, 1053-1057.

Iwasa, H., Kudo, T., Maimaiti, S., Ikeda, M., Maruyama, J., Nakagawa, K., and Hata, Y. (2013). The RASSF6 tumor suppressor protein regulates apoptosis and the cell cycle via MDM2 protein and p53 protein. The Journal of biological chemistry *288*, 30320-30329.

Januchowski, R., Zawierucha, P., Rucinski, M., Nowicki, M., and Zabel, M. (2014). Extracellular matrix proteins expression profiling in chemoresistant variants of the A2780 ovarian cancer cell line. BioMed research international *2014*, 365867.

Jeyaseelan, R., Poizat, C., Baker, R.K., Abdishoo, S., Isterabadi, L.B., Lyons, G.E., and Kedes, L. (1997). A novel cardiac-restricted target for doxorubicin. CARP, a nuclear modulator of gene expression in cardiac progenitor cells and cardiomyocytes. The Journal of biological chemistry *272*, 22800-22808.

Justice, R.W., Zilian, O., Woods, D.F., Noll, M., and Bryant, P.J. (1995). The Drosophila tumor suppressor gene warts encodes a homolog of human myotonic dystrophy kinase and is required for the control of cell shape and proliferation. Genes & development *9*, 534-546.

Kang, W., Tong, J.H., Chan, A.W., Lee, T.L., Lung, R.W., Leung, P.P., So, K.K., Wu, K., Fan, D., Yu, J., *et al.* (2011). Yes-associated protein 1 exhibits oncogenic property in gastric cancer and its nuclear accumulation associates with poor prognosis. Clinical cancer research : an official journal of the American Association for Cancer Research *17*, 2130-2139.

Kapoor, A., Yao, W., Ying, H., Hua, S., Liewen, A., Wang, Q., Zhong, Y., Wu, C.J., Sadanandam, A., Hu, B., *et al.* (2014). Yap1 activation enables bypass of oncogenic Kras addiction in pancreatic cancer. Cell *158*, 185-197.

Keshet, R., Adler, J., Ricardo Lax, I., Shanzer, M., Porat, Z., Reuven, N., and Shaul, Y. (2015). c-Abl antagonizes the YAP oncogenic function. Cell death and differentiation *22*, 935-945.

Kim, M., Kim, T., Johnson, R.L., and Lim, D.S. (2015). Transcriptional co-repressor function of the hippo pathway transducers YAP and TAZ. Cell reports *11*, 270-282.

Kim, N.G., Koh, E., Chen, X., and Gumbiner, B.M. (2011). E-cadherin mediates contact inhibition of proliferation through Hippo signaling-pathway components. Proceedings of the National Academy of Sciences of the United States of America *108*, 11930-11935.

Kojic, S., Nestorovic, A., Rakicevic, L., Belgrano, A., Stankovic, M., Divac, A., and Faulkner, G. (2010). A novel role for cardiac ankyrin repeat protein Ankrd1/CARP as a co-activator of the p53 tumor suppressor protein. Archives of biochemistry and biophysics *502*, 60-67.

Komuro, A., Nagai, M., Navin, N.E., and Sudol, M. (2003). WW domain-containing protein YAP associates with ErbB-4 and acts as a co-transcriptional activator for the carboxyl-terminal fragment of ErbB-4 that translocates to the nucleus. The Journal of biological chemistry *278*, 33334-33341.

Kudo, T., Ikeda, M., Nishikawa, M., Yang, Z., Ohno, K., Nakagawa, K., and Hata, Y. (2012). The RASSF3 candidate tumor suppressor induces apoptosis and G1-S cell-cycle arrest via p53. Cancer research *72*, 2901-2911.

Kussie, P.H., Gorina, S., Marechal, V., Elenbaas, B., Moreau, J., Levine, A.J., and Pavletich, N.P. (1996). Structure of the MDM2 oncoprotein bound to the p53 tumor suppressor transactivation domain. Science *274*, 948-953.

Labbe, E., Lock, L., Letamendia, A., Gorska, A.E., Gryfe, R., Gallinger, S., Moses, H.L., and Attisano, L. (2007). Transcriptional cooperation between the transforming growth factor-beta and Wnt pathways in mammary and intestinal tumorigenesis. Cancer research *67*, 75-84.

Lallemand, D., Curto, M., Saotome, I., Giovannini, M., and McClatchey, A.I. (2003). NF2 deficiency promotes tumorigenesis and metastasis by destabilizing adherens junctions. Genes & development *17*, 1090-1100.

Lei, Q.Y., Zhang, H., Zhao, B., Zha, Z.Y., Bai, F., Pei, X.H., Zhao, S., Xiong, Y., and Guan, K.L. (2008). TAZ promotes cell proliferation and epithelial-mesenchymal transition and is inhibited by the hippo pathway. Molecular and cellular biology *28*, 2426-2436.

Lei, Y., Henderson, B.R., Emmanuel, C., Harnett, P.R., and deFazio, A. (2015). Inhibition of ANKRD1 sensitizes human ovarian cancer cells to endoplasmic reticulum stress-induced apoptosis. Oncogene *34*, 485-495.

Levine, A.J. (1997). p53, the cellular gatekeeper for growth and division. Cell *88*, 323-331.

Levy, D., Adamovich, Y., Reuven, N., and Shaul, Y. (2008a). Yap1 phosphorylation by c-Abl is a critical step in selective activation of proapoptotic genes in response to DNA damage. Molecular cell *29*, 350-361.

Levy, D., Reuven, N., and Shaul, Y. (2008b). A regulatory circuit controlling Itch-mediated p73 degradation by Runx. The Journal of biological chemistry *283*, 27462-27468.

Li, C., Srivastava, R.K., Elmets, C.A., Afaq, F., and Athar, M. (2013). Arsenic-induced cutaneous hyperplastic lesions are associated with the dysregulation of Yap, a Hippo signaling-related protein. Biochemical and biophysical research communications *438*, 607-612.

Li, M., Lu, J., Zhang, F., Li, H., Zhang, B., Wu, X., Tan, Z., Zhang, L., Gao, G., Mu, J.*, et al.* (2014). Yes-associated protein 1 (YAP1) promotes human gallbladder tumor growth via activation of the AXL/MAPK pathway. Cancer letters *355*, 201-209.

Li, X., Tao, J., Cigliano, A., Sini, M., Calderaro, J., Azoulay, D., Wang, C., Liu, Y., Jiang, L., Evert, K.*, et al.* (2015a). Co-activation of PIK3CA and Yap promotes development of hepatocellular and cholangiocellular tumors in mouse and human liver. Oncotarget *6*, 10102-10115.

Li, Y., Zhou, H., Li, F., Chan, S.W., Lin, Z., Wei, Z., Yang, Z., Guo, F., Lim, C.J., Xing, W.*, et al.* (2015b). Angiomotin binding-induced activation of Merlin/NF2 in the Hippo pathway. Cell research *25*, 801-817.

Li, Z., Zhao, B., Wang, P., Chen, F., Dong, Z., Yang, H., Guan, K.L., and Xu, Y. (2010). Structural insights into the YAP and TEAD complex. Genes & development *24*, 235-240.

Liu, C., Pan, Y., Wang, X., Lu, J., Huang, B., and Li, X. (2010). Activation of RASSF2A by p300 induces late apoptosis through histone hyperacetylation. Cell biology international *34*, 1133-1139.

Liu, L., Broaddus, R.R., Yao, J.C., Xie, S., White, J.A., Wu, T.T., Hamilton, S.R., and Rashid, A. (2005). Epigenetic alterations in neuroendocrine tumors: methylation of RAS-association domain family 1, isoform A and p16 genes are associated with metastasis. Modern pathology : an official journal of the United States and Canadian Academy of Pathology, Inc *18*, 1632-1640.

Liu, L., Guo, C., Dammann, R., Tommasi, S., and Pfeifer, G.P. (2008). RASSF1A interacts with and activates the mitotic kinase Aurora-A. Oncogene *27*, 6175-6186.

Liu, L., Yoon, J.H., Dammann, R., and Pfeifer, G.P. (2002). Frequent hypermethylation of the RASSF1A gene in prostate cancer. Oncogene *21*, 6835-6840.

Liu, L.L., Zhang, M.F., Pan, Y.H., Yun, J.P., and Zhang, C.Z. (2014). NORE1A sensitises cancer cells to sorafenib-induced apoptosis and indicates hepatocellular carcinoma prognosis. Tumour biology : the journal of the International Society for Oncodevelopmental Biology and Medicine *35*, 1763-1774.

Liu, X.H., Bauman, W.A., and Cardozo, C. (2015). ANKRD1 modulates inflammatory responses in C2C12 myoblasts through feedback inhibition of NF-kappaB signaling activity. Biochemical and biophysical research communications *464*, 208-213.

Macheiner, D., Heller, G., Kappel, S., Bichler, C., Stattner, S., Ziegler, B., Kandioler, D., Wrba, F., Schulte-Hermann, R., Zochbauer-Muller, S.*, et al.* (2006). NORE1B, a candidate tumor suppressor, is epigenetically silenced in human hepatocellular carcinoma. Journal of hepatology *45*, 81-89.

Macias, M.J., Wiesner, S., and Sudol, M. (2002). WW and SH3 domains, two different scaffolds to recognize proline-rich ligands. FEBS letters *513*, 30-37.

Maruyama, R., Akino, K., Toyota, M., Suzuki, H., Imai, T., Ohe-Toyota, M., Yamamoto, E., Nojima, M., Fujikane, T., Sasaki, Y.*, et al.* (2008). Cytoplasmic RASSF2A is a proapoptotic mediator whose expression is epigenetically silenced in gastric cancer. Carcinogenesis *29*, 1312-1318.

Matallanas, D., Romano, D., Yee, K., Meissl, K., Kucerova, L., Piazzolla, D., Baccarini, M., Vass, J.K., Kolch, W., and O'Neill, E. (2007). RASSF1A elicits apoptosis through an MST2 pathway directing proapoptotic transcription by the p73 tumor suppressor protein. Molecular cell *27*, 962-975.

Mazelin, L., Panthu, B., Nicot, A.S., Belotti, E., Tintignac, L., Teixeira, G., Zhang, Q., Risson, V., Baas, D., Delaune, E.*, et al.* (2016). mTOR inactivation in myocardium from infant mice rapidly leads to dilated cardiomyopathy due to translation defects and p53/JNK-mediated apoptosis. Journal of molecular and cellular cardiology *97*, 213-225.

Mikhailov, A.T., and Torrado, M. (2008). The enigmatic role of the ankyrin repeat domain 1 gene in heart development and disease. The International journal of developmental biology *52*, 811-821.

Miller, M.K., Bang, M.-L., Witt, C.C., Labeit, D., Trombitas, C., Watanabe, K., Granzier, H., McElhinny, A.S., Gregorio, C.C., and Labeit, S. (2003). The Muscle Ankyrin Repeat Proteins: CARP, ankrd2/Arpp and DARP as a Family of Titin Filament-based Stress Response Molecules. Journal of Molecular Biology *333*, 951-964.

Mineo, M., Ricklefs, F., Rooj, A.K., Lyons, S.M., Ivanov, P., Ansari, K.I., Nakano, I., Chiocca, E.A., Godlewski, J., and Bronisz, A. (2016). The Long Non-coding RNA HIF1A-AS2 Facilitates the Maintenance of Mesenchymal Glioblastoma Stem-like Cells in Hypoxic Niches. Cell reports *15*, 2500-2509.

Mizuno, T., Murakami, H., Fujii, M., Ishiguro, F., Tanaka, I., Kondo, Y., Akatsuka, S., Toyokuni, S., Yokoi, K., Osada, H., *et al.* (2012). YAP induces malignant mesothelioma cell proliferation by upregulating transcription of cell cycle-promoting genes. Oncogene *31*, 5117-5122.

Modena, P., Lualdi, E., Facchinetti, F., Veltman, J., Reid, J.F., Minardi, S., Janssen, I., Giangaspero, F., Forni, M., Finocchiaro, G., *et al.* (2006). Identification of tumor-specific molecular signatures in intracranial ependymoma and association with clinical characteristics. Journal of clinical oncology : official journal of the American Society of Clinical Oncology *24*, 5223-5233.

Mohamed, J.S., and Boriek, A.M. (2012). Loss of desmin triggers mechanosensitivity and up-regulation of Ankrd1 expression through Akt-NF-kappaB signaling pathway in smooth muscle cells. FASEB journal : official publication of the Federation of American Societies for Experimental Biology *26*, 757-765.

Momand, J., Zambetti, G.P., Olson, D.C., George, D., and Levine, A.J. (1992). The mdm-2 oncogene product forms a complex with the p53 protein and inhibits p53-mediated transactivation. Cell *69*, 1237-1245.

Moran-Jones, K., Gloss, B.S., Murali, R., Chang, D.K., Colvin, E.K., Jones, M.D., Yuen, S., Howell, V.M., Brown, L.M., Wong, C.W., *et al.* (2015). Connective tissue growth factor as a novel therapeutic target in high grade serous ovarian cancer. Oncotarget *6*, 44551-44562.

Mosavi, L.K., Cammett, T.J., Desrosiers, D.C., and Peng, Z.Y. (2004). The ankyrin repeat as molecular architecture for protein recognition. Protein science : a publication of the Protein Society *13*, 1435-1448.

Muramatsu, T., Imoto, I., Matsui, T., Kozaki, K., Haruki, S., Sudol, M., Shimada, Y., Tsuda, H., Kawano, T., and Inazawa, J. (2011). YAP is a candidate oncogene for esophageal squamous cell carcinoma. Carcinogenesis *32*, 389-398.

Muranen, T., Selfors, L.M., Hwang, J., Gallegos, L.L., Coloff, J.L., Thoreen, C.C., Kang, S.A., Sabatini, D.M., Mills, G.B., and Brugge, J.S. (2016). ERK and p38 MAPK Activities Determine Sensitivity to PI3K/mTOR Inhibition via Regulation of MYC and YAP. Cancer research.

Neto-Silva, R.M., de Beco, S., and Johnston, L.A. (2010). Evidence for a growth-stabilizing regulatory feedback mechanism between Myc and Yorkie, the Drosophila homolog of Yap. Developmental cell *19*, 507-520.

Ni, L., Li, S., Yu, J., Min, J., Brautigam, C.A., Tomchick, D.R., Pan, D., and Luo, X. (2013). Structural basis for autoactivation of human Mst2 kinase and its regulation by RASSF5. Structure *21*, 1757-1768.

O'Neill, E., Rushworth, L., Baccarini, M., and Kolch, W. (2004). Role of the kinase MST2 in suppression of apoptosis by the proto-oncogene product Raf-1. Science *306*, 2267-2270.

Oka, T., Remue, E., Meerschaert, K., Vanloo, B., Boucherie, C., Gfeller, D., Bader, G.D., Sidhu, S.S., Vandekerckhove, J., Gettemans, J., *et al.* (2010). Functional complexes between YAP2 and ZO-2 are PDZ domain-dependent, and regulate YAP2 nuclear localization and signalling. Biochem J *432*, 461-472.

Oliner, J.D., Pietenpol, J.A., Thiagalingam, S., Gyuris, J., Kinzler, K.W., and Vogelstein, B. (1993). Oncoprotein MDM2 conceals the activation domain of tumour suppressor p53. Nature *362*, 857-860.

Orr, B.A., Bai, H., Odia, Y., Jain, D., Anders, R.A., and Eberhart, C.G. (2011). Yes-associated protein 1 is widely expressed in human brain tumors and promotes glioblastoma growth. Journal of neuropathology and experimental neurology *70*, 568-577.

Paramasivam, M., Sarkeshik, A., Yates, J.R., 3rd, Fernandes, M.J., and McCollum, D. (2011). Angiomotin family proteins are novel activators of the LATS2 kinase tumor suppressor. Molecular biology of the cell *22*, 3725-3733.

Park, J.H., Liu, L., Kim, I.H., Kim, J.H., You, K.R., and Kim, D.G. (2005). Identification of the genes involved in enhanced fenretinide-induced apoptosis by parthenolide in human hepatoma cells. Cancer research *65*, 2804-2814.

Peng, H.W., Slattery, M., and Mann, R.S. (2009). Transcription factor choice in the Hippo signaling pathway: homothorax and yorkie regulation of the microRNA bantam in the progenitor domain of the Drosophila eye imaginal disc. Genes & development *23*, 2307-2319.

Praskova, M., Khoklatchev, A., Ortiz-Vega, S., and Avruch, J. (2004). Regulation of the MST1 kinase by autophosphorylation, by the growth inhibitory proteins, RASSF1 and NORE1, and by Ras. Biochem J *381*, 453-462.

Ragione, F.D., Russo, G.L., Oliva, A., Mercurio, C., Mastropietro, S., Pietra, V.D., and Zappia, V. (1996). Biochemical characterization of p16INK4- and p18-containing complexes in human cell lines. The Journal of biological chemistry *271*, 15942-15949.

Reddy, B.V., and Irvine, K.D. (2013). Regulation of Hippo signaling by EGFR-MAPK signaling through Ajuba family proteins. Developmental cell *24*, 459-471.

Reeves, M.E., Firek, M., Chen, S.T., and Amaar, Y. (2013). The RASSF1 Gene and the Opposing Effects of the RASSF1A and RASSF1C Isoforms on Cell Proliferation and Apoptosis. Molecular biology international *2013*, 145096.

Richter, A.M., Haag, T., Walesch, S., Herrmann-Trost, P., Marsch, W.C., Kutzner, H., Helmbold, P., and Dammann, R.H. (2013). Aberrant Promoter Hypermethylation of RASSF Family Members in Merkel Cell Carcinoma. Cancers *5*, 1566-1576.

Richter, A.M., Pfeifer, G.P., and Dammann, R.H. (2009). The RASSF proteins in cancer; from epigenetic silencing to functional characterization. Biochim Biophys Acta *1796*, 114-128.

Richter, A.M., Schagdarsurengin, U., Rastetter, M., Steinmann, K., and Dammann, R.H. (2010). Protein kinase A-mediated phosphorylation of the RASSF1A tumour suppressor at Serine 203 and regulation of RASSF1A function. Eur J Cancer *46*, 2986-2995.

Richter, A.M., Zimmermann, T., Haag, T., Walesch, S.K., and Dammann, R.H. (2015). Promoter methylation status of Ras-association domain family members in pheochromocytoma. Frontiers in endocrinology *6*, 21.

Risch, A., and Plass, C. (2008). Lung cancer epigenetics and genetics. International journal of cancer *123*, 1-7.

Rong, R., Jiang, L.Y., Sheikh, M.S., and Huang, Y. (2007). Mitotic kinase Aurora-A phosphorylates RASSF1A and modulates RASSF1A-mediated microtubule interaction and M-phase cell cycle regulation. Oncogene *26*, 7700-7708.

Rong, R., Jin, W., Zhang, J., Sheikh, M.S., and Huang, Y. (2004). Tumor suppressor RASSF1A is a microtubule-binding protein that stabilizes microtubules and induces G2/M arrest. Oncogene *23*, 8216-8230.

Rosenbluh, J., Nijhawan, D., Cox, A.G., Li, X., Neal, J.T., Schafer, E.J., Zack, T.I., Wang, X., Tsherniak, A., Schinzel, A.C.*, et al.* (2012). beta-Catenin-driven cancers require a YAP1 transcriptional complex for survival and tumorigenesis. Cell *151*, 1457-1473.

Sasaki, H., Hikosaka, Y., Kawano, O., Yano, M., and Fujii, Y. (2010). Hypermethylation of the large tumor suppressor genes in Japanese lung cancer. Oncology letters *1*, 303-307.

Saucedo, L.J., and Edgar, B.A. (2007). Filling out the Hippo pathway. Nature reviews Molecular cell biology *8*, 613-621.

Schagdarsurengin, U., Richter, A.M., Hornung, J., Lange, C., Steinmann, K., and Dammann, R.H. (2010). Frequent epigenetic inactivation of RASSF2 in thyroid cancer and functional consequences. Molecular cancer *9*, 264.

Schagdarsurengin, U., Wilkens, L., Steinemann, D., Flemming, P., Kreipe, H.H., Pfeifer, G.P., Schlegelberger, B., and Dammann, R. (2003). Frequent epigenetic inactivation of the RASSF1A gene in hepatocellular carcinoma. Oncogene *22*, 1866-1871.

Schmidt, M.L., Calvisi, D.F., and Clark, G.J. (2016). NORE1A Regulates MDM2 Via beta-TrCP. Cancers *8*.
Schutte, U., Bisht, S., Heukamp, L.C., Kebschull, M., Florin, A., Haarmann, J., Hoffmann, P., Bendas, G., Buettner, R., Brossart, P.*, et al.* (2014). Hippo signaling mediates proliferation, invasiveness, and metastatic potential of clear cell renal cell carcinoma. Translational oncology *7*, 309-321.

Scurr, L.L., Guminski, A.D., Chiew, Y.E., Balleine, R.L., Sharma, R., Lei, Y., Pryor, K., Wain, G.V., Brand, A., Byth, K.*, et al.* (2008). Ankyrin repeat domain 1, ANKRD1, a novel determinant of cisplatin sensitivity expressed in ovarian cancer. Clinical cancer research : an official journal of the American Association for Cancer Research *14*, 6924-6932.

Seidel, C., Schagdarsurengin, U., Blumke, K., Wurl, P., Pfeifer, G.P., Hauptmann, S., Taubert, H., and Dammann, R. (2007). Frequent hypermethylation of MST1 and MST2 in soft tissue sarcoma. Molecular carcinogenesis *46*, 865-871.

Shao, D.D., Xue, W., Krall, E.B., Bhutkar, A., Piccioni, F., Wang, X., Schinzel, A.C., Sood, S., Rosenbluh, J., Kim, J.W.*, et al.* (2014). KRAS and YAP1 converge to regulate EMT and tumor survival. Cell *158*, 171-184.

Sharp, T.V., Al-Attar, A., Foxler, D.E., Ding, L., de, A.V.T.Q., Zhang, Y., Nijmeh, H.S., Webb, T.M., Nicholson, A.G., Zhang, Q.*, et al.* (2008). The chromosome 3p21.3-encoded gene, LIMD1, is a critical tumor suppressor involved in human lung cancer development. Proceedings of the National Academy of Sciences of the United States of America *105*, 19932-19937.

Shen, L., Chen, C., Wei, X., Li, X., Luo, G., Zhang, J., Bin, J., Huang, X., Cao, S., Li, G.*, et al.* (2015). Overexpression of ankyrin repeat domain 1 enhances cardiomyocyte apoptosis by promoting p53 activation and mitochondrial dysfunction in rodents. Clin Sci (Lond) *128*, 665-678.

Shimizu, S., Narita, M., and Tsujimoto, Y. (1999). Bcl-2 family proteins regulate the release of apoptogenic cytochrome c by the mitochondrial channel VDAC. Nature *399*, 483-487.

Shivakumar, L., Minna, J., Sakamaki, T., Pestell, R., and White, M.A. (2002). The RASSF1A Tumor Suppressor Blocks Cell Cycle Progression and Inhibits Cyclin D1 Accumulation. Molecular and cellular biology *22*, 4309-4318.

Shukla, S., Mirza, S., Sharma, G., Parshad, R., Gupta, S.D., and Ralhan, R. (2006). Detection of RASSF1A and RARbeta hypermethylation in serum DNA from breast cancer patients. Epigenetics *1*, 88-93.

Silvis, M.R., Kreger, B.T., Lien, W.H., Klezovitch, O., Rudakova, G.M., Camargo, F.D., Lantz, D.M., Seykora, J.T., and Vasioukhin, V. (2011). alpha-catenin is a tumor suppressor that controls cell accumulation by regulating the localization and activity of the transcriptional coactivator Yap1. Science signaling *4*, ra33.

Snijders, A.M., Schmidt, B.L., Fridlyand, J., Dekker, N., Pinkel, D., Jordan, R.C., and Albertson, D.G. (2005). Rare amplicons implicate frequent deregulation of cell fate specification pathways in oral squamous cell carcinoma. Oncogene *24*, 4232-4242.

Song, H., Oh, S., Oh, H.J., and Lim, D.S. (2010). Role of the tumor suppressor RASSF2 in regulation of MST1 kinase activity. Biochemical and biophysical research communications *391*, 969-973.

Song, M.S., Song, S.J., Kim, S.Y., Oh, H.J., and Lim, D.S. (2008). The tumour suppressor RASSF1A promotes MDM2 self-ubiquitination by disrupting the MDM2-DAXX-HAUSP complex. The EMBO journal *27*, 1863-1874.

Song, S.J., Kim, S.J., Song, M.S., and Lim, D.S. (2009a). Aurora B-mediated phosphorylation of RASSF1A maintains proper cytokinesis by recruiting Syntaxin16 to the midzone and midbody. Cancer research *69*, 8540-8544.

Song, S.J., Song, M.S., Kim, S.J., Kim, S.Y., Kwon, S.H., Kim, J.G., Calvisi, D.F., Kang, D., and Lim, D.S. (2009b). Aurora A regulates prometaphase progression by inhibiting the ability of RASSF1A to suppress APC-Cdc20 activity. Cancer research *69*, 2314-2323.

Stein, C., Bardet, A.F., Roma, G., Bergling, S., Clay, I., Ruchti, A., Agarinis, C., Schmelzle, T., Bouwmeester, T., Schubeler, D.*, et al.* (2015). YAP1 Exerts Its Transcriptional Control via TEAD-Mediated Activation of Enhancers. PLoS genetics *11*, e1005465.

Steinhardt, A.A., Gayyed, M.F., Klein, A.P., Dong, J., Maitra, A., Pan, D., Montgomery, E.A., and Anders, R.A. (2008). Expression of Yes-associated protein in common solid tumors. Human pathology *39*, 1582-1589.

Steinmann, K., Richter, A.M., and Dammann, R.H. (2011). Epigenetic silencing of erythropoietin in human cancers. Genes & cancer *2*, 65-73.

Strano, S., Munarriz, E., Rossi, M., Castagnoli, L., Shaul, Y., Sacchi, A., Oren, M., Sudol, M., Cesareni, G., and Blandino, G. (2001). Physical interaction with Yes-associated protein enhances p73 transcriptional activity. The Journal of biological chemistry *276*, 15164-15173.

Strazisar, M., Mlakar, V., and Glavac, D. (2009). LATS2 tumour specific mutations and down-regulation of the gene in non-small cell carcinoma. Lung Cancer *64*, 257-262.

Strunnikova, M., Schagdarsurengin, U., Kehlen, A., Garbe, J.C., Stampfer, M.R., and Dammann, R. (2005). Chromatin inactivation precedes de novo DNA methylation during the progressive epigenetic silencing of the RASSF1A promoter. Molecular and cellular biology *25*, 3923-3933.

Sudol, M., Bork, P., Einbond, A., Kastury, K., Druck, T., Negrini, M., Huebner, K., and Lehman, D. (1995). Characterization of the mammalian YAP (Yes-associated protein) gene and its role in defining a novel protein module, the WW domain. The Journal of biological chemistry *270*, 14733-14741.

Sudol, M., Shields, D.C., and Farooq, A. (2012). Structures of YAP protein domains reveal promising targets for development of new cancer drugs. Seminars in cell & developmental biology *23*, 827-833.

Sugawara, W., Arai, Y., Kasai, F., Fujiwara, Y., Haruta, M., Hosaka, R., Nishida, K., Kurosumi, M., Kobayashi, Y., Akagi, K.*, et al.* (2011). Association of germline or somatic TP53 missense mutation with oncogene amplification in tumors developed in patients with Li-Fraumeni or Li-Fraumeni-like syndrome. Genes, chromosomes & cancer *50*, 535-545.

Sugawara, W., Haruta, M., Sasaki, F., Watanabe, N., Tsunematsu, Y., Kikuta, A., and Kaneko, Y. (2007). Promoter hypermethylation of the RASSF1A gene predicts the poor outcome of patients with hepatoblastoma. Pediatric blood & cancer *49*, 240-249.

Sun, G., and Irvine, K.D. (2013). Ajuba family proteins link JNK to Hippo signaling. Science signaling *6*, ra81.

Tanaka, I., Osada, H., Fujii, M., Fukatsu, A., Hida, T., Horio, Y., Kondo, Y., Sato, A., Hasegawa, Y., Tsujimura, T.*, et al.* (2015). LIM-domain protein AJUBA suppresses malignant mesothelioma cell proliferation via Hippo signaling cascade. Oncogene *34*, 73-83.

Tao, H., Yang, J.J., Hu, W., Shi, K.H., and Li, J. (2016). HDAC6 Promotes Cardiac Fibrosis Progression through Suppressing RASSF1A Expression. Cardiology *133*, 18-26.

Tapon, N., Harvey, K.F., Bell, D.W., Wahrer, D.C., Schiripo, T.A., Haber, D., and Hariharan, I.K. (2002). salvador Promotes both cell cycle exit and apoptosis in Drosophila and is mutated in human cancer cell lines. Cell *110*, 467-478.

Tebaldi, T., Zaccara, S., Alessandrini, F., Bisio, A., Ciribilli, Y., and Inga, A. (2015). Whole-genome cartography of p53 response elements ranked on transactivation potential. BMC genomics *16*, 464.

Tian, Y., Hou, Y., Zhou, X., Cheng, H., and Zhou, R. (2011). Tumor suppressor RASSF1A promoter: p53 binding and methylation. PloS one *6*, e17017.

Tomlinson, V., Gudmundsdottir, K., Luong, P., Leung, K.Y., Knebel, A., and Basu, S. (2010). JNK phosphorylates Yes-associated protein (YAP) to regulate apoptosis. Cell death & disease *1*, e29.

Torrado, M., Nespereira, B., Bouzamayor, Y., Centeno, A., Lopez, E., and Mikhailov, A.T. (2006). Differential atrial versus ventricular ANKRD1 gene expression is oppositely regulated at diastolic heart failure. FEBS letters *580*, 4182-4187.

Torrado, M., Nespereira, B., Lopez, E., Centeno, A., Castro-Beiras, A., and Mikhailov, A.T. (2005). ANKRD1 specifically binds CASQ2 in heart extracts and both proteins are co-enriched in piglet cardiac Purkinje cells. Journal of molecular and cellular cardiology *38*, 353-365.

van Loo, P.F., Mahtab, E.A., Wisse, L.J., Hou, J., Grosveld, F., Suske, G., Philipsen, S., and Gittenberger-de Groot, A.C. (2007). Transcription factor Sp3 knockout mice display serious cardiac malformations. Molecular and cellular biology *27*, 8571-8582.

Varelas, X., Miller, B.W., Sopko, R., Song, S., Gregorieff, A., Fellouse, F.A., Sakuma, R., Pawson, T., Hunziker, W., McNeill, H.*, et al.* (2010). The Hippo pathway regulates Wnt/beta-catenin signaling. Developmental cell *18*, 579-591.

Varelas, X., Sakuma, R., Samavarchi-Tehrani, P., Peerani, R., Rao, B.M., Dembowy, J., Yaffe, M.B., Zandstra, P.W., and Wrana, J.L. (2008). TAZ controls Smad nucleocytoplasmic shuttling and regulates human embryonic stem-cell self-renewal. Nature cell biology *10*, 837-848.

Wang, K.C., Yeh, Y.T., Nguyen, P., Limqueco, E., Lopez, J., Thorossian, S., Guan, K.L., Li, Y.J., and Chien, S. (2016). Flow-dependent YAP/TAZ activities regulate endothelial phenotypes and atherosclerosis. Proceedings of the National Academy of Sciences of the United States of America *113*, 11525-11530.

Wang, Y., Dong, Q., Zhang, Q., Li, Z., Wang, E., and Qiu, X. (2010). Overexpression of yes-associated protein contributes to progression and poor prognosis of non-small-cell lung cancer. Cancer science *101*, 1279-1285.

Wu, S., Huang, J., Dong, J., and Pan, D. (2003). hippo encodes a Ste-20 family protein kinase that restricts cell proliferation and promotes apoptosis in conjunction with salvador and warts. Cell *114*, 445-456.

Wu, S., Liu, Y., Zheng, Y., Dong, J., and Pan, D. (2008). The TEAD/TEF family protein Scalloped mediates transcriptional output of the Hippo growth-regulatory pathway. Developmental cell *14*, 388-398.

Xia, Y., Zhang, Y.L., Yu, C., Chang, T., and Fan, H.Y. (2014). YAP/TEAD co-activator regulated pluripotency and chemoresistance in ovarian cancer initiated cells. PloS one *9*, e109575.

Xie, Q., Chen, J., Feng, H., Peng, S., Adams, U., Bai, Y., Huang, L., Li, J., Huang, J., Meng, S.*, et al.* (2013). YAP/TEAD-mediated transcription controls cellular senescence. Cancer research *73*, 3615-3624.

Xiong, Y., Zhang, H., and Beach, D. (1993). Subunit rearrangement of the cyclin-dependent kinases is associated with cellular transformation. Genes & development *7*, 1572-1583.

Xu, B., Li, S.H., Zheng, R., Gao, S.B., Ding, L.H., Yin, Z.Y., Lin, X., Feng, Z.J., Zhang, S., Wang, X.M.*, et al.* (2013). Menin promotes hepatocellular carcinogenesis and epigenetically up-regulates Yap1 transcription. Proceedings of the National Academy of Sciences of the United States of America *110*, 17480-17485.

Xu, T., and Rubin, G.M. (1993). Analysis of genetic mosaics in developing and adult Drosophila tissues. Development *117*, 1223-1237.

Yang, Q., Zage, P., Kagan, D., Tian, Y., Seshadri, R., Salwen, H.R., Liu, S., Chlenski, A., and Cohn, S.L. (2004). Association of epigenetic inactivation of RASSF1A with poor outcome in human neuroblastoma. Clinical cancer research : an official journal of the American Association for Cancer Research *10*, 8493-8500.

Yu, F.X., and Guan, K.L. (2013). The Hippo pathway: regulators and regulations. Genes & development *27*, 355-371.

Yu, F.X., Zhao, B., Panupinthu, N., Jewell, J.L., Lian, I., Wang, L.H., Zhao, J., Yuan, H., Tumaneng, K., Li, H.*, et al.* (2012). Regulation of the Hippo-YAP pathway by G-protein-coupled receptor signaling. Cell *150*, 780-791.

Yuan, Y., Li, D., Li, H., Wang, L., Tian, G., and Dong, Y. (2016). YAP overexpression promotes the epithelial-mesenchymal transition and chemoresistance in pancreatic cancer cells. Molecular medicine reports *13*, 237-242.

Zagurovskaya, M., Shareef, M.M., Das, A., Reeves, A., Gupta, S., Sudol, M., Bedford, M.T., Prichard, J., Mohiuddin, M., and Ahmed, M.M. (2009). EGR-1 forms a complex with YAP-1 and upregulates Bax expression in irradiated prostate carcinoma cells. Oncogene *28*, 1121-1131.

Zanconato, F., Forcato, M., Battilana, G., Azzolin, L., Quaranta, E., Bodega, B., Rosato, A., Bicciato, S., Cordenonsi, M., and Piccolo, S. (2015). Genome-wide association between YAP/TAZ/TEAD and AP-1 at enhancers drives oncogenic growth. Nature cell biology *17*, 1218-1227.

Zender, L., Spector, M.S., Xue, W., Flemming, P., Cordon-Cardo, C., Silke, J., Fan, S.T., Luk, J.M., Wigler, M., Hannon, G.J.*, et al.* (2006). Identification and validation of oncogenes in liver cancer using an integrative oncogenomic approach. Cell *125*, 1253-1267.

Zhang, L., Ren, F., Zhang, Q., Chen, Y., Wang, B., and Jiang, J. (2008). The TEAD/TEF family of transcription factor Scalloped mediates Hippo signaling in organ size control. Developmental cell *14*, 377-387.

Zhang, N., Bai, H., David, K.K., Dong, J., Zheng, Y., Cai, J., Giovannini, M., Liu, P., Anders, R.A., and Pan, D. (2010). The Merlin/NF2 tumor suppressor functions through the YAP oncoprotein to regulate tissue homeostasis in mammals. Developmental cell *19*, 27-38.

Zhang, W., Nandakumar, N., Shi, Y., Manzano, M., Smith, A., Graham, G., Gupta, S., Vietsch, E.E., Laughlin, S.Z., Wadhwa, M.*, et al.* (2014). Downstream of mutant KRAS, the transcription regulator YAP is essential for neoplastic progression to pancreatic ductal adenocarcinoma. Science signaling *7*, ra42.

Zhao, B., Li, L., Lei, Q., and Guan, K.L. (2010a). The Hippo-YAP pathway in organ size control and tumorigenesis: an updated version. Genes & development *24*, 862-874.

Zhao, B., Li, L., Lu, Q., Wang, L.H., Liu, C.Y., Lei, Q., and Guan, K.L. (2011). Angiomotin is a novel Hippo pathway component that inhibits YAP oncoprotein. Genes & development *25*, 51-63.

Zhao, B., Li, L., Tumaneng, K., Wang, C.Y., and Guan, K.L. (2010b). A coordinated phosphorylation by Lats and CK1 regulates YAP stability through SCF(beta-TRCP). Genes & development *24*, 72-85.

Zhao, B., Wei, X., Li, W., Udan, R.S., Yang, Q., Kim, J., Xie, J., Ikenoue, T., Yu, J., Li, L.*, et al.* (2007). Inactivation of YAP oncoprotein by the Hippo pathway is involved in cell contact inhibition and tissue growth control. Genes & development *21*, 2747-2761.

Zhao, B., Ye, X., Yu, J., Li, L., Li, W., Li, S., Yu, J., Lin, J.D., Wang, C.Y., Chinnaiyan, A.M.*, et al.* (2008). TEAD mediates YAP-dependent gene induction and growth control. Genes & development *22*, 1962-1971.

Zhou, X.H., Yang, C.Q., Zhang, C.L., Gao, Y., Yuan, H.B., and Wang, C. (2014). RASSF5 inhibits growth and invasion and induces apoptosis in osteosarcoma cells through activation of MST1/LATS1 signaling. Oncology reports *32*, 1505-1512.

Zhou, Y., Huang, T., Cheng, A.S., Yu, J., Kang, W., and To, K.F. (2016). The TEAD Family and Its Oncogenic Role in Promoting Tumorigenesis. International journal of molecular sciences *17*.

Zou, Y., Evans, S., Chen, J., Kuo, H.C., Harvey, R.P., and Chien, K.R. (1997). CARP, a cardiac ankyrin repeat protein, is downstream in the Nkx2-5 homeobox gene pathway. Development *124*, 793-804.

ACKNOWLEGMENTS

I would like to express my sincere gratitude to my advisor Prof. Dr. Reinhard Dammann for the continuous support and motivation. His experience, charisma and enthusiasm encouraged me during my work and my private life in Giessen. I could not have imagined having a better mentor for my PhD project.

My sincere thanks also for my labmates for the nice time together and for all the fun we had in the last years. I will always remember all of you and this beautiful time at the Dammann lab. To Antje, thank you for your friendship, time and good advises. I will always miss you. Dear Sara, I will always remember you and your patience with my temperament and thank you so much for your help. Dear Daniela, thanks for your patience and support. My sincere thanks and love to Michelle and Steffen for your friendship and the nice time together.

My special thanks to my friends Aiganish, Linda, Diana, German, Grace and Nayong for supporting me during my studies and my life in general. Also, I would like to express my sincere gratitude to Prof. Dr. Wolfgang Hagmann for supporting me throughout the writing of my last two theses. I will never forget you and your instructions.

I would like also to express my profound gratitude and love to the family Schmidhuber and to my beloved Claude, who supported me in good and in bad moments. I am truly thankful for your patience and for your unconditional love every single day.

Tambien les quiero agradecer a mis amigas y amigos, quienes se han convertido en mi familia, por su cariño incondicional que traspasa tiempo y distancias. A Nora, Nathy, Johis, Ursula, y David porque con ustedes empece esta aventura y a mis amigos en Ecuador, a quienes siempre llevare en mi corazón, en especial a Wilmi y Marujita. Finalmente quiero agradecer de todo corazón a Dios y a toda mi familia, en especial a mis padres Mauricio Jiménez y Teresa Carrera, a mis hermanos Javier y Fernanda, sobrinos, a mis tios, tias, primas, primos y por supuesto a mi Balou. Gracias por su apoyo y amor durante todo este largo tiempo. Los amo mucho.

Adry